

1 **Scale-dependent perspectives on the geomorphology and evolution of beach-dune systems.**

2

3 draft manuscript submitted to *Earth-Science Reviews*

4 revised submission, March 2017

5

6

7

8

9

10

11

12

13

14 Ian J. Walker*, School of Geographical Sciences and Urban Planning, School of Earth and Space
15 Exploration, Arizona State University, Tempe, AZ, USA.

16 *corresponding author: ianjwalker@asu.edu, 250-721-7347

17

18 Robin G.D. Davidson-Arnott, Dept. of Geography, University of Guelph, Guelph, ON, Canada.

19

20 Bernard O. Bauer, Earth & Environmental Sciences, University of British Columbia – Okanagan,
21 Kelowna, BC, Canada.

22

23 Patrick A. Hesp, School of the Environment, Flinders University, Bedford Park, South Australia
24 5041.

25

26 Irene Delgado-Fernandez, Dept. of Geography, Edge Hill University, Ormskirk, Lancashire, UK.

27

28 Jeff Ollerhead, Dept. of Geography and Environment, Mount Allison University, Sackville, NB,
29 Canada.

30

31 Thomas A.G. Smyth, Department of Geography and Environmental Science, Liverpool Hope
32 University, Hope Park, Liverpool, L16 9JD.

33	TABLE OF CONTENTS	
34	1. Introduction and purpose	4
35	2. Conceptual Foundations: Effectiveness and Scale of Geomorphic Events	6
36	3. Study Area: Greenwich Dunes, Prince Edward Island, Canada.....	12
37	4. Plot scale	17
38	4.1 Airflow dynamics over the beach-dune profile.....	18
39	4.1.1 Classic models of boundary layer flow over low hills.....	18
40	4.1.2 Advances in flow dynamics over complex dune terrain.....	20
41	4.1.3 New perspectives on turbulence and coherent flow structures.....	24
42	4.1.4 Advances in understanding topographic steering of near surface flow and sand	
43	transport vectors	29
44	4.1.5 Innovative Computational Fluid Dynamics (CFD) modeling of flow over foredunes ...	39
45	4.2 Instantaneous sediment transport across the beach-dune profile	41
46	4.2.1. Classic ideas on equilibrium ‘saturated’ sand transport	41
47	4.2.2. Improved understanding of the fetch effect on beaches and sand delivery to foredunes	
48	43	
49	4.2.3. Advances in understanding of fetch and moisture interactions on beaches.....	46
50	4.2.4. Exploring wind unsteadiness, transport response, and intermittency	51
51	4.2.5. New observations of vertical sediment flux variations and transport events (flurries)	
52	55	
53	4.2.6. Observations of flux divergence and spatial-temporal patterns of erosion and	
54	deposition	60
55	5. Landform scale	64
56	5.1 Modeling sediment delivery to coastal dunes	65
57	5.1.1 Classic approaches to modelling long-term aeolian sand drift	65
58	5.1.2 New efforts to assess the regime of aeolian transport events in beach-dune systems	
59	66	
60	5.1.3 Advances in modelling the effect of supply-limited conditions on predicted sand	
61	transport to foredunes	72
62	5.2. Beach-dune interaction.....	76
63	5.2.1. Classic understanding of sand supply and coastal dune evolution.....	76
64	5.2.2. Assessing annual to decadal beach-dune interaction	78
65	5.2.3. Decadal scale observations of extreme overwash and foredune recovery	85
66	6. Landscape scale.....	90
67	6.1 The classic view of the response of coastlines to sea-level rise: the Bruun model	90
68	6.2 A new perspective on the response of beach-dune systems to sea-level rise: the RD-A model	
69	91	
70	7. Summary and Conclusions	96
71	7.1 The persistent challenges of scale in beach-dune geomorphology.....	96
72	8. Acknowledgements.....	104
73	9. References	106

76 **Abstract:**

77 Despite widespread recognition that landforms are complex Earth systems with process-
78 response linkages that span temporal scales from seconds to millennia and spatial scales from
79 sand grains to landscapes, research that integrates knowledge across these scales is fairly
80 uncommon. As a result, understanding of geomorphic systems is often scale-constrained due
81 to a host of methodological, logistical, and theoretical factors that limit the scope of how Earth
82 scientists study landforms and broader landscapes.

83 This paper reviews recent advances in understanding of the geomorphology of beach-dune
84 systems derived from over a decade of collaborative research from Prince Edward Island (PEI),
85 Canada. A comprehensive summary of key findings is provided from short-term experiments
86 embedded within a decade-long monitoring program and a multi-decadal reconstruction of
87 coastal landscape change. Specific attention is paid to the challenges of scale integration and
88 the contextual limitations research at specific spatial and/or temporal scales imposes.

89 A conceptual framework is presented that integrates across key scales of investigation in
90 geomorphology and is grounded in classic ideas in Earth surface sciences on the effectiveness
91 of formative events at different scales. The paper uses this framework to organize the review
92 of this body of research in a 'scale aware' way and, thereby, identifies many new advances in
93 knowledge on the form and function of subaerial beach-dune systems.

94 Finally, the paper offers a synopsis of how greater understanding of the complexities at
95 different scales can be used to inform the development of predictive models, especially those
96 at a temporal scale of decades to centuries, which are most relevant to coastal management

97 issues. Models at this (landform) scale require an understanding of controls that exist at both
98 'landscape' and 'plot' scales. Landscape scale controls such as sea level change, regional
99 climate, and the underlying geologic framework essentially provide bounding conditions for
100 independent variables such as winds, waves, water levels, and littoral sediment supply.
101 Similarly, an holistic understanding of the range of processes, feedbacks, and linkages at the
102 finer plot scale is required to inform and verify the assumptions that underly the physical
103 modelling of beach-dune interaction at the landform scale.
104

105 **1. Introduction and purpose**

106 Despite widespread recognition that landforms are complex systems with process-
107 response linkages that span temporal scales from seconds to millennia and spatial scales from
108 sand grains to landscapes, research that integrates knowledge across these scales is fairly
109 uncommon (Bauer and Sherman, 1999). Our understanding of Earth surface systems is often
110 scale-constrained due to a host of methodological, logistical, and theoretical factors that limit,
111 either explicitly or implicitly, the span of what can be (or is being) studied (Sherman, 1995). As
112 such, it is not surprising that traditional geomorphic research was incapable of providing critical
113 insights into the conceptual bridges between fundamental process-response dynamics (studied
114 at micro or meso scales) and long-term processes and controls that govern landform evolution
115 over centuries and longer. This remains a key challenge for many Earth scientists and it is
116 particularly true for aeolian-coastal geomorphology research that focuses on the evolution and
117 maintenance of beach-dune systems that straddle the highly dynamic terrestrial-marine
118 interface (Short and Hesp, 1982).

119 This paper reviews recent advances in understanding of beach-dune systems derived from
120 over a decade of extensive and collaborative research that began in 2002 at the Greenwich
121 Dunes on Prince Edward Island (PEI), Canada. The paper provides a comprehensive summary of
122 findings from several short-term experiments embedded within a decade-long monitoring
123 program and a longer-term (multi-decadal) reconstruction of coastal landscape change.
124 Furthermore, the review situates the results from this specific research collaboration in a
125 broader (global) context with research from elsewhere to draw attention to the challenges

126 associated with scale integration in geomorphology. In particular, emphasis is placed on the
127 constraints that neighboring (smaller and larger) scale perspectives impose on the
128 understanding of knowledge derived at the scale of the event-based, instrumented field (plot
129 scale) experiment. For example, measurements of net accretion along the toe of a coastal
130 foredune using traditional cross-shore topographic profiles at monthly or seasonal intervals
131 cannot reveal information about whether there was a gradual accumulation of sand through
132 time, or deposition from a single event. Similarly, such survey data do not provide any
133 information about potential intervening events that may have caused foredune erosion via
134 wave scarping, nor can these data be used to extrapolate to long-term scenarios of dune
135 maintenance and evolution without knowledge of the erosion-deposition tendencies over
136 seasons, years and decades. Thus, without appropriate context, such survey data are of limited
137 utility, revealing only what happened at a particular place and time.

138 Section 2 of the paper presents a conceptual framework based on classic ideas in Earth
139 surface sciences that guide thinking on scale awareness and the effectiveness of geomorphic
140 events in landform and landscape evolution. This framework provides the structure for an
141 extensive review of scale-dependent research on beach-dune systems that is 'scale aware' and
142 identifies critical gaps in knowledge. The review is grounded in the extensive research from the
143 PEI study site (described in Section 3) but also considers a wide range of contributions, both
144 classic and contemporary, from around the world. Sections 4 through 6 each provide a brief
145 synthesis of classic knowledge and the state of the science up to the early 2000s. This is
146 followed by focused summaries of major advances at distinct spatial-temporal scales (plot,

147 landform, landscape for Sections 4-6 respectively) over the last 15 or so years. Section 7 offers
148 an overarching summary of key advances at each scale, issues of integration between them,
149 and presents future research opportunities and challenges.

150 Given the significant range of spatial and temporal scales covered in this review, the
151 domain of long-term Quaternary studies is not incorporated. It is acknowledged, however, that
152 glacio-isostatic adjustments and altered rates of relative sea-level (RSL) rise, for example, exert
153 key controls on the evolution of global coastlines that, in turn, may have implications for littoral
154 cell sediment budgets and influence millennial-scale evolution of beach-dune systems.

155

156 **2. Conceptual Foundations: Effectiveness and Scale of Geomorphic Events**

157 Advances in Earth sciences are typically incremental, often building on the research of past
158 generations of scientists. Modern process geomorphologists, are often motivated by earlier
159 works on complex system behaviour (or 'process-response' dynamics) in geomorphic
160 environments. Wolman and Miller (1960), for example, argued that the largest magnitude
161 events in Earth surface systems are not necessarily those that perform the greatest amount of
162 work. 'Catastrophic' storms may have immense capacity to alter pre-existing landscapes over
163 short time spans, but events of moderate magnitude may account for greater cumulative work
164 in a system because of their more frequent recurrence within the historical sequence of events
165 that yield landscape evolution. In contrast, seemingly innocuous events individually may not
166 cause major landscape disruption, but can be significant in landscape dynamics because of the
167 sustained work they perform over decades. Wolman and Gerson (1978) further argued that the

168 degree to which an event may leave an indelible imprint on the landscape (referred to as
169 geomorphic 'effectiveness') is not a simple, linear function of event magnitude but, rather,
170 depends on: (i) the historical sequencing of events and their timing; (ii) the antecedent
171 conditions that predispose a landscape for rapid change; and (iii) the capacity for a landscape to
172 recover from the change imparted by the most recent event. Thus, a large catastrophic event
173 may alter the landscape significantly, but the system may rebuild to the pre-event state under
174 every-day processes that cause landscape change. In contrast, even small landscape
175 disturbances may persist for decades if there is little capacity in the system to recover to the
176 prior state.

177 The effectiveness of a geomorphic event, which must include its magnitude-threshold-
178 frequency characterization, is also closely linked to the idea of equilibrium behavior (Thorn and
179 Welford, 1994) by virtue of implicitly embedding events into a historical sequence that yields
180 landscape change. The notion of 'embeddedness' was described masterfully by Schumm and
181 Lichty (1965) who asserted that the spatial-temporal scale at which a geomorphic system is
182 examined has implications for how system equilibrium may be manifested or perceived.

183 Although Schumm and Lichty (1965) referred to each of the scale domains as representative of
184 time, their framework implicitly embodies spatial dimensions. Based on these seminal
185 perspectives on geomorphic effectiveness and the conceptual foundation established by
186 Schumm and Lichty (1965) for general geomorphic systems, this paper provides a 'scale aware'
187 approach for reviewing recent advances on beach-dune dynamics using a dominantly spatial
188 reference terminology. Specifically, three characteristic scales of interest are identified: (1) the

189 experimental 'plot' scale, which operates on 'steady' time scales of seconds to days and length
190 scales of metres; (2) the 'landform' scale, which functions on 'graded' time (months to years)
191 and on length scales of hundreds of metres; and (3) the 'landscape' scale, which operates on
192 'cyclic' time (decades to centuries) across length scales of kilometres. Table 1 proposes a list of
193 variables applicable to a beach-dune system across the three scale ranges, which coincides with
194 our predisposition to investigate geomorphic processes and landform dynamics at scales
195 relevant to the human management of coastal resources. It is acknowledged that a different
196 definition of scale may be needed to create a similar classification for other coastal systems
197 (e.g., rocky, muddy, ice-dominated, etc.). Furthermore, challenges that exist at key scale
198 transitions (plot-landform, landform-landscape) are identified and recent efforts to bridge them
199 are discussed.

200 At the landscape (largest) scale, the dominant research interests of a coastal
201 geomorphologist might include characterizing and classifying the dynamic nature of the coast
202 according to whether the shoreline is prograding, aggrading, or retrograding, how wide and
203 steep the beach is, and whether the foredune is receding or advancing and growing or
204 shrinking. These factors are closely tied to the geometry and morphology of the beach-dune
205 system (Short and Hesp, 1982; Hesp, 1988; Sherman and Bauer, 1993; Bauer and Sherman,
206 1999; Houser and Ellis, 2013; Hesp and Walker, 2013), and they collectively define the
207 "dependent" variables (i.e., those that geomorphologists are interested to understand and
208 predict). The main "independent" variables (i.e., those that serve as controls or drivers of
209 system change and allow geomorphologists to gain insight into the dependent variables) are

210 the geological framework of the coast (i.e., tectonic/isostatic setting, structural controls, rock
211 type/history, fracture patterns, submarine bathymetry), eustatic sea-level trends, regional
212 climatology, and exposure to oceanographic forcing (e.g., wave climatology, coastal currents,
213 tidal fluctuations). Time is a relevant variable, simply because it takes time for major landforms
214 to respond and adjust toward equilibrium.

215 Many of the landscape scale variables listed toward the bottom of Table 1 are considered
216 “indeterminate” (i.e., those that have large variance but little impact on system dynamics at the
217 scale of interest) because there is often insufficient information to adequately parameterize
218 them and predict their state. For example, the degree to which a beach may have surface salt
219 crusts, snow cover, and flotsam during an individual transport event is of limited importance to
220 understanding whether there was (or will be) shoreline progradation or landward translation of
221 the beach-dune profile at the scale of decades to centuries.

222 At the plot (smallest) scale, the research focus is on prediction of sediment transport at
223 discrete locations over short time spans with the intent of understanding erosion and
224 deposition across the beach-dune system as it relates to foredune maintenance and evolution.
225 Thus, sediment transport rate and the pattern of flux divergence (leading to erosion or
226 deposition) are the primary dependent variables in the system, whereas the primary driver is
227 the near-surface wind vector (speed, direction) consistent with standard formulations of
228 aeolian sediment transport models (e.g., Bagnold, 1941; Kawamura, 1951). In addition, there
229 are a large number of supply-limiting surface controls, such as moisture content, snow cover,
230 salt crusts, textural gradations, roughness elements (e.g., woody debris, wrack, foot prints,

231 bedforms, lag deposits), that dictate the spatial-temporal pattern of sand transport across a
232 beach-dune system (Sherman, 1990; Ellis and Sherman, 2013). Table 1 also catalogues
233 "parameters", which are defined as controlling variables that are largely time-invariant at the
234 scale of inquiry, although at larger scales they may be treated as time dependent variables. For
235 example, in most plot-scale studies of sediment transport across a beach, it is reasonable to
236 assume that foredune geometry is unchanged over periods of hours to days, that vegetation
237 cover is constant because of slow growth rates (unless buried by a large event), and the
238 tendency for the shoreline to erode or accrete is relatively unaltered if nearshore forcing is
239 constant. Long-term factors such as mean wave conditions, climate patterns, relative sea-level
240 trend and the geological context are not relevant at the plot scale, whereas at the landscape
241 scale, these are dominant independent variables. As shown by Schumm and Lichty (1965), the
242 specific combination of independent and dependent variables defining the dynamics of
243 geomorphic systems will change depending on the scale of investigation.

244 Between the landscape and plot scales is the landform (intermediate) scale, which spans a
245 period of time long enough to include seasonal cycles of adjustment as well as multiple extreme
246 events. Table 1 shows that there is no overlap between the list of variables that are dependent
247 (i.e., predictable) or independent (i.e., imposed) at the landscape versus plot scales, suggesting
248 that knowledge gained at these end-member frames of reference is largely incommensurate.
249 Research at the landform scale provides rich opportunities to connect these disparate
250 knowledge domains, although research at the landform scale requires a commitment to

251 longitudinal experimental designs that span a decade or more, which is often logistically
252 challenging to maintain.

253 In many respects, the landform scale is the most challenging and demanding to conduct
254 research in as it retains the requirements of a short-term (plot-scale) assessment with the need
255 to scale up to a medium-term (landform-scale) understanding of processes that span a much
256 wider range of variables. Moreover, the contextual controls imposed by the broader landscape
257 scale are also relevant for understanding landform scale adjustments. Foredune maintenance
258 and evolution is best understood with observations that span periods of many years to
259 decades, and this category of understanding offers greater utility for management strategies
260 intended to mitigate damage from human alteration of the coast and/or within a framework of
261 climate non-stationarity and global sea-level rise (e.g., Davidson-Arnott, 2005; McLean and
262 Shen, 2006; Hesp, 2013). Indeed, this was one of the key motivations for our research at
263 Greenwich Dunes and our research partnership with Parks Canada.

264

265 **Table 1:** A proposed classification of system variables for beach-dune interaction that integrates
 266 across key spatial-temporal scales of reference from the plot scale (seconds to days, metres), to
 267 landform scale (months to years, 100s of metres), and up to landscape scale (decades to
 268 centuries, kilometres). This conceptualization is limited in scope to sandy coastal systems and
 269 scales relevant for human management of coastal systems, rather than the long-term
 270 geological evolution of the coastline.
 271

Beach-Dune Variable	Status of Variable During Spatial-Temporal Frame of Reference		
	LANDSCAPE	LANDFORM	PLOT
Time	Independent	Not Relevant	Not Relevant
Geological Context	Independent	Parameter	Not Relevant
Sea-Level Transgression	Independent	Parameter	Not Relevant
Climatology	Independent	Independent	Not Relevant
Coastal Oceanography	Independent	Independent	Not Relevant
Shoreline Progradation/Erosion	Dependent	(In)dependent	Parameter
Vegetation Cover (Biogeography)	Dependent	(In)dependent	Parameter
Foredune Size And Geometry	Dependent	Dependent	Parameter
Beach Width And Slope	Dependent	Dependent	Independent
Surface Moisture & Snow/Ice	Indeterminate	Dependent	Independent
Salt Crusts	Indeterminate	Dependent	Independent
Surface Debris	Indeterminate	Dependent	Independent
Human Influences	Indeterminate	Dependent	Independent
Wind Approach Angle	Indeterminate	Dependent	Independent
Wind Speed	Indeterminate	Dependent	Independent
Sediment Transport Rate	Indeterminate	Dependent	Dependent
Erosion/Deposition Patterns	Indeterminate	Dependent	Dependent

272

273 3. Study Area: Greenwich Dunes, Prince Edward Island, Canada

274 The Greenwich Peninsula is located on the northeastern shore of Prince Edward Island (PEI)
 275 in the Gulf of St. Lawrence in eastern Canada. The Greenwich Dunes complex was incorporated
 276 by Parks Canada Agency (PCA) into PEI National Park in 2000 to protect an area of established
 277 foredunes backed by wetlands, ponds, stabilized transgressive dunes, and a large parabolic
 278 dune complex (Figure 1). Much of the northeastern coast of PEI consists of horizontally-
 279 bedded, red sandstone, with some siltstone and mudstone, of Permian-Carboniferous age (van

280 de Pol, 1983), that erodes readily. During the Holocene, the coast of PEI evolved under marine
281 transgression and bedrock erosion. Shoreline retreat averaged about 0.5 m a^{-1} over the past
282 6,000 years (Forbes et al., 2004), which is similar to recession rates over the past half century
283 along the NE coast (Webster, 2012). Sand supply associated with marine erosion and
284 transgression is stored primarily as a thin wedge on the beach and inner shoreface, in barrier
285 islands and mainland dune systems, and in flood and ebb tidal deltas associated with inlets of
286 the barrier systems (Forbes et al, 2004; Coldwater Consulting, 2011). Today, low bedrock cliffs
287 and headlands are typical with extensive sections of barrier islands and spits that enclose
288 lagoons and shallow estuaries. The tidal range is micro-tidal ($\sim 1.0 \text{ m}$) with a mixed, semi-
289 diurnal regime. Recent estimates of relative sea-level (RSL) rise for Charlottetown, PEI, give
290 rates of land subsidence (due to glacial isostatic effects) of -1.45 mm a^{-1} and an estimated
291 eustatic rise in sea level of $+1.07 \text{ mm a}^{-1}$, producing an estimated RSL rise of about $+0.25 \text{ m}$
292 century^{-1} (James et al., 2012). This value is roughly consistent with estimates of long-term RSL
293 rise for the past 6,000 years of $+0.3 \text{ m century}^{-1}$ (Forbes et al., 2004; Webster, 2012).

294 Prince Edward Island experiences a cool, temperate climate with a strong marine influence.
295 Daily average temperatures range from a low of -8°C in February to a high of 19°C in August
296 with maximum temperatures seldom exceeding 30°C . Average annual precipitation is about
297 1200 mm with less than 25% falling as snow, although winter snowfall amounts are highly
298 variable. Prevailing winds at the site are from the SW, although strong northerly winds are
299 common in March and April. Dominant winds from the NW, N and NE are driven by the passage
300 of mid-latitude cyclones, which occur frequently in late fall through winter (October through

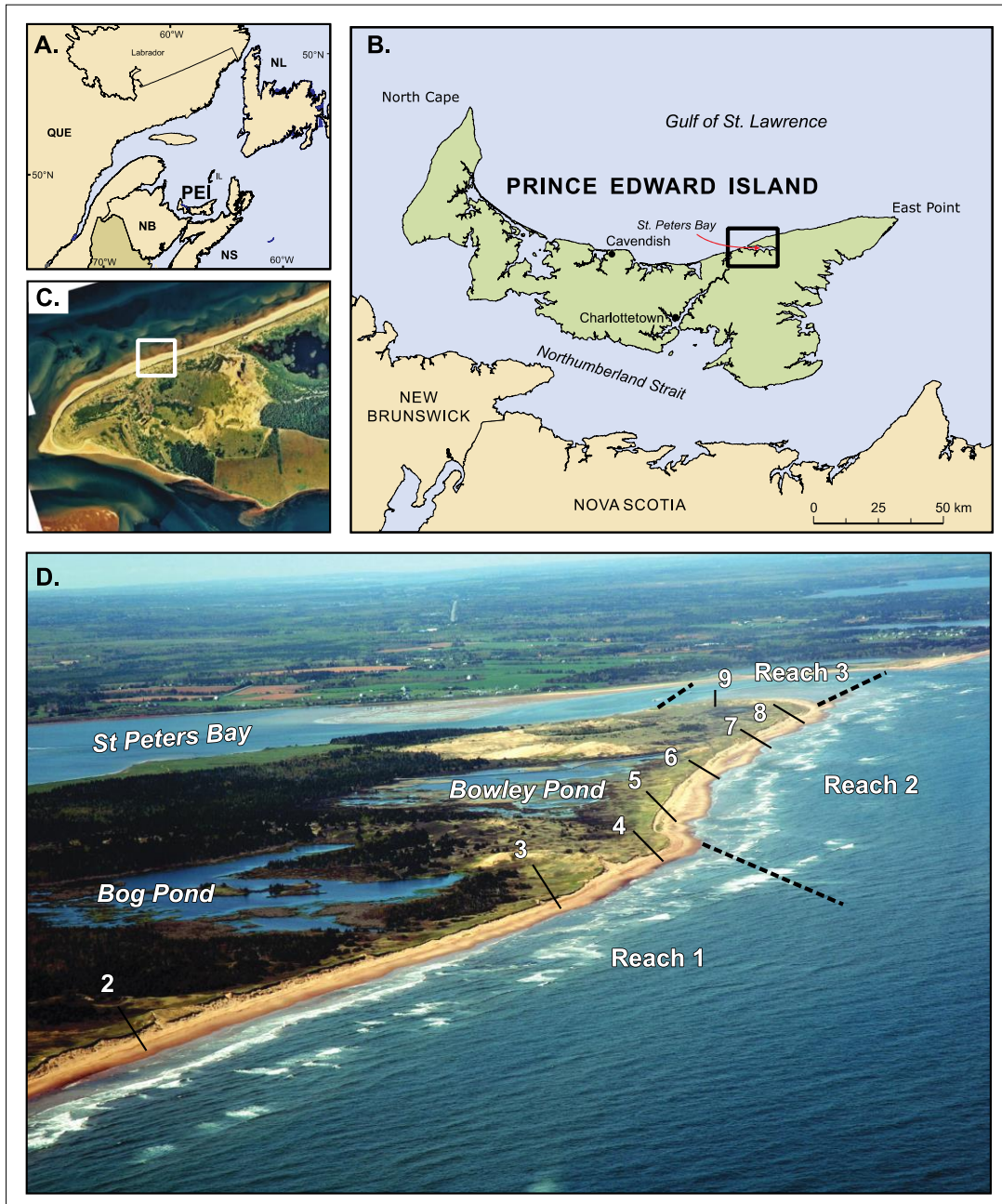
301 March) and exert significant control on precipitation and wind patterns in PEI (Manson et al.,
302 2002; Forbes et al., 2004; Manson et al., 2015). Occasionally, hurricanes also track NE from the
303 Caribbean, particularly in September and October. While the direct impact of hurricanes and
304 post-tropical storms is generally moderate, storms tracking close to the area can interact with
305 other mid-latitude systems to produce intense wind and wave conditions and storm surges that
306 may persist for many hours. Extensive coastal erosion, flooding, and localized overwash of
307 mainland and barrier dune systems is associated with extreme storms, as appears to have been
308 the case for a major fall gale in 1923 (see section 5.2.3).

309 Foredunes at the site range in height from 8 to 12 m and have fairly uniform, straight
310 seaward stoss slopes and a complex, undulating dune crest with intermittent depositional lobes
311 and blowouts (Hesp and Walker, 2012). The foredune toe is occasionally scarped by waves
312 during major storms but aeolian processes rapidly rebuild the slope by scarp in-filling. Incipient
313 dunes up to 1 m high and 5-6 m wide also develop and can persist for 2-4 years between major
314 storms. The dominant vegetation on the foredune is American Beach Grass (*Ammophila*
315 *breviligulata*), whereas the annual Sea Rocket (*Cakile edentula*) is common on the backshore
316 and occasionally Saltwort (*Salsola sp.*) is present. Beach Pea (*Lathyrus japonicas*) and Seaside
317 Goldenrod (*Solidago sempiverens*) are common on lee slopes during the summer and fall
318 months and shrubs such as Bayberry (*Myrica pensylvanica*) are found in more sheltered areas.

319

320

321 **Figure 1:** Location of study area showing: a) location of PEI in the Gulf of St. Lawrence and
 322 surrounding provinces; b) the Greenwich Dunes and St. Peter's Estuary area; c) vertical aerial
 323 photograph of Greenwich Dunes and the entrance to St. Peters Bay; d) oblique aerial
 324 photograph of the beach and dune system at Greenwich Dunes including the locations of
 325 characteristic study reaches (1-3) and cross-shore topographic profiles (see Ollerhead et al.
 326 2013, and Figs. 21 and 25).



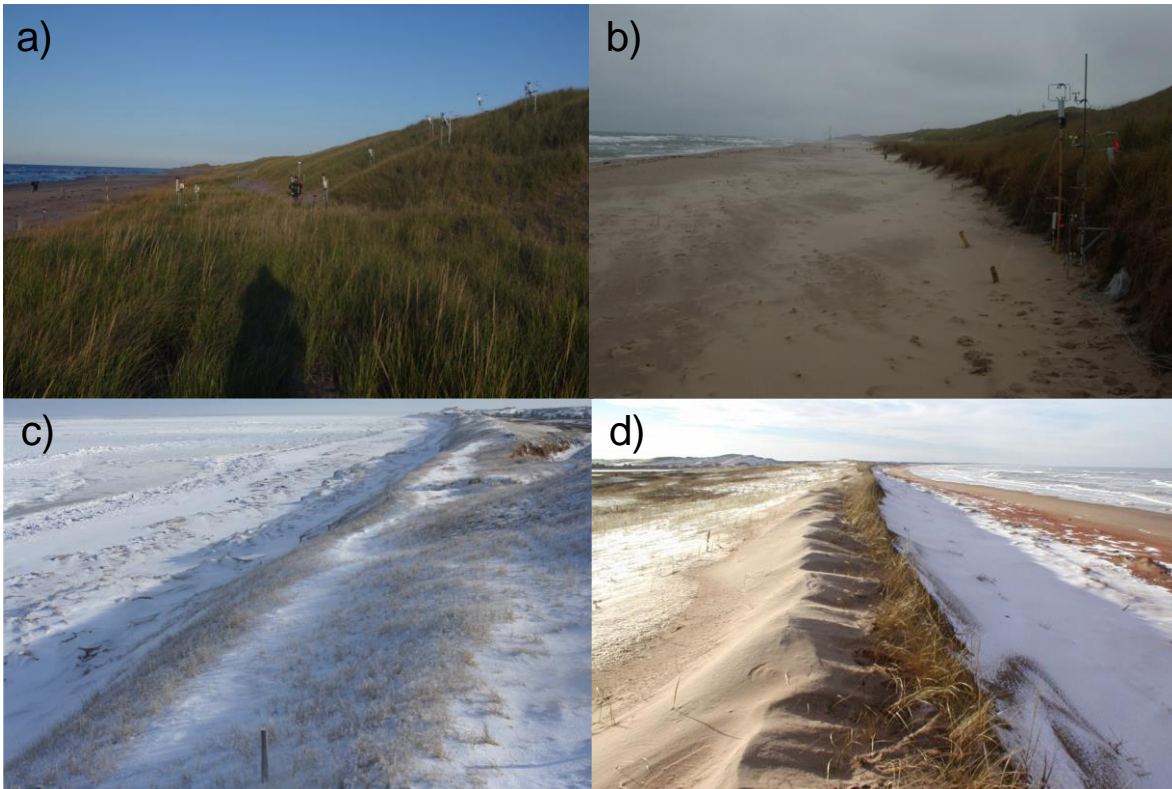
327

328 For the purposes of coastal erosion and dune dynamics monitoring for PCA, the study site
329 was divided into three reaches (Figure 1d, each described in section 5.2.2). Representative
330 profiles across the beach and foredune were established within each reach and surveyed
331 annually between 2002 and 2012 (Ollerhead et al., 2013). Net littoral sediment transport is
332 from E to W and there is evidence of about 100 m of westward progradation into the estuary
333 over the past 80 years with several small foredune ridges formed over this time (Mathew et al.,
334 2010). The littoral sediment budget is negative in Reach 1 with measured recession of the
335 foredune of 0.5-1.0 m a⁻¹ over the observation period. In contrast, the sediment budget in
336 Reach 2 transitions from negative to positive, with Line 7 having a neutral budget (Ollerhead et
337 al., 2013).

338 Plot scale field experiments were conducted in Reach 2 just west of Bowley Pond near Line
339 7 (Figs. 1d, 2a, b) to measure wind flow and sediment transport on the beach and foredune in
340 May-June 2002, October 2004, October 2007, and April-May 2010. Beach width at this location
341 was 30-40 m and sediments consisted of dominantly quartz sand with some feldspar with a
342 mean grain size of 0.26 mm.

343

344 **Figure 2:** Site photographs of the beach and foredune system at Greenwich Dunes, PEI. The
345 uppermost photos show the site for plot scale experiments in 2004 with a wide, vegetated
346 incipient dune a) before the arrival of Tropical Storm Nicole and during the storm in b) with a
347 visible eroded scarp at the foredune toe and active sand transport and deposition. Photo c)
348 shows shorefast ice, snow cover, and vegetation dieback typical of the winter season. Photo d)
349 illustrates distinct depositional lobes landward of the foredune crest that result from onshore
350 sand transport and deposition in the winter months.



351
352 **4. Plot scale**

353 For most of the 20th century, aeolian geomorphologists have worked within a paradigm of
354 steady, uniform flow for which (dry) sand flux is controlled mainly by the strength of the wind
355 under what is referred to as 'transport-limited' conditions. These conditions were replicated
356 well within wind tunnel experiments that dealt primarily with horizontal, uniform beds of
357 unimodal sediments, which also facilitated the development of theoretical models based on the

358 fundamental physics of saltation. Plot scale field experiments were often sited to minimize
359 topographic and surface complexity so as to conform to the paradigm. The development of
360 ultrasonic 2D and 3D anemometers and fast-response sediment sensors has allowed aeolian
361 geomorphologists to make high frequency measurements of turbulent wind flow and sand
362 transport, which has enabled a shift away from the steady-state paradigm toward consideration
363 of more natural conditions (e.g., Stout and Zobeck, 1997; Bauer et al., 1998; Sterk et al., 1998;
364 Davidson-Arnott et al., 2005; Walker, 2005; Bauer et al., 2013). The plot scale experiments at
365 PEI were specifically designed to explore the characteristics and effects of unsteady, non-
366 uniform flow together with spatial and temporal variations in topography and surface
367 characteristics.

368 This section provides a summary of research that was designed to characterize the complex
369 flow dynamics over the beach and foredune and related patterns of sand transport. A summary
370 and critique of traditional models of airflow dynamics and surface shear stress over low hills is
371 provided as a starting point. More comprehensive reviews of secondary flow dynamics over
372 dunes in general, and related semi-coherent flow structures over dunes, are provided by
373 Walker and Hesp (2013) and Bauer et al. (2013), respectively.

374 4.1 Airflow dynamics over the beach-dune profile

375 4.1.1 *Classic models of boundary layer flow over low hills*

376 Theory on boundary layer flows over flat surfaces were extended to low symmetrical hills
377 by climatologists (see Walker and Hesp, 2013), and seized upon by aeolian geomorphologists
378 interested in predicting sand transport over dunes (e.g., Howard et al., 1978; Walmsley et al.,

379 1982; Lancaster et al., 1996; Jensen and Zeman, 1985; Lancaster, 1985; Walmsley and Howard,
380 1985; Mulligan, 1988; Weng et al., 1991; Frank and Kocurek, 1996a; Wiggs et al., 1996b;
381 McKenna Neuman et al., 1997, 2000; Walker and Nickling, 2002). The Jackson and Hunt (JH)
382 model (Jackson and Hunt, 1975; Hunt et al., 1988) delineated 'inner' and 'outer' flow regions
383 that resulted from topographically-forced streamline perturbations. Outer flow in the JH model
384 is modified only by the pressure field, whereas within the inner region turbulent momentum
385 transfers and surface shear effects are also considered and create two sub-layers: i) the thin,
386 inner surface layer (ISL) where fluid shear is in equilibrium with surface roughness (i.e., the
387 constant stress region) and ii) the overlying shear stress layer (SSL) where shear effects
388 decrease with height until negligible. The JH model established a new theoretical framework for
389 understanding boundary layer flow dynamics, successfully characterizing: i) flow stagnation and
390 deceleration immediately upwind of hills and ii) flow acceleration or 'speed-up' on the
391 windward (stoss) slope.

392 Rasmussen (1989) was among the first to apply a modified version of the JH model to a
393 foredune. Due to varying roughness and slope transitions, he found that the depth of the ISL,
394 from which surface shear stress is derived, was very thin and therefore traditional velocity-
395 profiles measured using bulky instruments were of limited utility in estimating sand
396 transport. Similarly, Hesp (1983) and Arens et al. (1995) found that flow accelerations up the
397 windward slope deviated from those predicted by the JH model due to vegetation effects. They
398 also noted that, as winds became more oblique, the effective slope (i.e., aspect ratio) of the
399 dune decreased, reducing flow acceleration and the transport rate on the stoss slope. Arens et

400 al. (1995) noted a decline in sand flux up the stoss slope at a rate that was dependent on
401 incident wind speed. At slow speeds, the decline in sand flux was drastic, whereas at faster
402 speeds sand traveled farther inland because of turbulent suspension. This effect was
403 pronounced for steeper dunes and occurred despite changes in vegetation density.

404 These early studies revealed that the ability to simulate flow dynamics over foredunes
405 using climatological models was limited. Field experiments in the 1990s and 2000s also
406 showed that typical foredune terrain leads to flow separation and flow reversal, unlike flow
407 over a low hill (see Walker et al., 2006; Walker and Hesp, 2013). Empirical models of flow
408 behavior in the lee of transverse desert dunes also emerged (e.g., Sweet and Kocurek, 1990;
409 Frank and Kocurek, 1996; Wiggs et al., 1996; Walker and Nickling, 2002; 2003) and provided
410 new conceptual foundations upon which flow dynamics over more complex, vegetated dunes
411 could be understood.

412 *4.1.2 Advances in flow dynamics over complex dune terrain*

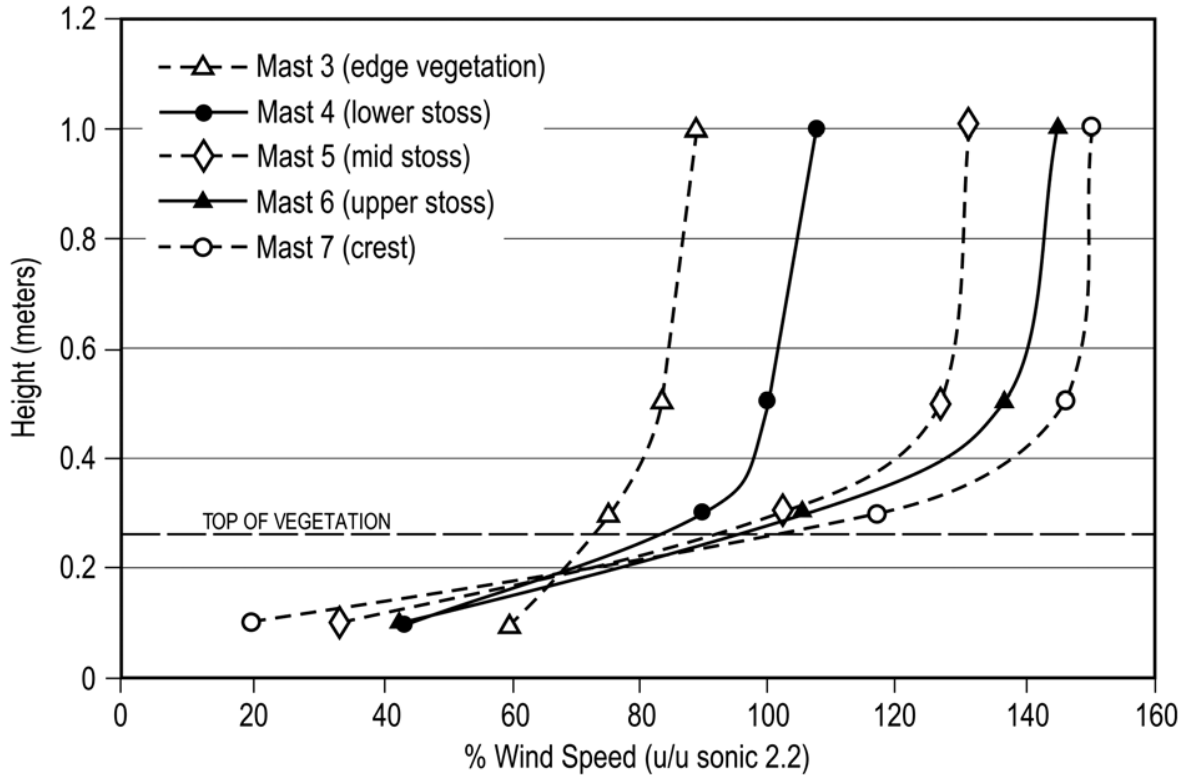
413 A vegetated foredune induces flow deceleration upwind of the dune toe, promoting
414 deposition of sand at the bottom of the dune slope (e.g., Arens, 1996a; Davidson-Arnott and
415 Law, 1996; Hesp, 1989; Sarre, 1989; Wal and McManus, 1993; Hesp, 2002). Beyond the
416 foredune toe and up the stoss slope, the protrusion of the foredune into the boundary layer
417 results in the compression of flow streamlines, increasing surface shear stress and wind speed
418 toward a maximum at the crest. Accordingly, non-log-linear velocity profiles are common (Fig.
419 3). This type of topographic forcing on flow speed and shear stress distributions over aeolian
420 dunes has been documented widely (see Walker and Hesp, 2013). The effect is most

421 pronounced with wind perpendicular to the crest line and decreases steadily as the wind
422 direction becomes more oblique (Hesp et al., 2005; 2015; Smyth and Hesp, 2015; Walker et al.,
423 2006; 2009b).

424 In the PEI plot scale research, conventional velocity profiles were measured as part of some
425 experiments (e.g., Hesp et al. 2009), although several drawbacks to this approach are
426 recognized. Conventional anemometers (rotating cups, propeller-fuselage, sonic anemometry)
427 are bulky compared to the shallow depth of the ISL. Thus, it is difficult to estimate shear stress
428 in the thin constant flux region (where the Law of the Wall applies). Some researchers have
429 measured velocity profiles that extend above the ISL (into the overlying SSL) as a proxy for
430 estimating shear stress over desert dunes (e.g., Mulligan, 1988; Lancaster et al., 1996; Wiggs et
431 al., 1996b). However, this often produces segmented and/or non-linear profiles (e.g., Bauer et
432 al., 1990; 1996; Hesp et al., 2005; 2013; see Fig. 3). Additionally, a vegetation canopy over the
433 foredune stoss slope imposes other limitations for applying boundary layer theory to estimate
434 surface shear stress. Thus, careful sampling and assessment of flow conditions within the near
435 surface zone is required if reliable sediment transport predictions are to be achieved (Bauer et
436 al., 2004). This remains difficult with existing instrument designs (Walker, 2005).

437

438 **Figure 3:** Percentage wind speed profiles up the PEI foredune stoss slope from an experiment in
 439 2002 (see Hesp et al. 2005; 2013). Speed observations at positions 3–7 are normalized against
 440 windspeed measured by a sonic anemometer at 2.2 m on a mast on the upper beach. Wind
 441 speed is topographically accelerated upslope above the vegetation, while within the vegetation,
 442 drag increases upslope and speeds decelerate.
 443



444
 445 The PEI experiments included measurements during flow conditions moderately above the
 446 threshold for sand transport in 2002 and substantially above threshold in 2004. In both studies,
 447 flow across the foredune was characterized by significant flow compression and
 448 acceleration. However, during the 2002 experiment a significant reduction in wind speed
 449 (deceleration) resulted over the foredune from enhanced drag exerted by the vegetation
 450 canopy as observed in other studies (e.g., Arens et al., 1995). During the gale event in 2004,
 451 there was a marked speed up above the vegetation, but also significant penetration of high-
 452 speed flow into the vegetation that, at times, produced sediment entrainment within the plant

453 canopy (Hesp et al., 2005, 2009; 2013; Walker et al., 2009; see Fig. 3). The vertical (W) velocity
454 component of the flow field was positive (upwards) across the stoss slope under slow wind
455 conditions but shifted to negative (downwards) during gale conditions. In addition, a jet
456 developed approximately 1 m above the vegetation canopy and extended from the upper stoss
457 slope to the foredune crest during the gale event (Hesp et al., 2009; 2013). Formation of jet
458 flow is common over distinct topographic breaks (e.g., Bowen and Lindley, 1977; Hsu, 1977,
459 1987; Tsoar et al., 1985; Arens, 1996a), but had not been observed on foredune stoss slopes
460 (Hesp and Smyth, 2016a). These two phenomena, flow speed up within the plant canopy and
461 jet flow development, are important for moving sediment to the lee of the dune during strong
462 wind events (e.g., Arens, 1996a; Peterson et al., 2011; Hesp et al., 2009; 2013; Hesp and Smyth,
463 2016a).

464 Tall grassy vegetation exerts significant aerodynamic roughness that likely varies with wind
465 speed as the plants flex downward and become more streamlined under extreme winds (e.g.,
466 Hesp et al., 2009). This dynamic behavior of the vegetation layer makes it difficult to
467 parameterize surface roughness as an aerodynamic roughness length (z_0) or with a
468 displacement height (d). This quandary is also a major limitation with current numerical
469 modelling approaches (Smyth, 2016). As a result, time-averaged and spatially coarse velocity
470 profiles over foredunes are likely inaccurate for characterizing the highly spatially and
471 temporally variable surface shear stresses that drive sand transport.

472 4.1.3 *New perspectives on turbulence and coherent flow structures*

473 Much work has been done recently to describe time-averaged conditions and turbulent
474 structures in flow over aeolian dunes (see Walker and Hesp, 2013) similar to earlier research in
475 rivers (e.g., McLean and Smith, 1986; Nelson and Smith, 1989; Bennett and Best, 1995; Venditti
476 and Bauer, 2005). Nevertheless, the relationship between turbulence intensity, Reynolds shear
477 stress ($RS = -\rho \overline{u' w'}$ where u' , w' are horizontal, vertical velocity fluctuations and ρ is fluid
478 density), and sand transport across aeolian dunes remained essentially unexplored until the
479 early 2000s following work on sand transport and turbulence over flat sand surfaces (e.g.,
480 Bauer et al., 1998; Sterk et al., 1998; Leenders et al., 2005; Baas, 2006).

481 Research over desert dunes and in wind tunnels demonstrated that RS at the toe of a dune
482 often exceeds time-averaged, streamwise shear stress ($\tau = \rho u_*^2$, where u_* is shear velocity
483 derived from velocity profiles) (e.g., Wiggs et al., 1996; Walker and Nickling, 2002; 2003;
484 Parsons et al., 2004; Baddock et al., 2011; Weaver and Wiggs, 2011; Smyth and Hesp, 2015).
485 Wiggs et al. (1996) argued that semi-coherent flow structures in the upwind boundary layer
486 were conveyed toward the bed at the dune toe by concave streamline curvature in this
487 region. These structures, which cause fluctuations in local RS, were thought to aid the
488 maintenance of grain transport across the beach and through the flow deceleration region at
489 the dune toe. Toward the dune crest, surface shear stress increases as a result of streamline
490 compression and flow acceleration, assisted by streamline convexity that suppresses vertical
491 motions and enhances horizontal fluctuations. These patterns of turbulence modification have
492 been documented in flow over desert dunes (see Wiggs et al. 1996; Walker and Nickling, 2002;

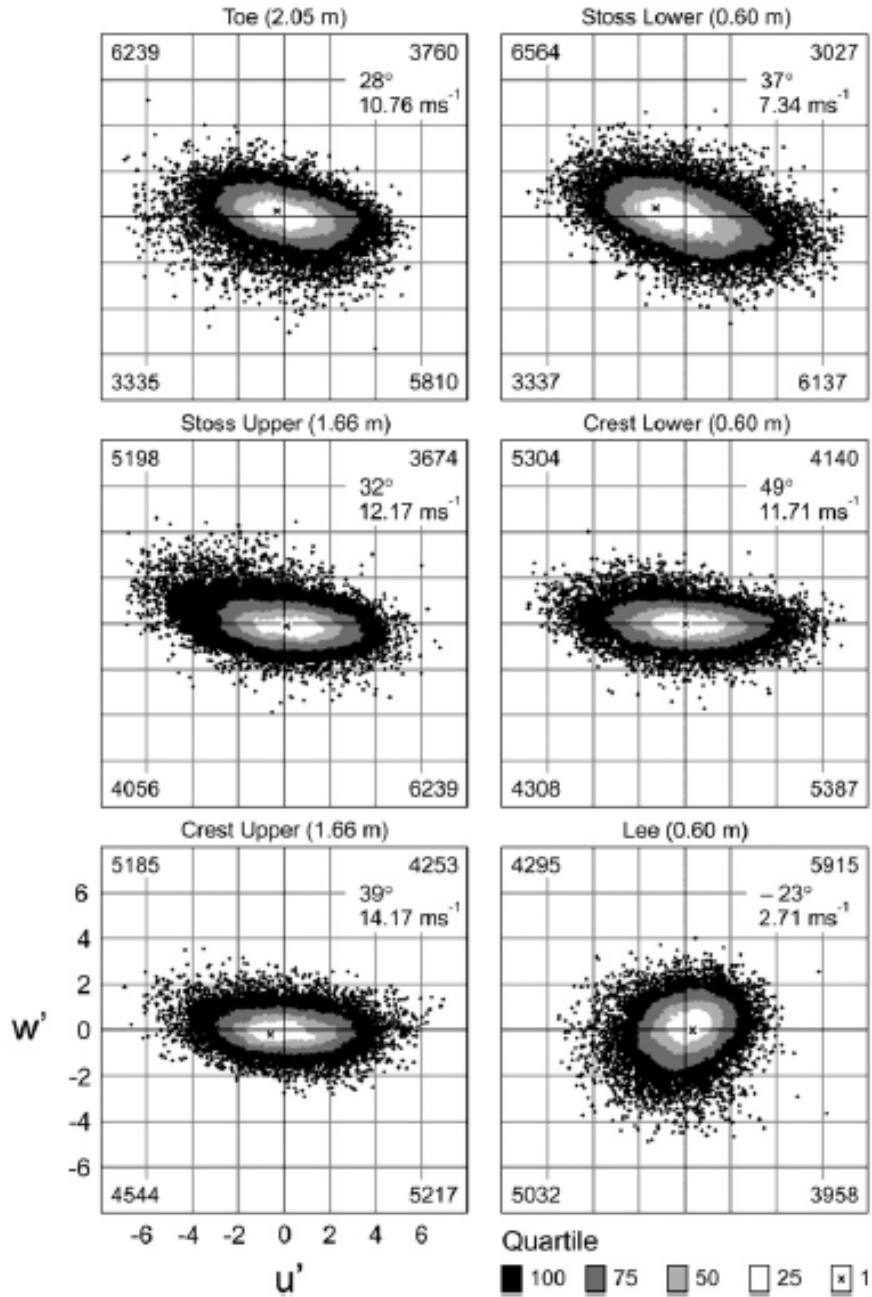
493 2003; Walker and Hesp, 2013) and over the foredunes at the PEI study site (Chapman et al.
494 2012; 2013).

495 Research in fluvial systems has shown that ejection and sweep events and larger macro-
496 structures (e.g., kolks, boils) are often associated with enhanced sediment entrainment and
497 transport via suspension (e.g., Jackson, 1976; Drake et al., 1988; Best, 1993; Robert et al., 1996;
498 Roy et al., 1996, 2004; Best and Kostachuk, 2002; Kostaschuk et al., 2008, 2009; Shugar et al.,
499 2010). However, few studies have focused on bed load transport, which is more comparable to
500 the saltation-dominated mode of transport over aeolian dunes (cf., Drake et al., 1988; Valyrakis
501 et al., 2010). Some of the experiments at PEI were dedicated to exploring the relationships
502 between turbulent stresses (including semi-coherent structures) and sediment transport
503 (Chapman et al. 2012; 2013) over foredunes using ultrasonic anemometry to acquire high-
504 frequency (1-32 Hz) measurements of 3D velocity vectors (U, V, W) at two sampling heights
505 across a transect extending from the upper beach to the lee of the dune crest. Sand transport
506 intensity was measured using Laser Particle Counters (LPCs) positioned at 0.014 m and
507 higher. Quadrant analysis was used to assess the distribution of quasi-instantaneous
508 components of the RS signals over the foredune as a means to interpret potential links between
509 fluid stress and resulting sand transport (Chapman et al., 2013).

510 Chapman et al. (2012) showed that the activity level in each of the four quadrants varied
511 with height and position across the beach-dune profile (Fig. 4). Q2 activity ($u' < 0, w' > 0$), which is
512 often associated with 'ejections', and Q4 activity ($u' > 0, w' < 0$), which is associated with 'sweeps',
513 generally dominated the turbulence structure over Q1 ($u' > 0, w' > 0$) and Q3 ($u' < 0, w' < 0$) activity,

514 which conform to 'outward' and 'inward' interactions, respectively. Such Q2-Q4 skew is a
515 characteristic signature of a turbulent boundary layer and was particularly evident across the
516 beach, dune toe, and lower stoss slope of the foredune. In contrast, as the dune crest is
517 approached, Q2 activity declines whereas Q1 becomes more dominant. The frequency of
518 ejection and sweep activity is reduced toward the crest. In the lee of the crest, where flow
519 separation occurs, the quadrant distributions were more symmetrical due to mixed, multi-
520 directional flow. In terms of correlations between quadrant signatures and sand transport,
521 Chapman et al., (2013) found that Q4 activity was most frequently associated with transport on
522 the beach (52%), foredune toe (60%), and stoss locations (100%), whereas Q1 activity was
523 dominant at the crest (25 to 86%), followed by Q4 (13 to 59%). Q3 activity appeared to be
524 largely irrelevant in terms of correlation with observed sand transport at any location.
525

526 **Figure 4:** Quasi-instantaneous (32 Hz) quadrant plots derived from a 10-minute Run at 1700 h
 527 on 11 October 2004 during a gale force event. Average incident flow angle and resultant speed
 528 for each location are shown in the top right. Quadrant counts (in each corner) represent the
 529 total number of observations (modified from Chapman et al. 2012: Fig. 10).



530
 531

532 Understanding the dominance of certain quadrants over others at varying positions across
533 the beach-dune profile provides insight into why there is generally a poor correlation between
534 sand transport and time-averaged RS, contrary to what might be expected across an extensive
535 horizontal sand surface. Specifically, fluid fluctuations that yield activity signatures in Q2 and
536 Q4 provide positive contributions to RS, whereas those in Q1 and Q3 are negative
537 contributions. If either couplet dominates the distribution (as with diagonally-skewed ellipsoids
538 shown in Fig. 4), there will be either positive or negative momentum transfer toward, or away
539 from, the bed, respectively. However, when the activity signatures are balanced (i.e., a circular
540 pattern), the positive and negative quantities balance each other in the time-averaged RS.
541 Thus, it is possible to have intense activity in Q1 and Q4, as we find at the dune crest, which
542 implies significant turbulent fluctuations in the streamwise (positive) direction, but poor
543 correlation with vertical fluctuations. This situation yields a small value of RS, despite
544 significant potential in the flow field to sustain sediment transport. As a result, the relationship
545 between sand transport and turbulence across beach-dune profiles is complex and cannot be
546 described well using RS alone (Chapman et al. 2013). Figure 5 presents a conceptual model that
547 summarizes these relations.

548 Other research has examined the distribution of Reynolds normal stresses (i.e., u'^2 , w'^2)
549 and turbulent kinetic energy (TKE) in flow over desert dunes (e.g., Baddock et al., 2011; Weaver
550 and Wiggs, 2011). Increasing evidence suggests that positive streamwise velocity fluctuations
551 are associated with the bulk of aeolian transport (e.g. Bauer et al., 1998; Sterk et al., 1998;
552 Schönfeldt and von Löwis, 2003; Leenders et al., 2005; Baddock et al., 2011; Weaver and Wiggs,

553 2011; Wiggs and Weaver, 2012). As such, the relationship between near-surface turbulence,
554 especially RS, and sand transport is not as straightforward as in traditional equations that relate
555 sand flux to surface stress directly and unambiguously.

556 *4.1.4 Advances in understanding topographic steering of near surface flow and sand transport*
557 *vectors*

558 Interaction of regional wind flow with surface topography results in deviations in the
559 magnitude and directionality of near-surface flow vectors - a phenomenon termed 'topographic
560 steering'. The mechanics of topographic steering are driven largely by pressure differences that
561 the flow field encounters along streamlines that traverse the dune toe (deceleration, positive
562 pressure gradient) and stoss slope (acceleration, negative pressure gradient). More in-depth
563 explanations of this mechanism are provided by Walker and Hesp (2013) and Hesp et al. (2015)
564 and references therein.

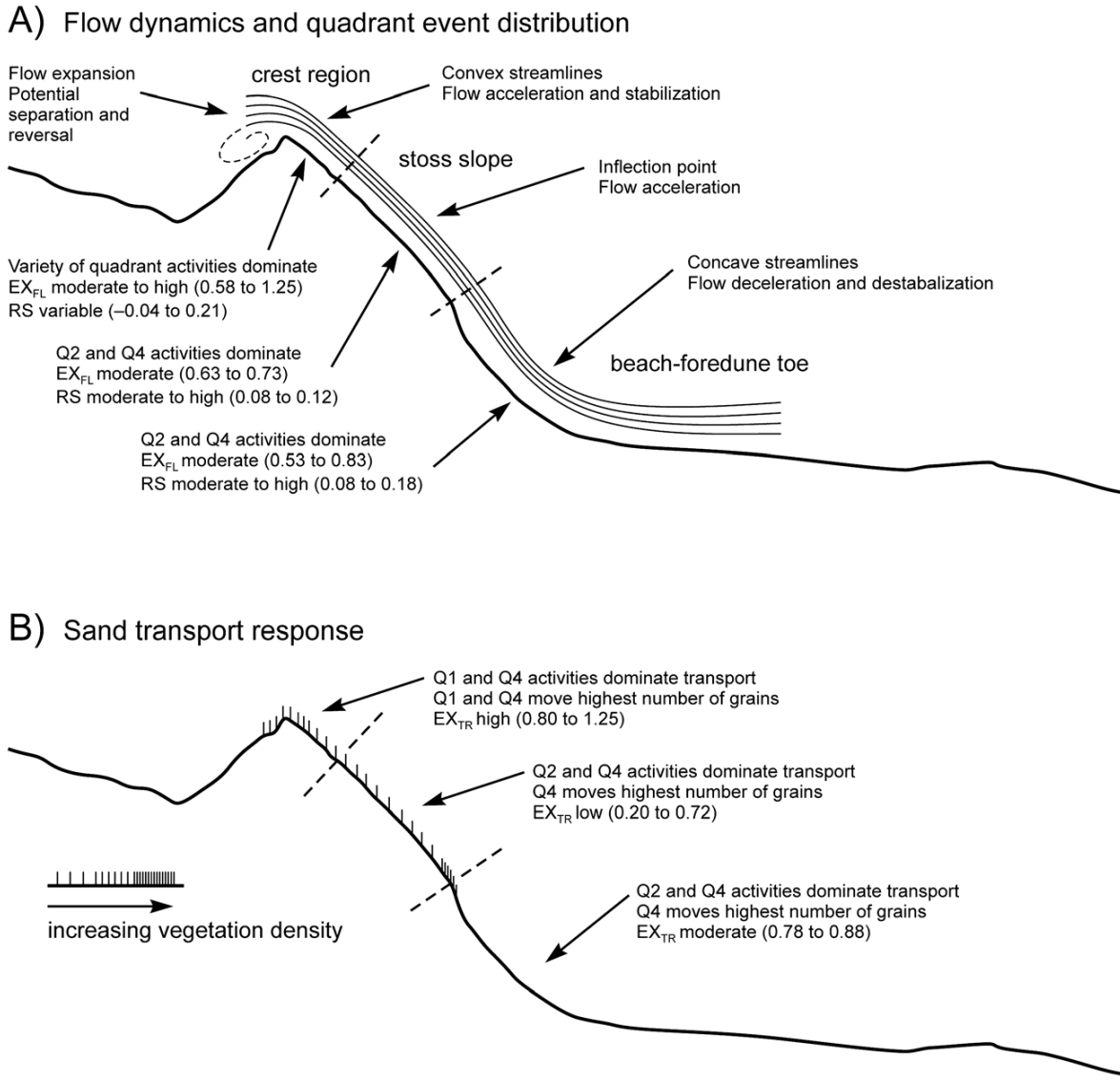
565 Early work on topographic steering over beaches and foredunes (e.g., Svasek and Terwindt,
566 1974; Bradley, 1983; Mikklesen, 1989; Rasmussen, 1989; Arens et al., 1995; Hesp and Pringle,
567 2001) demonstrated that winds approaching a foredune at an oblique angle tend to be
568 deflected toward crest-normal and that this effect is greatest when incident angles are
569 between 30° and 60° to the crestline. Highly oblique winds less than 30° to the foredune crest
570 (where 90° is directly on shore) are generally deflected parallel to the crestline. Recent research
571 at the PEI site (Walker et al., 2006, 2009a, b; Bauer et al., 2012; Hesp et al., 2015) and
572 elsewhere (e.g., Lynch et al., 2008; 2009; 2013; Jackson et al., 2011; Delgado-Fernandez et al.,
573 2013, Smyth et al., 2011, 2012), suggests a common set of flow responses over morphologically

574 simple foredunes. Bauer et al. (2012) presented a conceptual model (Fig. 7) of flow-form
575 interaction over foredunes for a variety of flow approach angles from onshore (crest-
576 perpendicular) through oblique, and offshore that also incorporates knowledge of resultant
577 sediment transport vectors (Bauer et al., 2015).

578 From these collective empirical results, it is now clear that topographic steering plays a
579 significant role in determining the near surface wind field and, consequently, the sediment
580 transport pathways across the beach-dune profile during onshore, oblique, and offshore
581 regional wind flows. To extend understanding beyond these empirical observations, a more
582 detailed computational fluid dynamics (CFD) simulation of flow over the PEI foredune (Hesp et
583 al., 2015) was conducted to simulate near-surface flow response in 10° increments from
584 onshore (0°) to alongshore (90°) wind approach angles. The results are summarized below into:
585 I) crest perpendicular winds – onshore and offshore; II) crest oblique winds – onshore and
586 offshore; and III) shore parallel winds.

587

588 **Figure 5:** Conceptual model showing observed streamline behaviour, flow dynamics, Reynolds
 589 stress (RS) quadrant event activity, and sand transport responses over a foredune. (Chapman et
 590 al. 2013: Fig. 7).
 591

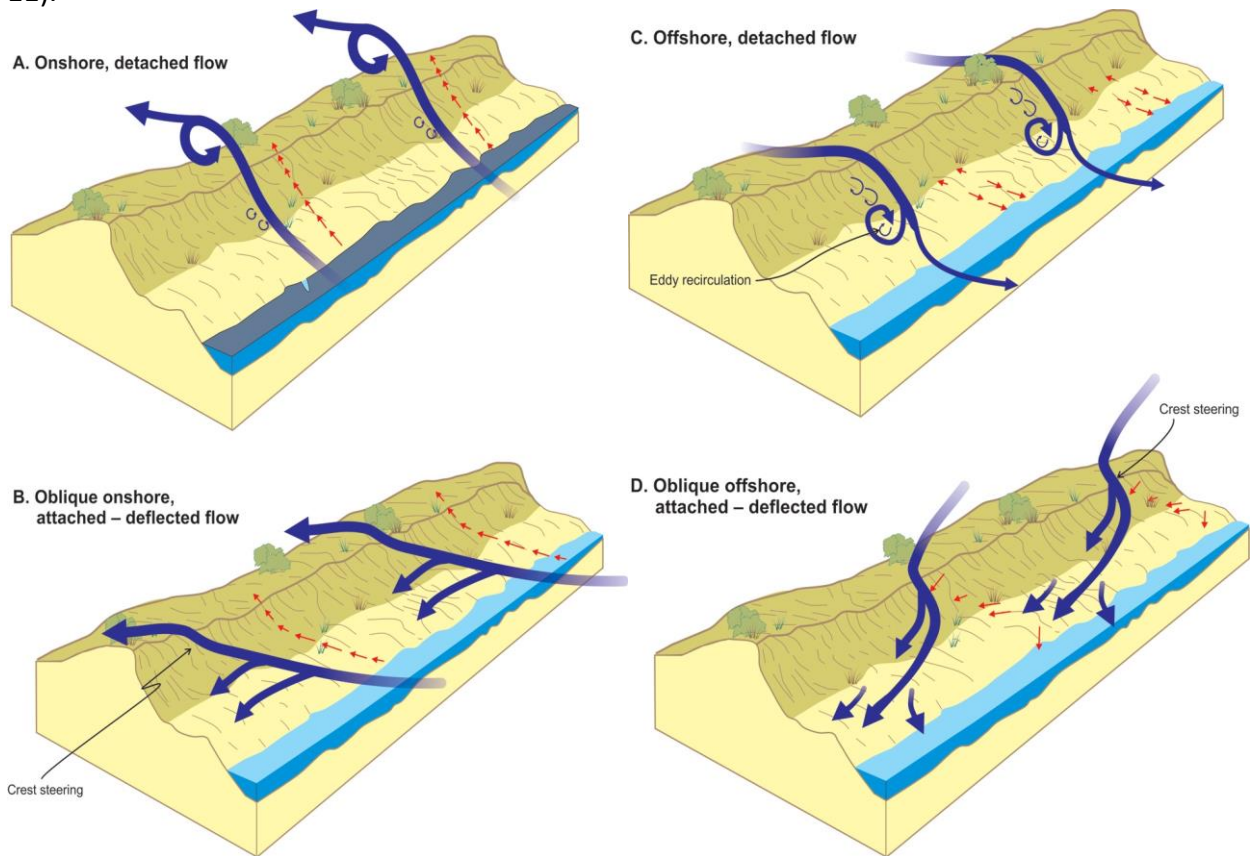


592

593

594

595 **Figure 6:** Conceptual model of flow–form interaction and topographic steering over a large
 596 foredune for variable wind approach directions. Large solid arrows correspond to near-surface
 597 wind flows and small arrows show likely sediment transport directions. (Bauer et al. 2012: Fig.
 598 11).



599

600

601 I. Crest perpendicular winds

602 Crest perpendicular winds are accelerated up the stoss (upwind) slope of the dune and, if
 603 the foredune ridge is sufficiently high and steep, flow detachment occurs at the crest. A

604 recirculation cell occupies the dune lee with a reattachment point located somewhere

605 downwind depending on dune height and topographical complexity. Flow reversals at the bed

606 are not uncommon (Fig. 6A and C) (e.g., Delgado-Fernandez et al., 2011; Jackson et al., 2011).

607 During offshore winds, when the beach is in the 'lee' of the foredune ridge, anemometers

608 located above the foredune crest and on tall beach towers record the regional (offshore) wind
609 flow, while those close to the surface show drastically reduced flow speed and often reversed
610 and highly variable wind directions, which are typical of lee side eddy circulation in general
611 (Walker and Nickling, 2002; Jackson et al., 2011; Delgado-Fernandez et al., 2013; Bauer et al.,
612 2012; 2015). The results of the PEI work on onshore and offshore flow conditions support
613 detailed findings of others in Northern Ireland (Lynch et al., 2009; 2010; 2013; Jackson et al.,
614 2011; Delgado-Fernandez et al., 2013) who documented distinct flow recirculation in the lee of
615 a large foredune during offshore winds. During strong winds from either onshore or offshore
616 directions, flow acceleration towards the crest can result in sand transport high enough above
617 the bed to be incorporated within and above the lee-side flow separation eddy and deposited
618 on the lower part of the downwind slope and beyond (Arens 1995; Peterson et al., 2011; Hesp
619 et al., 2013). During offshore winds, some sand may be entrained near the crest and
620 transported onto the upper seaward slope of the foredune, while on the beach, onshore
621 transport may occur both seaward and landward from the point of flow reattachment, thus
622 leading to a pronounced transport discontinuity (Bauer et al., 2012; 2015; Davidson-Arnott et
623 al., 2012).

624 ii. Oblique winds

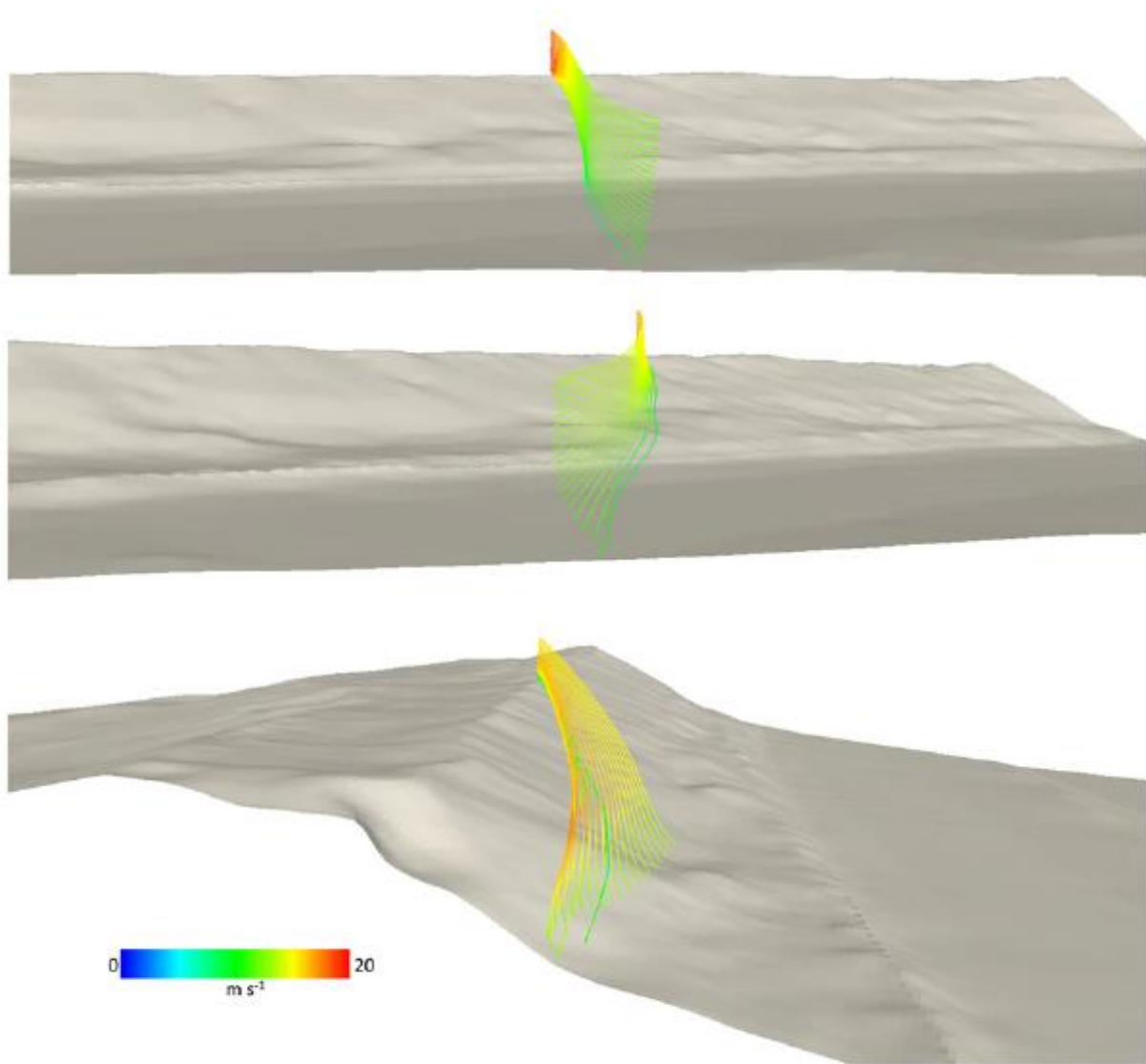
625 Winds approaching a foredune at an oblique angle are deflected toward crest-normal along
626 the stoss slope (Fig. 6B and D) (Walker et al., 2006; 2009b; Hesp et al., 2015). The degree of
627 deflection is dependent on incidence angle as well as height above the surface, with the most
628 pronounced steering near the surface and nearer to the crest where flow acceleration effects

629 are most prevalent (Arens et al., 1995; Mikkelsen, 1989; Walker et al. 2006; 2009b; Walker and
630 Shugar, 2013; Hesp et al., 2015). Significant onshore steering of near-surface flow vectors can
631 occur (as much as 37° from the incident wind as in Walker et al. 2009b), even during highly
632 oblique winds.

633 Figure 7 shows CFD-generated flow streamlines in near-surface boundary layer flow (from
634 0.66 to 2 m) over the PEI foredune and depicts the resulting degree of streamline deflection for
635 three incident wind approach directions (20°, 40° and 80°)(Hesp et al. 2015). The lowest
636 streamlines show the strongest response to topographic forcing and display the greatest degree
637 of deflection, similar to that observed empirically at the PEI site by Walker et al. (2006; 2009b).
638 Near-surface flow speed responses show that the greatest speed-up occurs for winds that are
639 most directly onshore when the dune has the steepest aspect ratio and then decreases as the
640 incident wind becomes increasingly oblique. For example, at 0.66 m above the bed the wind
641 speed at the foredune crest for incident wind directions from 50° to 30° to the crest is on
642 average 25% lower than for winds in the 30° to 0° range (Fig. 8). Beyond the crest, flow
643 separation occurs for onshore to moderately oblique winds and is manifest as a fairly simple
644 reversing roller vortex, as in Fig. 6A above and as captured in smoke visualization by Walker
645 (2005: Fig. 6). Flow separation and expansion results in notable flow deceleration leeward of
646 the crest, particularly closer to the surface (Fig. 8B). However, as the flow trends towards more
647 alongshore (from 50° to 70°), the degree of lee-side flow deceleration declines. This generally
648 reflects a change in the effective aspect ratio imposed by the dune, such that from onshore (0°)
649 to oblique-alongshore (~60°), incident winds still encounter a relatively steep and asymmetric

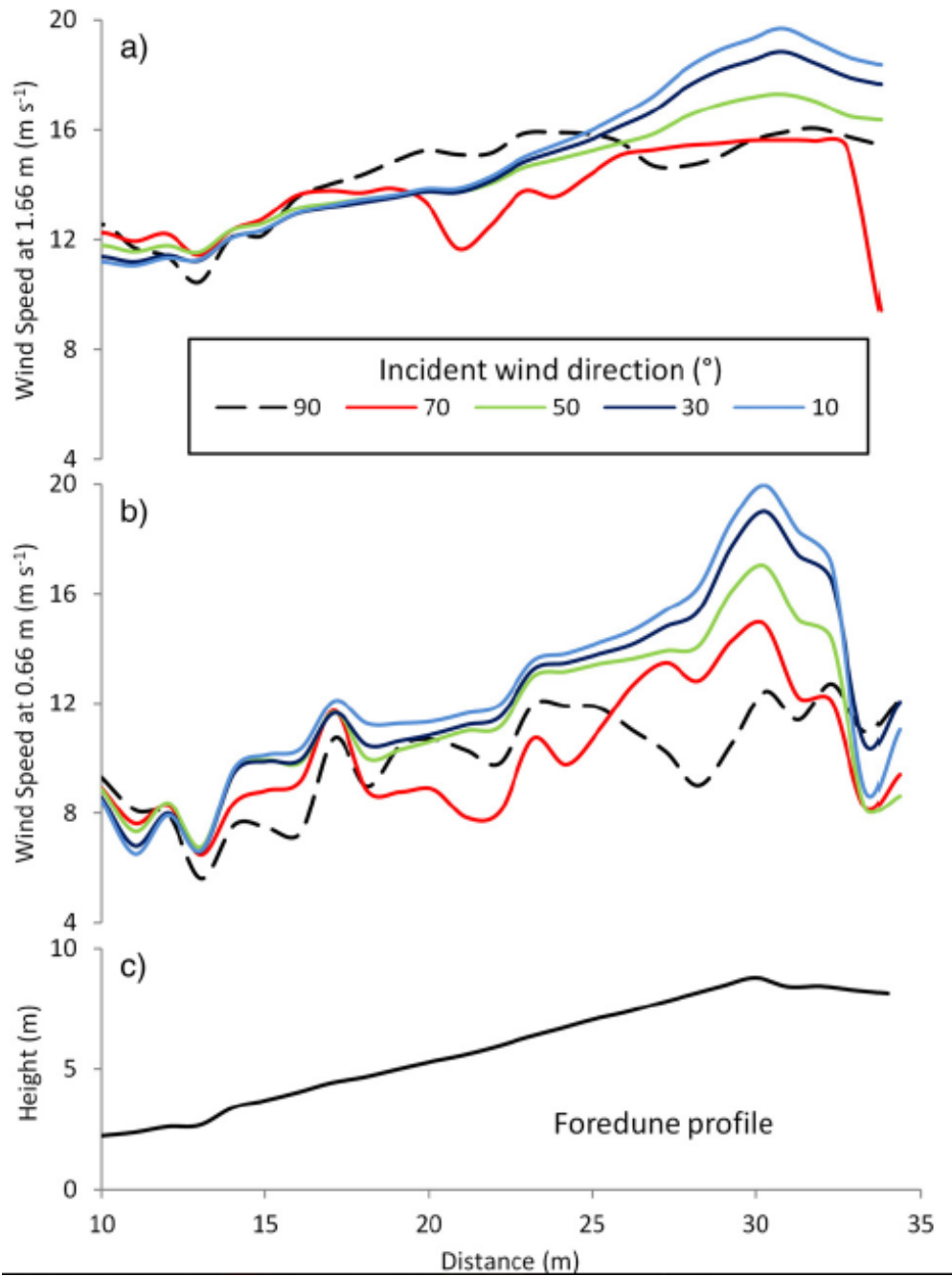
650 topography. Beyond this range, as the incident wind approaches crest-parallel, there is
651 significantly less topographic forcing due to the decline in dune aspect ratio, and little to no
652 flow separation in the lee, as evident in the markedly different surface velocity distribution.

653 **Figure 7:** Examples of topographic steering of lower boundary layer flow (0.66 to 2 m)
654 streamlines generated by a field-validated CFD simulation (Hesp et al., 2015) for three incident
655 wind approach directions: 20° (oblique-onshore, uppermost), 40° (oblique, middle) and 80°
656 (oblique-alongshore, lowermost). The lowest streamlines show the strongest response to
657 variations in surface morphological changes and display the greatest degree of deflection.
658 (Hesp et al. 2015: Fig. 8, reproduced with permission).
659



660
661

662 **Figure 8:** Near-surface wind speed responses generated by the CFD simulation of Hesp et al.
663 (2015) showing speeds at 1 m intervals across the foredune at heights of 1.66 m(a) and 0.66 m
664 (b) above the dune profile (c) for five incident wind directions. (Hesp et al. 2015: Fig. 7,
665 reproduced with permission).
666



667

668

669 III. Alongshore winds

670 As the incident wind becomes more oblique (i.e., alongshore), the reduction in mean wind
671 speed at the dune toe and the increase in wind speed toward the crest become less
672 pronounced due to the declining effects of flow stagnation and streamline compression over
673 the effectively less steep dune form (Arens et al. 1995; Parsons et al., 2004). Overall, there is
674 also less spatial variability in near-surface flow speed over the dune (Fig. 8), although this does
675 depend on the variability in surface morphology as well as **vegetation cover and distribution**.

676 The reduced flow acceleration effect over the dune for highly oblique flows can often result
677 in increased sand transport potential along the beach (vs. into the foredune). However, the
678 greater drag on wind flow over the vegetated surface of the lower stoss slope can also produce
679 rapid wind speed decreases and some topographic steering towards the foredune toe, which
680 may enhance sand transport from the upper beach onto the lower stoss slope. Transport
681 potential over the stoss slope also decreases as a consequence of vegetation-induced drag,
682 thereby creating a large disparity between sand transport on the stoss slope versus that on the
683 beach.

684 If the foredune is scarped as a result of storm wave erosion, flow deflection patterns may
685 be significantly different, than that for a non-scarped dune. Winds above the scarp may be
686 deflected onshore towards the crest (Hesp et al., 2013) while flow seaward of the scarp is
687 deflected along the beach during oblique and alongshore winds (Hesp and Smyth, 2016a),
688 which may aid in the development of a dune ramp that rebuilds the eroded region (see
689 Ollerhead et al., 2013).

690 The geomorphic implications of these flow deflection phenomena are important for several
691 reasons. First, oblique winds can transport sediment onto a foredune or away from it
692 depending on the angle of incident wind or the presence of a dune scarp, thereby affecting
693 sediment supply to the dune. Second, deflected surface winds can influence net transport
694 pathways and sedimentation patterns on the foredune, as has also been documented over
695 transverse desert dunes. Third, transport conditions on the beach may be decoupled from
696 those on the foredune at certain approach angles. Fourth, fetch distances and sand transport
697 pathways into, and over, foredunes may be greater or less than predicted depending on the
698 nature and magnitude of flow deflection. Finally, sedimentary strata may be deposited more
699 crest transverse than the regional wind regime would indicate, thereby confounding paleo-
700 environmental interpretations of relict dunes. Thus, assessments of landscape-scale dune
701 evolution using regional wind statistics from nearby weather stations or relict dune morphology
702 must also consider the confounding effects of topographic steering on near-surface flow
703 patterns and the overall foredune sediment budget (Hesp and Hyde, 1996; Walker et al., 2006).
704 In some settings (e.g., offshore oriented wind regimes), this may exert significant control on the
705 total sand supply to, and/or the distribution of sand within, the foredune system (Hesp, 2002;
706 and Davidson Arnott and Law, 1996; Walker et al. 2006; 2009a; 2009b; Lynch et al., 2009; 2010;
707 2013; Jackson et al., 2011; Bauer et al. 2012; Delgado-Fernandez et al., 2013), as discussed in
708 Section 5.

709 At the plot scale, the nature and degree of topographic forcing on near-surface flow
710 vectors is now conceptually understood and supported by rich empirical datasets and recent

711 CFD simulations (e.g., Parsons et al., 2004; Beyers et al., 2010; Jackson et al., 2011; Hesp et al.,
712 2015). Implementation of this understanding into predictive models remains a challenge.

713 *4.1.5 Innovative Computational Fluid Dynamics (CFD) modeling of flow over foredunes*

714 The development of robust CFD modeling has significantly advanced our understanding of
715 flow dynamics over dunes. Due to the logistical limitations of deploying field instrumentation to
716 measure wind flow over complex terrain (Walker, 2005), CFD simulations are being used
717 increasingly as a proxy and/or in conjunction with field measurements to accurately model
718 complex flow behavior over aeolian landforms (e.g., Parsons et al., 2004; Omidyeganeh et al.,
719 2013; Pelletier et al. 2015; Hesp et al., 2015; Hesp and Smyth, 2016a; Smyth, 2016).

720 CFD is a numerical method of solving fluid flow by converting the Navier-Stokes (N-S)
721 equations to algebraic equations and solving them iteratively within a gridded computational
722 domain of a study area. Unlike the Jackson and Hunt (1975) model, which solved the N-S
723 equations linearly, CFD is capable of solving complex turbulent flow using a range of methods.
724 The two most common approaches are Reynolds-Averaged Navier-Stokes (RANS) and Large
725 Eddy Simulation (LES). RANS separates velocity and pressure into mean and fluctuating
726 components, which are substituted into the original N-S equations producing a steady state
727 solution of the mean flow dynamics. Unsteady or transient RANS (URANS and TRANS
728 respectively) can also be calculated by retaining the unsteady terms, instead of averaging,
729 making the dependent variables not only a function of space but also of time. LES produces a
730 transient solution of flow dynamics by modelling smaller scale vortices, which are close to
731 homogenous, and simulating larger-scale turbulence, which largely depends on geometry and

732 boundary conditions. The locations in the mesh where the N-S equations are simulated (i.e.,
733 the N-S equations are solved) depends on the spatial resolution of the mesh and a spatial filter.
734 Where the cells are larger (smaller) than the filter, the flow is calculated exactly (modelled
735 using approximations).

736 Direct Numerical Simulation (DNS) of the N-S equations without any turbulence modelling
737 is also possible. However, the computational power required to solve all scales of turbulence
738 spatially and temporally makes the computational cost prohibitively expensive for use at high
739 Reynolds numbers over aeolian landforms. To date, most studies of wind flow over aeolian
740 landforms have been performed using RANS turbulence modelling, with the exception of
741 Jackson et al. (2011) who compared RANS, LES and a hybrid RANS-LES model with measured
742 data. In addition, Omidyeganeh et al. (2013) conducted an LES study of flow over a barchan
743 dune at a relatively high Reynolds number, more akin to flow conditions found in fluvial
744 environments. Building on this work, Pelletier et al. (2015) quantified turbulent shear stresses
745 that produce grain flows on the slip faces of aeolian barchan dunes. Smyth (2016) provides a
746 comprehensive review of recent progress in the use of CFD in aeolian research.

747 Despite recent advances, several limitations remain in CFD modelling of flow over aeolian
748 landforms (Smyth, 2016). Most notable for research on coastal dunes is the ability to
749 accurately model surface roughness imposed by vegetation. Vegetation drastically reduces
750 wind velocity and shearing force exerted near the surface, which causes sediment to be
751 deposited, which may over time result in increasing dune mass. In the majority of CFD codes,
752 vegetation is simply parameterized as a fixed, surface roughness length. This parameter limits

753 the vertical resolution of the computational domain, as the cell closest to the surface (where
754 the roughness element resides) must equal twice the aerodynamic roughness length. The
755 problem is compounded by the recommendations of Franke et al. (2004), who advise that at
756 least two cells must exist between the surface and the area of interest inside the computational
757 domain. This remains a key challenge in aeolian geomorphology as sediment transport is driven
758 by flow dynamics very close to the surface within the ISL (see section 4.1.1), yet roughness
759 lengths can extend to tens of centimetres within and through the ISL.

760 4.2 Instantaneous sediment transport across the beach-dune profile

761 4.2.1. *Classic ideas on equilibrium 'saturated' sand transport*

762 A great deal of effort has been devoted to understanding the detailed physics of aeolian
763 saltation, usually under ideal conditions such as dry, unimodal sand on a flat, extensive surface
764 without vegetation or moisture controls. Many aspects of saltation (e.g., grain-fluid
765 momentum transfer, impact cratering, boundary layer adjustments) have also been simulated
766 using complex analytical and numerical models (e.g., Bagnold, 1941; Anderson and Haff, 1991;
767 Durán and Herrmann, 2006; Kok and Renno, 2009) but, in general, there is a presumption that
768 the transport rate is in steady-state equilibrium with the wind. This has been referred to as the
769 'saturated' flux condition (Sauermann et al., 2001). In parallel, a large number of empirical
770 studies have tested the performance of the basic predictive relations under natural field
771 situations, with often disappointing performance. In early experiments, sand transport was
772 measured with integrating traps over periods of 10-20 minutes and compared to values of u_*
773 derived from the wind profile. Measured flux rates in the field were often much less than the

774 maximum theoretical rate predicted for saturated sand transport (e.g., Sarre, 1988; Bauer et al.,
775 1990; Sherman et al., 1998; Sherman et al., 2011). Sherman and Hotta (1990) summarized how
776 the basic transport equations have been modified to accommodate the influence (usually
777 singly) of supply-limiting factors such as surface moisture, binding salts, topographic slope, and
778 sediment texture, which tend to reduce the maximum transport rate below that from standard
779 models (see review in Ellis and Sherman, 2013).

780 In the 1990s, a number of fast response sensors for high frequency measurement of sand
781 transport were developed and tested in the field, including: acoustic impact sensors (Spaan and
782 van den Abeele, 1991; Arens, 1996; Ellis et al., 2009); piezoelectric impact sensors (Stockton
783 and Gillette, 1990; Stout and Zobeck, 1997; Baas, 2004); and electronic balance traps (Jackson,
784 1996; Bauer and Namikas, 1998; McKenna Neuman et al., 2000). These sensors have permitted
785 field measurements of “instantaneous” sediment transport in combination with high frequency
786 measurements of wind flow. As a consequence, greater insight has been gained into the links
787 between wind turbulence and the resulting characteristics of aeolian transport, including
788 transport intermittency (e.g., Davidson-Arnott and Bauer, 2009; Davidson-Arnott et al., 2009;
789 Davidson-Arnott et al., 2012) and the event-based nature of saltation (e.g., “flurry”
790 characterization per Bauer and Davidson-Arnott, 2014). Advances in the ability to measure
791 surface moisture content have also enabled improved understanding of non-saturated flux
792 related to supply-limited conditions (e.g., Yang and Davidson-Arnott, 2005; Davidson-Arnott et
793 al., 2008; Bauer et al., 2009; Darke et al., 2009; Delgado-Fernandez et al., 2009).

794 4.2.2. *Improved understanding of the fetch effect on beaches and sand delivery to*
795 *foredunes*

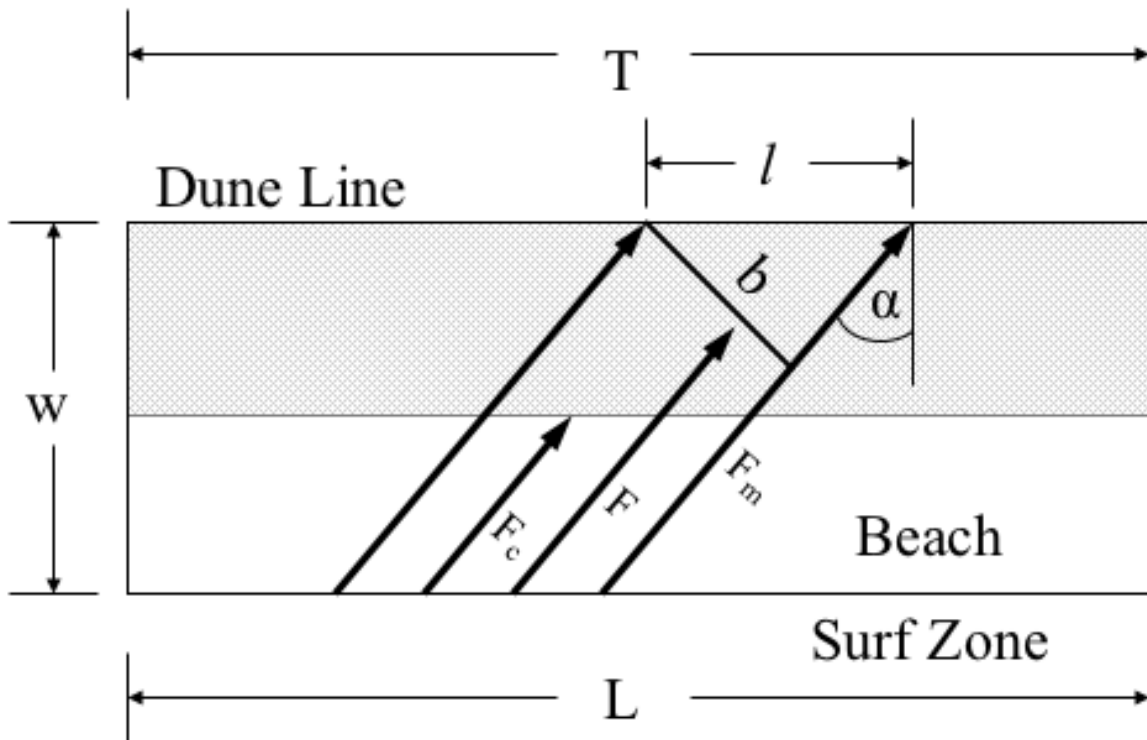
796 Increasing evidence collected from field studies from the 1970s to the 1990s identified a
797 persistent mismatch between measured and predicted transport rates on beaches (e.g., Svasek
798 and Terwindt, 1974; Sarre, 1988; Bauer et al., 1990; Davidson-Arnott and Law, 1990; Nordstrom
799 and Jackson, 1992; 1993). This compelled aeolian geomorphologists working on coasts to
800 contemplate the ways in which the beach-dune environment is different from desert surfaces
801 and wind-tunnel simulations. A primary factor involves the complexities of flow-transport
802 interactions from open water to sandy beach to foredune (Sherman and Bauer, 1993; Hesp and
803 Smyth, 2016b) that generates complex boundary layer adjustments, as well as specific
804 constraints on sediment transport imposed by the 'fetch' effect (Gillette et al., 1996; Bauer and
805 Davidson-Arnott, 2003; Delgado-Fernandez, 2010). Wind tunnel studies with dry, uniform sand
806 showed that the distance downwind from a sediment source boundary required for the
807 saltation cascade to achieve a constant transport rate (i.e., 'saturated' transport) was only a few
808 metres (e.g., Nickling, 1988; Shao and Raupach, 1992; Dong et al., 2004), although this may
809 depend somewhat on working section length, height and flow speed (Dong et al., 2004).
810 However, it has long been recognized for agricultural fields that, where some form of supply-
811 limiting factor exists, this distance can be significantly longer (Chepil and Milne, 1939). Coastal
812 geomorphologists began exploring how important the fetch effect was for reconciling
813 differences between measured and predicted transport rates across beaches, especially on the
814 foreshore and lower beach (e.g., Svasek and Terwindt, 1974; Davidson-Arnott and Law, 1990;

815 Bauer et al., 1990). Just as there is a time lag or period of adjustment between the response of
816 the saltation layer to a change in wind speed (e.g., Butterfield, 1999), there is a corresponding
817 spatial distance over which such process-response adjustments occur (e.g., Shao and Raupach,
818 1992). The downwind distance that is required to achieve equilibrium transport via the
819 saltation cascade is referred to as the 'critical fetch distance' (F_c). If one measures sediment
820 transport downwind of F_c , then it is reasonable to expect that an equilibrium model (e.g.,
821 Bagnold, 1941) could be applicable. Within the fetch-limited zone ($F < F_c$), however, measured
822 transport will always be less than that predicted by equilibrium-type models.

823 Figure 9 depicts the conceptual model of Bauer and Davidson-Arnott (2003), wherein the
824 influence of fetch on sand supply to a foredune is characterized geometrically as a function of
825 beach geometry (w/L) and incident flow angle (α). The model identifies the region landward
826 (downwind) of F_c where sediment transport rate reaches a maximum (equilibrium flux) state,
827 which, in turn, governs total transport into the foredune. Figure 10 shows various simulations
828 that depict the magnitude of normalized specific sediment transport (relative to maximum rate
829 per unit width) for a 1:1 ($w:L$) beach form for three different wind angles ($\alpha = 0^\circ, 20^\circ, 45^\circ$) and
830 three fetch ratios ($F_c/w = 0.2, 1.0, 1.3$). Essentially, the simulations reveal that F_c exerts an
831 important control on the amount of sand delivery to the foredune, but the proportion of
832 sediment delivered to the dune, relative to the amount eroded from the beach, is influenced
833 dominantly by angle of wind approach, not fetch. When angle of wind approach becomes more
834 oblique, the downwind portion of the beach closest to the dunes experiences enhanced sand
835 transport rates (ultimately reaching the equilibrium potential rate), however, the total amount

836 of sediment supplied to the foredune actually decreases relative to that during shore-normal
837 conditions as most of the sediment is lost to the downwind margin of the beach.

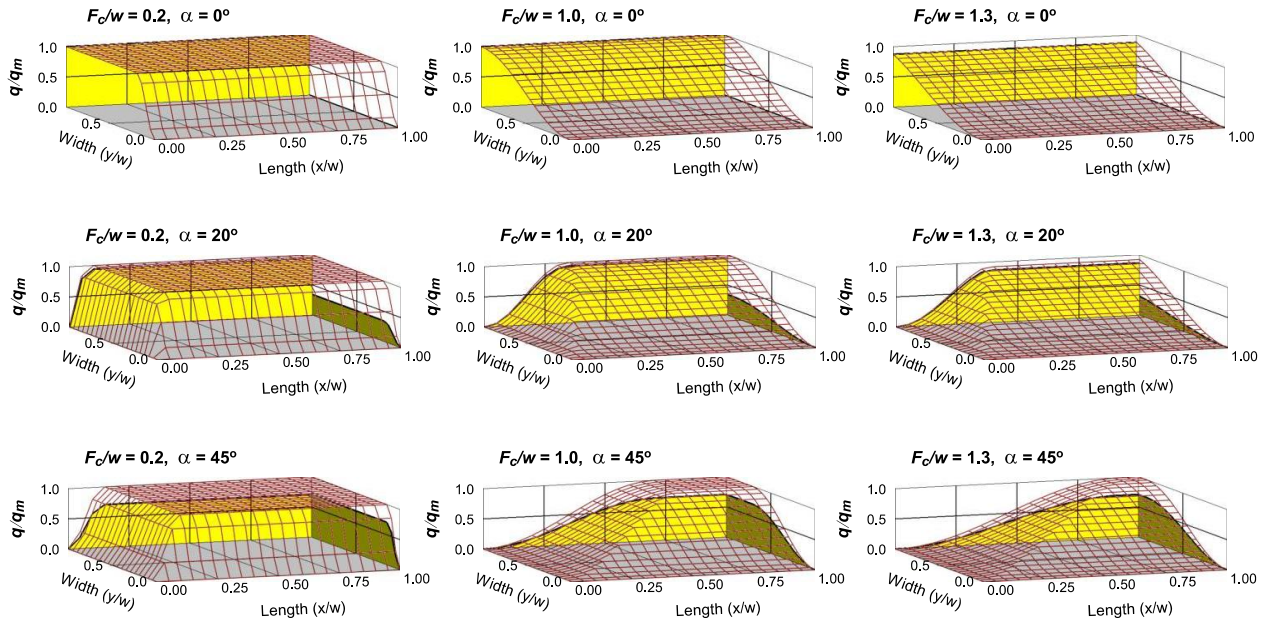
838 **Figure 9:** Conceptual model of Bauer and Davidson-Arnott (2003: Fig. 4) characterizing the fetch
839 effect on a rectangular beach of length, L , and width, w . The beach is defined as the zone of dry
840 sand between the limit of wave swash and the dune toe (limit of dune vegetation or significant
841 break in slope). Critical fetch length, F_c , is the distance for aeolian sand transport to reach its
842 maximum value (equilibrium flux rate). The shaded zone is the region where maximum values
843 exist, as determined by wind speed, incident wind approach angle, α , and sediment size. F_m is
844 maximum fetch resulting from the relationship between beach width relative to shore normal.
845 Distance l represents a unit of alongshore length at the dune toe mapped out by two parallel
846 streamlines of the wind field separated by perpendicular distance, b , such that $b = l (\cos \alpha)$. T
847 represents a total transport line, or alongshore length of a line parallel to the dune toe that will
848 receive sand transported from the beach for a given wind angle, α .



849

850

851 **Figure 10:** Distribution of normalized specific sediment transport (relative to maximum rate per
 852 per unit width) over a beach with geometry $w/L = 1.0$ for a combination of three wind angles ($\alpha =$
 853 $0^\circ, 20^\circ, 45^\circ$) and three fetch ratios ($F_c/w=0.2, 1.0, 1.3$) simulated by Bauer and Davidson-Arnott
 854 (2003: Fig. 9) based on the conceptual model presented in Fig. 9. The mesh grid shows
 855 magnitude of normalized specific transport parallel to the wind vectors and shaded portions of
 856 the axis planes indicate magnitude of transport across dune line or downwind margin of beach
 857 (as controlled by the $\cos \alpha$ effect). Zones of net transport and erosion on the beach correspond
 858 to level and sloping regions of the mesh grid, respectively, where steeply sloping regions
 859 indicate intense erosion.



860

861

862

4.2.3. Advances in understanding of fetch and moisture interactions on beaches

863

In addition to the fetch effect, there are a host of other confounding natural factors that

864

limit our ability to predict accurately the amount of sediment transport from beaches into

865

foredunes. It is well known, for example, that increased surface moisture reduces the

866

maximum rate of sand transport across a beach (e.g., Namikas and Sherman, 1995, McKenna

867

Neuman and Langston, 2006; Davidson-Arnott et al., 2008; Edwards et al., 2012). It is also

868

known that sand transport does not shut down completely during intense rain events, provided

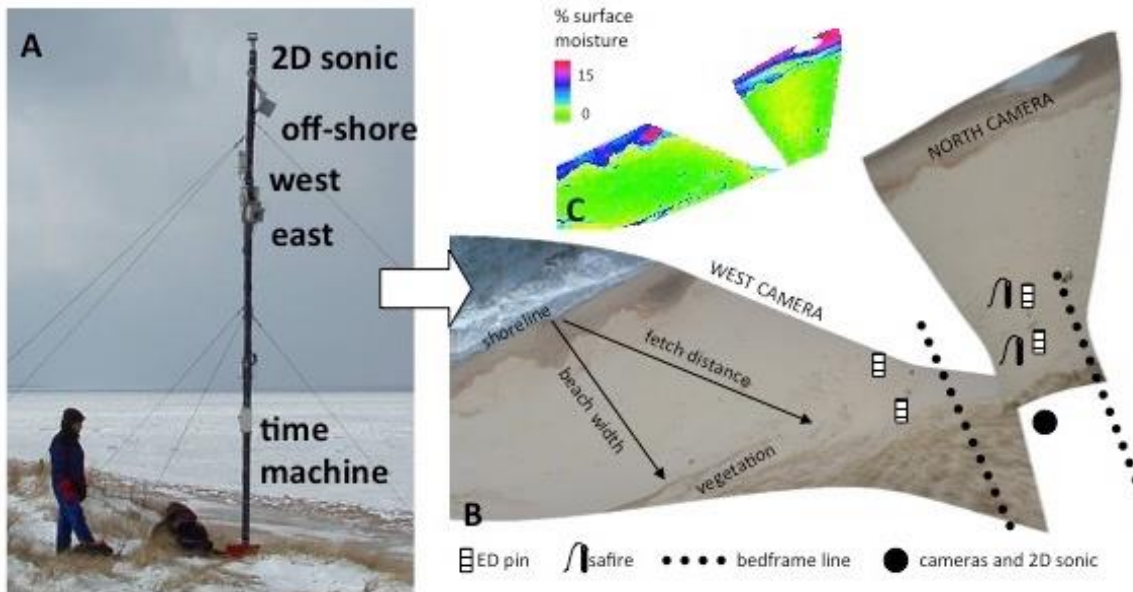
869 there is sufficient wind speed (e.g., Jackson and Nordstrom, 1998; McKenna Neuman and Scott,
870 1998; Hesp et al., 2009; Rotnicka, 2013). Wet portions of a beach, (e.g., foreshore,
871 groundwater emergence zones) are subject to greater transport intermittency and spatial
872 variability (e.g., Davidson-Arnott et al., 2005, 2008; Davidson-Arnott and Bauer, 2009), with the
873 result that the critical fetch distance, F_c , will increase with increasing surface moisture
874 (Davidson-Arnott and Dawson, 2001). All other factors equal, foredunes fronted by typically
875 dry (wet) beaches will experience enhanced (reduced) sediment delivery and dune
876 growth. Similar increases in F_c can be expected for other supply-limiting conditions such as the
877 presence of pebbles or flotsam (e.g., de Vries et al., 2014).

878 Until recently, surface moisture measurement in the field was estimated gravimetrically by
879 taking field samples to the laboratory – a tedious and time-consuming process. The Theta Probe
880 impedance sensor was initially tested on beach surfaces by Atherton et al. (2001) and Wiggs et
881 al. (2004), and this approach permitted rapid determination of average moisture at a sampling
882 point over a depth of 0.1 m. Yang and Davidson-Arnott (2005) demonstrated that the probe
883 length could be reduced to 0.02 m without significant loss in accuracy, thus permitting
884 measurements that were much more representative of the forces related to moisture content
885 very near the surface that constrain grain entrainment. Further evaluation of these instruments
886 was done by Edwards and Namikas (2009) and Edwards et al. (2012). Rapid changes in surface
887 elevation due to erosion and deposition in beach and foredune environments makes it difficult
888 to deploy impedance sensors over long periods by simply embedding the instrument in the

889 sand. Thus, repetitive sampling is required, with the prospect of unduly affecting the surface
890 conditions.

891 An alternate near-field remote sensing approach based on surface brightness signatures
892 from digital photographs has also been used to measure surface moisture (e.g., McKenna
893 Neuman and Langston, 2006; Darke and McKenna Neuman, 2008). This method was applied to
894 oblique photographs taken from cameras mounted on a tower on the dune crest at the PEI site
895 (Fig. 11), thus providing coverage of an area on the order of 100 m² (Darke et al., 2009) and for
896 a period of several months (Delgado-Fernandez et al., 2009; see section 5.1.2). Ortho-
897 rectification and incorporation of these photos into a GIS facilitated the mapping of a number
898 of other variables, in addition to moisture, on a regular basis (Delgado Fernandez and Davidson-
899 Arnott, 2011; Delgado-Fernandez et al., 2012).

900 **Figure 11:** Components of the PEI long-term monitoring station located at the crest of the
901 foredune (A). A 2D sonic anemometer was located at the top of a 5-m mast, with three digital
902 SLR cameras below to take oblique, overlapping colour photographs of the beach and foredune
903 toe region for ortho-rectification (B), and moisture mapping (C). Modified from Delgado
904 Fernandez and Davidson-Arnott (2011: Fig. 2) and Delgado-Fernandez et al. (2009).



905

906 The control on aeolian transport imposed by surface moisture is ordinarily thought of as
907 either a spatial phenomenon (i.e., zones or patches of wet or dry sand) or a temporal
908 phenomenon (i.e., increasing moisture during storms and subsequent drying via
909 evaporation). However, surface moisture exerts a supply-limiting control on aeolian sediment
910 transport on beaches that varies in both space and time coincidentally. Indeed, the moisture
911 state of a beach surface will often interact with the fetch effect to yield very complex process-
912 response feedback loops (e.g., Nordstrom and Jackson, 1992; 1993; Bauer et al., 2009).

913 Consider the scenario of a wide beach that has experienced uniform surface drying via
914 solar radiation for several hours and sand at the surface retains a moisture content of about
915 4%. A short-lived, onshore wind event begins that has the capacity to entrain sediment from
916 the dry surface layer. Sediment stripped from the upper foreshore is transported to the
917 foredune toe and deposited. As there is no supply of dry sediment to the foreshore from
918 upwind, progressive erosion of the surface layer exposes wetter sediments beneath that are
919 increasingly more difficult to entrain. As a consequence, the critical fetch distance, F_c , required
920 for sand transport to reach its maximum (equilibrium) flux rate is effectively lengthened and
921 the equilibrium transport zone fronting the foredune becomes narrower (see Fig.
922 10). Eventually, the berm and lower beach are stripped of dry sediment, exposing more closely
923 packed, moist sediments, which further extends the F_c . In contrast, the upper beach and
924 foredune toe are zones of deposition, comprised of newly delivered sediment that is dry and
925 unconsolidated. The outcome of this scenario is that the system progresses from an initial
926 beach surface with uniform moisture conditions to one with distinct zones of erosion,

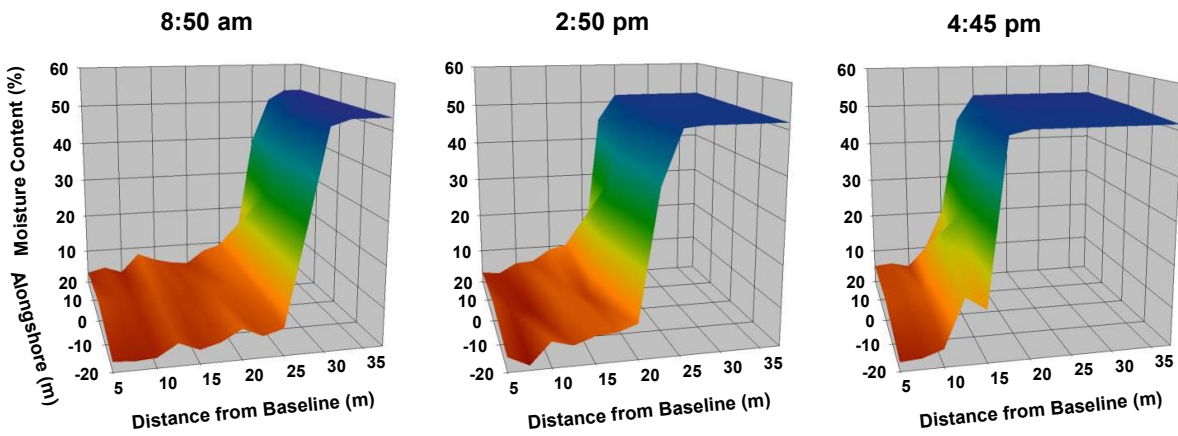
927 transportation, or deposition, in response to aeolian transport alone and without any changes
928 other meteorological or tidal conditions that control the moisture state of the beach. Delgado-
929 Fernandez (2010) and Delgado-Fernandez et al. (2012) describe field measurements consistent
930 with these trends.

931 A different scenario is presented in Figure 12, which shows surface moisture conditions
932 across the beach at the PEI site over an 8-hr interval (see Bauer et al., 2009). In the morning
933 (0850 h), the upper beach was relatively wide and dry, with moisture contents ranging from 2-
934 4% at the top of the beach, 4-6 % in the mid-beach, and saturated conditions in the foreshore
935 zone from wave run-up. Moisture contents over the beach decreased slightly as the sun rose
936 then increased with increasing wind speed and spray from wave breaking. As described below,
937 because of drying of the surface layer by wind, low transport activity occurred occasionally
938 even from areas that had 6% moisture or greater as a result of a relatively wide fetch zone.

939 During the day, wind speed increased progressively and, by 1000 h, sand transport was
940 active across the entire beach except on the lower foreshore. Wind direction also shifted from
941 essentially alongshore in the early morning to obliquely onshore by late morning. Despite a
942 relatively narrow beach (< 20 m wide at 1200 h), sand transport across the upper beach
943 remained active because of the oblique angle of wind approach, creating an effective fetch
944 length > 80 m. By 1450 h, a combination of enhanced wave set-up, run-up, and rising tide
945 caused the lower half the beach to become saturated and, by 1645 h, almost the entire beach
946 except a 5-m strip in front of the foredune was either totally or periodically inundated. So,
947 even though the wind field was competent to transport sediment, aeolian activity was inhibited

948 by excess surface moisture across most of the beach. These types of complex interactions on
949 beach-dune systems that involve changes in fetch distance that result from the interaction of
950 wind angle, wind speed, wave set-up, tidal excursions, and rainfall, and, in turn, they can have
951 significant implications for modelling sand supply to the foredune over a period of months to
952 years (see section 5.2.3)

953 **Figure 12:** Surface moisture contents across the beach at the PEI study site from the foredune
954 toe (baseline origin) to lower foreshore over an 8-hr interval during which wind speeds
955 increased above transport threshold by 1000h and wind direction shifted from alongshore to
956 obliquely onshore by late morning.



957

958 4.2.4. Exploring wind unsteadiness, transport response, and intermittency

959 Natural winds tend to be unsteady rather than constant, adding another level of
960 complexity to sediment transport processes at the plot scale. Rather than a constant state of
961 maximum flux, there is a semi-continuous state of disequilibrium between the time-varying
962 nature of the wind and the phase-lagged response of the saltation system (Butterfield, 1991,
963 Spies et al., 2000). This disequilibrium is most pronounced when wind speed fluctuates above
964 and below the entrainment threshold, leading to discontinuous and constantly varying rates of
965 sand transport. Stout and Zobeck (1997) proposed an 'intermittency' parameter that

966 characterizes the degree of transport continuity as a function of the number of data points in a
967 measurement period during which active transport occurs, expressed as a fraction of the total
968 number of data points in the period. A time series with continuous transport, during which
969 wind speed is consistently above the entrainment threshold, will have an intermittency value of
970 1, whereas a value of 0 indicates no transport. Davidson-Arnott et al. (2012) recommended
971 adoption of an 'activity parameter' (AP) rather than 'intermittency parameter' (IP) per Stout and
972 Zobeck (1997) because a large value for AP (or IP) indicates a very active transport system with
973 minimal intermittency (taken literally). It should be noted, that while the AP (or IP) is a fairly
974 simple concept, differences in the sampling effectiveness of different sensors make comparison
975 of AP values derived between sensors and studies difficult (Baas, 2005; Davidson-Arnott et al.
976 2009; Barchyn and Hugenholtz, 2010).

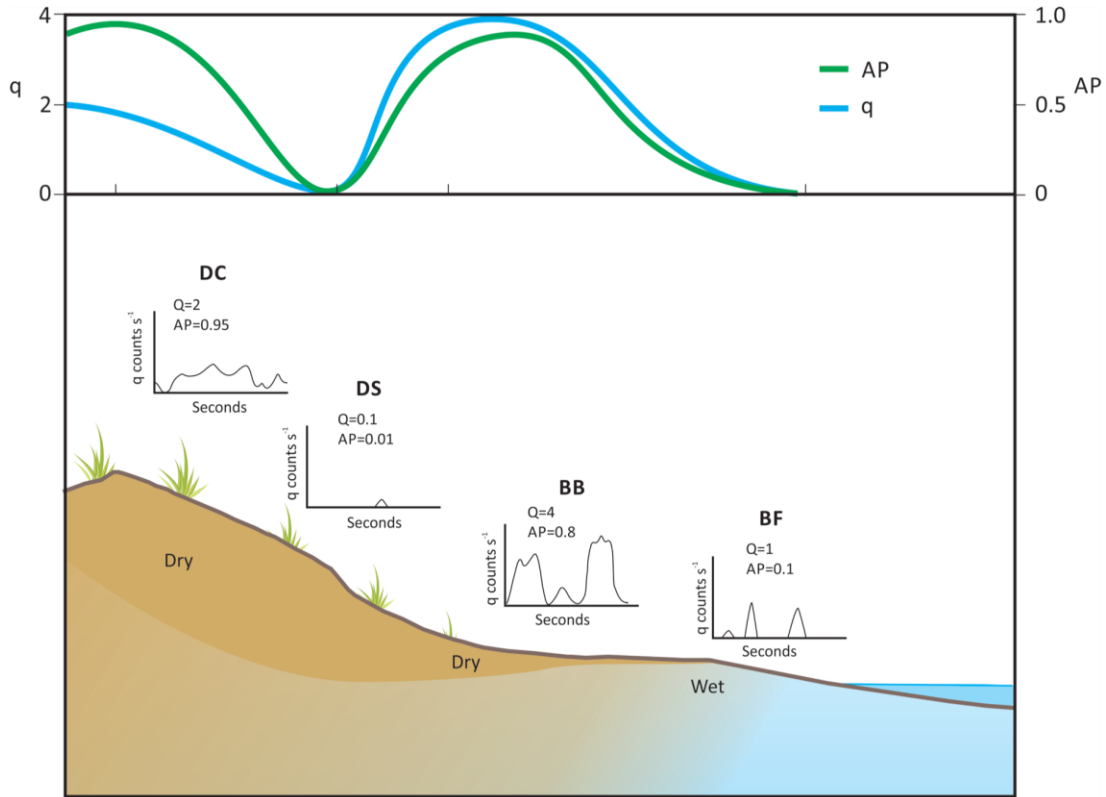
977 Field experiments at the Greenwich Dunes in PEI and elsewhere have shown that the sand
978 transport rate increases downwind from the limit of swash run-up toward the upper beach
979 (e.g., Nordstrom and Jackson, 1992; Bauer and Davidson-Arnott, 2003; Bauer et al., 2009;
980 Delgado-Fernandez, 2010; De Vries et al., 2014). A pattern of exponential increase in sand
981 transport rate with downwind distance is often evident in time-averaged measurements along
982 transects over beaches using depth-integrating traps (e.g., Davidson-Arnott and Law, 1990;
983 Davidson-Arnott et al., 2008). Consistent with the fetch effect, this suggests that there is an
984 increase in transport toward the saturated flux condition somewhere on the upper beach.
985 However, observations also indicate that there can be considerable variation across the beach-
986 dune profile, with some locations showing semi-continuous transport while others show

987 significant transport intermittency. This suggests that the increase in the time-averaged
988 transport rate at different positions across the beach-dune profile reflects both an increase in
989 the instantaneous transport rate (larger flux peaks) and an increase in the proportion of time
990 that transport occurs (Davidson–Arnott and Bauer, 2009).

991 There is also a positively reinforcing interaction between the fetch effect and the spatial
992 pattern of surface moisture that leads to an increase in overall sand transport rate downwind
993 toward the foredune. Figure 13 is a conceptual schematic of expected transport variation and
994 AP values across a beach-dune profile for an obliquely onshore wind, based on observations at
995 the PEI site. Sand transport on the beach foreshore (BF) is very intermittent, producing small
996 AP values and small total transport (q_s). Toward the beach backshore (BB), the effects of the
997 saltation cascade and decreasing moisture content produce an increase in activity and total
998 transport. Behind the beach is a near vertical scarp that, coupled with the presence of
999 vegetation, prevents most sand transported across the beach from reaching the foredune. As a
1000 consequence, both AP and q_s are very small at the dune toe and lower stoss slope (DS). Near
1001 the foredune crest (DC), sand is entrained from the upper stoss slope reflecting both small
1002 values for surface moisture and significant wind speed up towards the crest due to flow
1003 compression. This results in nearly continuous transport (large AP) at the crest but smaller
1004 values of sand transport in comparison to the back-beach.

1005

1006 **Figure 13:** Conceptual model of expected transport variation (q_s) and activity (AP) across a
 1007 beach-dune profile at beach foreshore (BF), back beach (BB), dune slope (DS) and dune crest
 1008 (DC) locations for an obliquely onshore wind, based on our field experiments at the Greenwich
 1009 Dunes.



1010
 1011 The consequence of these spatial-temporal controls on aeolian sand transport across the
 1012 beach-dune profile (including fetch length, moisture interactions, vegetation, and topographic
 1013 effects) is that there is often very poor correspondence between quasi-instantaneous (i.e., 1 Hz)
 1014 wind speed and sand transport at any given location (e.g., Davidson-Arnott et al., 2008;
 1015 Davidson-Arnott and Bauer, 2009). Indeed, regressions between transport flux and the cube of
 1016 wind speed often have very small R^2 values, suggesting poor explanatory power (see example
 1017 below in Fig. 15). The relationship usually improves with longer averaging intervals, which is

1018 consistent with the observation of Namikas et al. (2003) regarding u^* . Stout and Zobeck (1997)
1019 sought to use the observed fluctuations in wind speed and sand transport to derive a ‘time
1020 fraction equivalent’ threshold wind speed. However, measurements at the PEI site by Davidson-
1021 Arnott et al. (2005; 2008) and Davidson-Arnott and Bauer (2009) as well as others (e.g., Wiggs
1022 et al., 2004a, b) have shown that sand transport can occur when quasi-instantaneous wind
1023 measurements are below the calculated threshold of motion, and vice versa. In part, this is
1024 explained by the phase-lagged response of saltation to changes in wind speed (Spies et al.,
1025 2002), but there are also spatial dimensions involving the delivery of saltating sediments to a
1026 sensor location from upwind sources that have differing surface controls and wind patterns.

1027 *4.2.5. New observations of vertical sediment flux variations and transport events*
1028 *(flurries)*

1029 Aeolian sand transport is a near-surface phenomenon in that saltation layers are of limited
1030 vertical extent. The bulk of transport occurs in a very thin layer immediately above the surface
1031 by grains moving in saltation (saltons) and as surface creep (reptons). The grain concentration
1032 in a given volume of air decreases with increasing distance from the surface in a non-linear
1033 manner, as does the transport rate. Usually an exponential-decay function is used to describe
1034 vertical profiles of sand transport (Ellis et al., 2011; Rotnicka, 2013; Bauer and Davidson-Arnott,
1035 2014). Energetic saltons that rise higher into the air column tend to have larger particle speeds
1036 than low-energy saltons that are constrained to a near-surface layer and, therefore, the
1037 concentration profile and the flux profile are not ordinarily interchangeable unless information
1038 is available on the particle speed profile. Another source of confusion arises from the use of

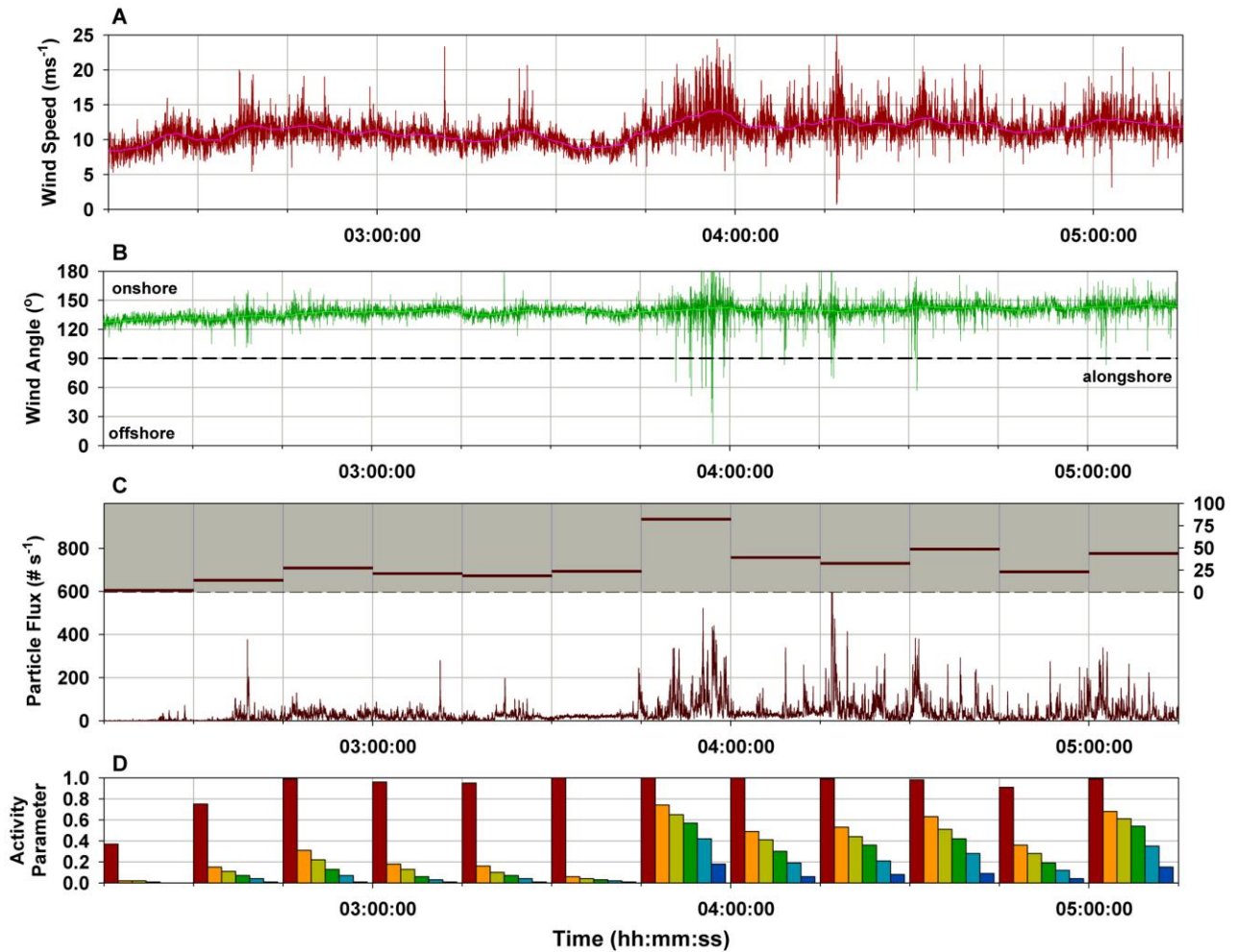
1039 three different transport quantities (mass, volume, particle count) to represent the vertical
1040 profile. These are, in theory, interchangeable but in practice there can be insurmountable
1041 challenges and uncertainty around grain size distributions, particle shapes, and mineral
1042 densities. There remains considerable debate in the literature regarding whether the vertical
1043 profile of sediment flux is smoothly continuous or layered (e.g., Butterfield, 1999; Dong et al.,
1044 2006; 2011; Farrell et al., 2012) and how the profile should be parameterized (e.g., Martin et
1045 al., 2013; Bauer and Davidson-Arnott, 2014).

1046 Insight into the nature of vertical mass flux profiles across beach-dune systems was
1047 facilitated with the adoption of the segmented sand trap in field studies (e.g., Williams, 1964;
1048 Rasmussen et al., 1989; Rasmussen and Mikkelsen, 1998; Sherman et al., 1994; 2014; Namikas,
1049 2003). The cumbersome nature of these first-generation traps was eliminated by the
1050 development of smaller and more sophisticated laser particle counters (LPCs) and acoustic
1051 sensors, which could be stacked vertically. Some key advantages of the LPCs used in the PEI
1052 experiments are that they are commercially available, relatively affordable, and manufactured
1053 to high technical standards. This implies that the results from one unit are precisely
1054 reproducible by another unit, eliminating the need for extensive cross-calibration (cf. Baas,
1055 2004 in regards to Safire-style piezoelectric probes). As with any field instrument, LPCs have
1056 certain shortcomings (see Barchyn et al., 2014 and references therein), the most challenging of
1057 which is the conversion of particle counts to mass flux. It is advisable to co-locate a passive,
1058 segmented trap such as a multi-layered 'hose trap' (Sherman et al., 2014) to verify results from
1059 the high-frequency sensors with direct mass flux measurements.

1060 In the PEI research, vertical arrays of LPCs yielded novel insights into the nature of aeolian
1061 saltation at the plot scale. Figure 14 shows time series of: (A) wind speed; (B) wind angle; (C)
1062 particle flux; and (D) AP during an intense wind event on 4 May 2010 at the PEI field site (from
1063 Bauer and Davidson-Arnott, 2014). The wind speed and particle flux traces suggest a crude
1064 correspondence for which the most intense and variable speed segments align with the
1065 greatest flux events. However, a simple regression analysis using the 1 Hz data (Fig. 15) reveals
1066 that the R^2 is only 0.33 ($P < 0.0001$), which is typical for raw, high-frequency data that have not
1067 been averaged. There are periods near the beginning of the time series when transport was not
1068 very active and a large number of intervals that had no transport whatsoever. Figure 14D
1069 shows APs for different layers in the vertical flux profile calculated over 15-minute
1070 intervals. The first (red) bar in each interval shows AP for the lowermost LPC (0.014 m), and
1071 each bar progressively declining to the right shows LPCs higher in the profile (up to 0.472 m).
1072 The lowermost LPC in the first interval had an AP of only 0.37 followed by 0.75 for the second
1073 interval, and 0.99 for the third interval. All subsequent intervals had APs in excess of 0.91 for
1074 the lowermost LPC (in most cases it was 0.99 or 1.00), indicating a very energetic transport
1075 system over a prolonged period. Of particular interest is the substantial difference in the
1076 nature of the vertical flux profiles before 1545 h relative to those afterward. In the earlier
1077 intervals, there was a rapid reduction in AP above the lowermost LPC with values typically < 0.2 ,
1078 which means that the majority of particle flux was contained in a near-surface layer of
1079 approximately 0.05 m height. In contrast, after 1545 h when the total transport rate increased,
1080 the AP of the mid-level LPCs was typically > 0.2 and often as large as 0.7, which indicates that

1081 there were significantly more energetic saltations higher in the profile. The uppermost LPC (at
1082 0.472 m) had APs between 0.05 and 0.15, whereas in the earlier period there were very few
1083 saltations recorded at this height. A detailed assessment of these flux profiles was undertaken by
1084 Bauer and Davidson-Arnott (2014), wherein it was demonstrated that the geometry of the
1085 vertical flux profiles (shape, slope) depended on the event-like nature of the sand transport
1086 time series. Specifically, during intervals when transport was highly intermittent (small AP),
1087 there were fewer significant transport events (referred to as sediment 'flurries') interspersed
1088 between longer periods of quiescence. In addition, these flurries tended to have shorter life-
1089 spans (several seconds), which means that the saltation system rarely achieved the equilibrium
1090 (saturated) transport state. Thus, there are intricate linkages between wind unsteadiness,
1091 transport intermittency, and the geometry of the vertical flux profile and these linkages are
1092 further complicated by topographic position and vegetation characteristics over the beach-
1093 dune profile.
1094

1095 **Figure 14:** Time series of: (A) wind speed; (B) wind approach angle; (C) particle flux; and (D)
 1096 Activity Parameter (AP, a measure of transport intermittency) recorded at 1 Hz for a three-hour
 1097 measurement period on the foredune crest on 4 May 2010. Wind speed and direction are from
 1098 the 3D sonic at 0.2 m above the bed adjacent to the vertical array of LPCs. Smoothed trend
 1099 lines are 5-minute moving averages. Particle flux is the vertically-integrated instantaneous (1
 1100 Hz) count summed over six LPCs in the vertical array (left-hand scale). Upper (grey-shaded)
 1101 panels show 15-minute mean counts (right-hand scale). Every 15-minute segment has six
 1102 vertical bars that indicates AP for each of the six sensors in the vertical array (left-most bar is
 1103 the lowest LPC and right-most bar is the highest LPC in the array).
 1104

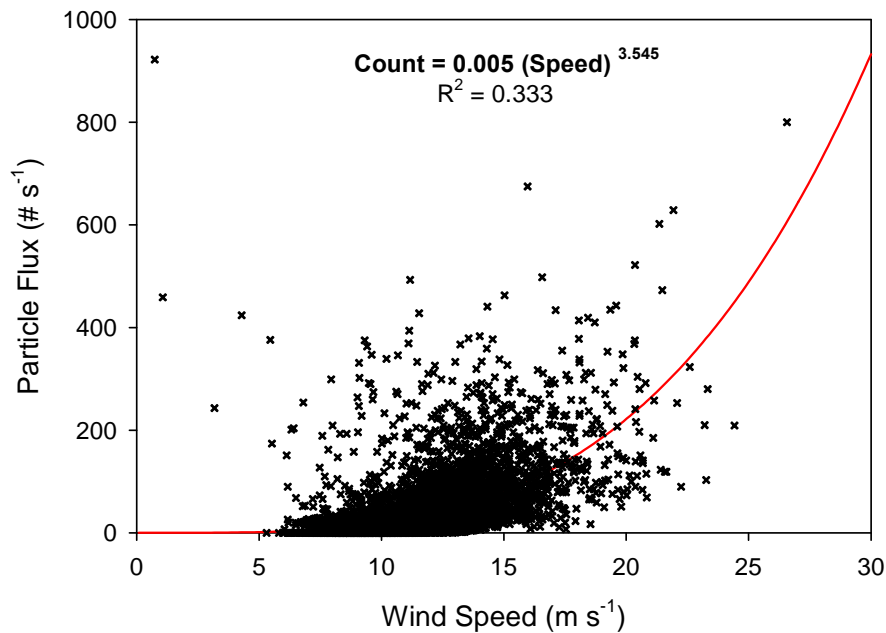


1105

1106

1107

1108 **Figure 15:** Regression of wind speed against particle flux (data in panels A and C, respectively,
1109 in Fig. 14) during an intense wind event on 4 May 2010 at the PEI field site.



1110

1111 *4.2.6. Observations of flux divergence and spatial-temporal patterns of erosion and*

1112 *deposition*

1113 The introduction and use of relatively affordable, fast-response sediment transport sensors

1114 in aeolian geomorphology has facilitated the deployment of dense arrays of instruments that

1115 enable the characterization of spatial-temporal patterns of transport rate across an entire

1116 beach-dune profile. Not only has this provided insight into the vertical structure of the saltation

1117 layer, as described above, but also into the potential correlation between fundamental scales of

1118 fluid events (i.e., coherent flow structures) and transport events such as aeolian streamers

1119 (Baas and Sherman, 2005; Bauer et al., 2013) or ‘flurries’ (Bauer and Davidson-Arnott, 2014).

1120 Initially, the objective of horizontal arrays of transport sensors was to quantify the spatial

1121 variability in transport rate relative to predictions from equilibrium models. Ellis et al. (2012)

1122 noted that there were only five field-based studies addressing this problem at that time, and
1123 four of them used integrating traps rather than fast-response sensors. The horizontal spacing
1124 between traps was usually several metres. Baas (2003) was the first to utilize a very closely
1125 spaced horizontal instrument array, which included both fast-response piezo-electric impact
1126 sensors (e.g., 'Safires') and hot-wire anemometry. Collectively, these studies demonstrated that
1127 there can be considerable spatial variability in transport rate, with the coefficient of variation
1128 across the array of traps ranging from about 0.1 to 1.0. In the Baas (2003) study, the sand
1129 surface in front of the array was meticulously groomed, thereby reducing the likelihood that
1130 the spatial variation in transport rate was due to surface controls. Nevertheless, it proved
1131 impossible to link the scales of the transport events (i.e., streamers) to the scales of fluid
1132 structures embedded in the wind field in a statistically reliable way.

1133 One of the more useful applications for data derived from spatial arrays of LPCs is to derive
1134 the sediment flux divergence, $\nabla \cdot q_s$, which is the spatial gradient (d/dx, d/dy, d/dz) in sediment
1135 volume flux (q_s). The flux divergence is used in a simplified version of the sediment
1136 conservation relation referred to as the Exner equation (Paola and Voller, 2005),

1137
$$\frac{\partial h}{\partial t} = -\frac{1}{(1-p)} \nabla \cdot q_s \quad (1)$$

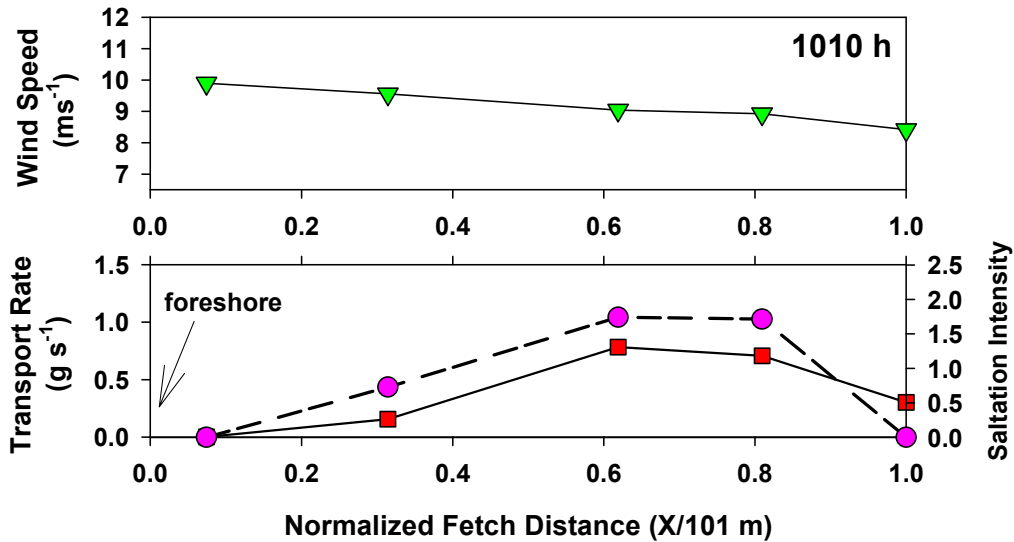
1138 where h is elevation of the bed, t is time, and p is sediment porosity. Figure 16 shows the cross-
1139 beach pattern of mean wind speed and mean sediment transport (time averaged flux and
1140 transport intensity) at four trap locations oriented along prevailing streamlines during an
1141 obliquely onshore wind event at the Greenwich Dunes site on 11 October 2004. Estimates of
1142 sediment transport were from integrating traps as well as co-located Safire sensors and both

1143 methods showed the same trend in transport. The rate of sand transport increased from a
1144 minimum at the foreshore, where conditions were extremely wet and fetch-limited, to a
1145 maximum on the upper beach, where conditions were dry and closer to equilibrium. An
1146 unexpected, but recurring decline in transport rate toward the dune toe was also measured,
1147 which is explained by the downstream reduction in wind speed associated with the vertical
1148 growth of the boundary layer, and flow stagnation imposed by the dune, thereby yielding a
1149 concomitant decrease in near-surface shear stress (Bauer et al., 2009; Walker and Hesp, 2013;
1150 Hesp et al. 2015). The flux divergence between neighboring trap locations suggests that there
1151 would be net erosion from the foreshore and across most of the beach, which is required to
1152 drive the increase in saltation flux in the downwind direction. However, the decrease in
1153 sediment flux between the last two stations indicates that this is a zone of deposition, which is
1154 typically observed during onshore transport events across beaches.

1155 Bauer et al. (2015) demonstrated that a similar pattern of sand accumulation at the toe of
1156 the dune occurs during offshore wind events because of eddy recirculation over the seaward
1157 (lee) slope of the foredune. A methodology for isolating the cross-shore sediment flux from the
1158 total sediment flux using the wind vectors was proposed. These patterns of flux divergence
1159 over beaches are critical to infilling wave-cut scarps at the dune toe and to rebuilding dune
1160 ramps that are essential to facilitating sand transport pathways onto the stoss slope of the
1161 foredune and toward the crest.

1162

1163 **Figure 16:** Patterns of mean wind speed, mean sediment transport rate derived from sand
 1164 traps (squares), and transport intensity measured from safire sand transport probes (circles) at
 1165 several trap locations from the foreshore to dune toe during an obliquely onshore wind event
 1166 at the Greenwich Dunes, PEI site on 11 October 2004. Normalized fetch distance for each trap
 1167 (aligned into local flow streamlines) is provided on the x-axis.



1168

1169 The complexity of spatial-temporal patterns of erosion and deposition across beach-dune

1170 systems during single events is becoming widely appreciated and increasingly quantified, yet

1171 the linkages between plot scale investigations and landform scale perspectives remain more

1172 challenging. Logistically, it is not yet feasible to conduct experiments at the intensity of the plot

1173 scale with continuous high-frequency monitoring over periods of years. Nor is it reasonable to

1174 maintain high-density instrument deployments over very large areas because of financial

1175 constraints. As a consequence, there can be substantial data gaps during periods in which

1176 significant geomorphic change may occur in locations where we did not (or were unable to)

1177 monitor. Thus, plot scale studies provide only a limited vignette within the broader frequency-

1178 magnitude-effectiveness regime that governs dune morphodynamics, and yet it is the broader

1179 landscape scale perspective that is of greater concern to coastal resource management. The

1180 next section explores research at the landform scale that attempts to bridge the divide
1181 between the plot scale and the landform scale (Table 1).

1182

1183 **5. Landform scale**

1184 The objectives of research at the landform scale in the PEI study were motivated by the
1185 need to make observations and to obtain data that provide insights into which processes at the
1186 plot scale may be most relevant for understanding and managing issues related to foredune
1187 morphodynamics in partnership with Parks Canada Agency (e.g., dune evolution, dune
1188 migration, coastal erosion). At the landform scale (Table 1), beach-dune sediment budgets and
1189 foredune growth over months to years are controlled initially by the volume of sand on the
1190 beach that is available to be transported to the foredune by aeolian processes and/or the
1191 propensity for sediment to be eroded from the upper beach and foredune by high-water
1192 events.

1193 Much effort has gone into developing predictive models based on standard deterministic
1194 equations used in plot scale studies (e.g., Hunter et al., 1983; Kroon and Hoekstra, 1990; Wahid,
1195 2008). The approach employed in the PEI research at the landform scale is similarly
1196 ‘reductionist’ (Bauer and Sherman, 1999) as it splits the problem of predicting aeolian transport
1197 into smaller and smaller components with the intent of scaling back up. Over time, it has
1198 certainly offered insights into the relationships between aeolian sediment transport and a
1199 range of controlling variables, but it has also highlighted other non-trivial issues such as how to
1200 combine multiple supply-limiting factors, or to upscale findings from plot scale studies to the

1201 landform scale. Ultimately, a main focus of research at the landform scale is to predict (model)
1202 sand delivery from the beach to the foredune, and then to examine the broader processes
1203 involved in beach-dune interaction as controls on foredune evolution.

1204 5.1 Modeling sediment delivery to coastal dunes

1205 5.1.1 *Classic approaches to modelling long-term aeolian sand drift*

1206 The most widely used approach for predicting aeolian sand supply and resulting dune form
1207 is the 'Fryberger method' (Fryberger and Dean, 1979), which uses the Lettau and Lettau (1977)
1208 equation to calculate aeolian sand transport (drift) at an annual scale. The Fryberger method
1209 was applied initially to desert dunes (e.g., Fryberger, 1980; Carson and Mclean, 1986; Wang et
1210 al., 2002) but has also been adopted for coastal dunes (e.g., Chapman 1990; Wal and McManus,
1211 1993; Davidson-Arnott and Law, 1996; Hesp and Hyde, 1996; Blumberg and Greeley, 1996,
1212 Walker and Barrie, 2006; Miot da Silva and Hesp, 2010). The wind speed at 10 m drives 'drift
1213 potentials' (DP) in compass directional classes to express total potential sand drift and resultant
1214 drift potential (RDP) associated with the wind regime in a particular area. In turn, these
1215 quantities can be related to dune size, shape, and mobility using statistical expressions. The
1216 method is relatively simple and only requires wind data from standard meteorological stations.
1217 Details of the method and discussion of procedural limitations, including inaccuracies resulting
1218 from how data are converted (e.g., units as knots vs. m s^{-1} , Bullard, 1997) and/or categorized
1219 during the calculations to introduce 'frequency bias' (Pearce and Walker, 2005), are provided
1220 elsewhere.

1221 The main limitation of the Fryberger method, especially in vegetated coastal foredune
1222 settings, is that it does not account for key supply-limiting factors, such as surface moisture or
1223 fetch effects (Nickling and Davidson-Arnott, 1990; Bauer and Davidson-Arnott, 2003), transport
1224 –limiting factors such as vegetation or beach wrack, or near-surface secondary flow effects such
1225 as topographic steering. As a result, measured transport and deposition is typically much less
1226 than predicted by the Fryberger method (e.g., Hunter et al., 1983; Sarre, 1989; Chapman, 1990;
1227 Davidson-Arnott and Law, 1996; Hesp and Hyde, 1996).

1228 *5.1.2 New efforts to assess the regime of aeolian transport events in beach-dune systems*

1229 Recognizing the limitations of the Fryberger approach to predicting sand supply from the
1230 beach to the foredune, Delgado-Fernandez et al. (2009; 2012; 2013a) developed a monitoring
1231 system that simultaneously measured wind velocity (hourly), sediment transport, and some key
1232 supply-limiting factors including surficial moisture content (see Darke et al., 2009) and beach
1233 width (cf. Lynch et al., 2006). Sediment transport was measured using several complementary
1234 methods, including piezoelectric ('Safire' style) saltation sensors and erosion-deposition pins
1235 permanently deployed from the upper beach toward the crest, bedframe volumetric surveys,
1236 and visual interpretation of aeolian transport conditions from fixed-mount camera imagery. The
1237 resulting data set permitted assessment of both the magnitude and frequency of wind events
1238 and associated sand transport events, as well as the development and testing of a modelling
1239 approach to predict sand supply to the foredune that accounts for supply-limited conditions
1240 operating at seasonal time scales (Delgado-Fernandez and Davidson-Arnott, 2011).

1241 To develop models capable of calculating sand supply to a foredune and, in turn, to better
1242 predict foredune evolution at the landform scale, it is important to evaluate the relative
1243 significance of event frequency, magnitude, and effectiveness following the concepts described
1244 in Wolman and Miller (1960) and Wolman and Gerson (1978)(see section 2). An effective wind
1245 event is defined as a period during which wind speed exceeds the threshold of motion for dry
1246 sand for more than two hours (based on an hourly photo acquisition rate), thus providing the
1247 potential for significant transport to occur. Additional supply-limiting factors to consider are
1248 the moisture state of the beach sand, wind approach angle, and available fetch distance, among
1249 others. Ultimately, the potential hourly sand transport rate (Q) can be converted into a
1250 potential hourly sand delivery into the dune based on the cosine function (Davidson-Arnott and
1251 Law, 1990; Bauer and Davidson-Arnott, 2003):

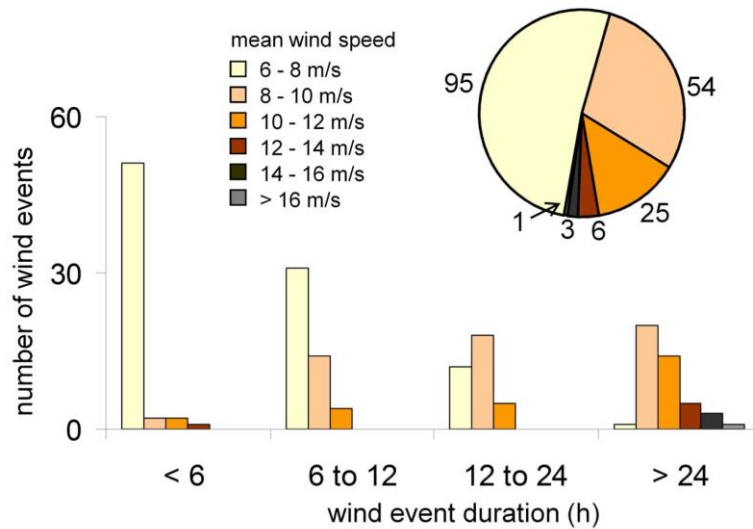
$$1252 \quad Q_n = Q \cos \alpha \quad (2)$$

1253 where α is the angle of the wind to shore perpendicular and Q_n is the hourly average sand
1254 transport into the foredune per metre alongshore ($\text{kg h}^{-1} \text{m}^{-1}$). Equation 2 can be summed for
1255 each hour to give the total potential transport for the event. Note that a transport event does
1256 not necessarily coincide with the duration of the wind event because of the threshold
1257 condition, which defines when sand transport is active. As such, transport events may occupy
1258 all or only a portion of an associated wind event and some wind events may have no transport
1259 associated with them at all.

1260 Delgado-Fernandez and Davidson-Arnott (2011) examined a total of 184 wind events
1261 during a 9-month period from 1 September 2007 to 31 May 2008. Most of these events

1262 (95/184) had mean wind speeds of $< 8 \text{ m s}^{-1}$ and, therefore, were of insufficient strength to
 1263 yield transport (Figure 17). Only about 25% of the events had wind speeds in excess of 12 m s^{-1}
 1264 and of sufficient duration ($> 12 \text{ hrs}$) to yield significant sediment transport.

1265 **Figure 17:** Wind event categorization according to wind speed magnitude and storm duration
 1266 (adapted from Delgado-Fernandez and Davidson-Arnott, 2011). In general, low magnitude
 1267 events were more frequent and of shorter duration than large magnitude events, which were
 1268 infrequent and of longer duration.



1269

1270 The relative magnitude of each wind storm ($Q_{m\%}$) as a potential sediment transporting
 1271 event was calculated based on hourly wind transport rates and event duration, and expressed
 1272 as percentage of the total amount of sediment transport predicted for the study period. An
 1273 expression proposed by Wolman and Miller (1960) was adapted for this purpose:

1274
$$Q_{m\%} = \frac{Q_i \cdot F}{Q_{tot}} \cdot 100 \quad (3)$$

1275 where Q_i is the sediment transport during a given event predicted by summing the potential
 1276 transport for each hour (per Delgado-Fernandez and Davidson-Arnott, 2011), F is the frequency
 1277 of the event, and Q_{tot} is the total sand transport predicted over the study period. Events were

1278 grouped into five magnitude classes prior to implementation of Equation 3 to simplify the
1279 frequency analysis. Roughly 50% of the potential transport was associated with large
1280 magnitude events ($> 81 \times 10^2 \text{ kg m}^{-1}$), while the smallest events ($< 3 \times 10^2 \text{ kg m}^{-1}$) contributed
1281 only 7.6% to the total potential transport despite accounting for more than 60% of the total
1282 number of events (Fig. 18A).

1283 Large magnitude wind events occurred mostly during the late fall and winter months.
1284 Events with an onshore component accounted for about half of the number of events but
1285 about 71% of the total potential transport. However, when the potential transport is modified
1286 by the cosine function (Eq. 2), the net potential transport (Q_n) into the dune is about 41% of the
1287 total transport predicted for all events (Fig. 18B). Despite the overall reduction in the number of
1288 events with only onshore conditions and the magnitude of predicted transport for those events,
1289 the percentage distributions associated with each category were very similar to the total
1290 population of all wind events (Fig. 18A). Infrequent, large magnitude wind events were still
1291 concentrated during the late fall and winter months and were responsible for approximately
1292 50% of potential sediment input to the dunes (as depicted in Figs. 2c, d).

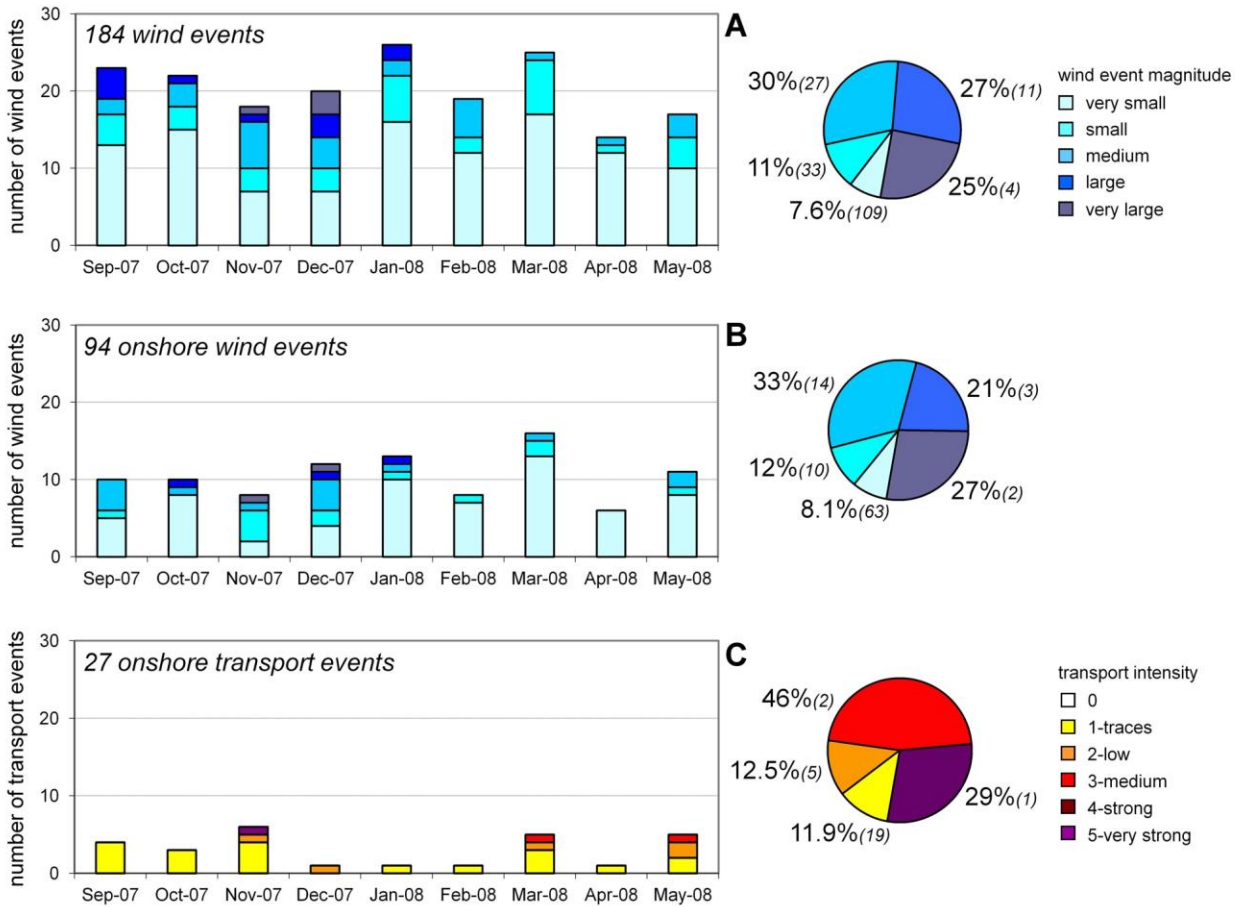
1293 Many of the wind events with very large transport potential (i.e., with extreme wind
1294 speeds) actually produced less (or no) total transport compared to more moderate events (Fig.
1295 18). The influences of one or more supply-limiting controls, such as fetch, wind angle, surface
1296 moisture, storm surge, wave runup, tide level, and the presence of snow and ice during the
1297 winter months (January through March) are critical in determining whether aeolian transport is
1298 active or not and, thereby, effective in moving sediment into the foredune. The wind vector is

1299 but one of many important variables to consider at this scale, which is a much different result
1300 than that obtained using the Fryberger method in the absence of appropriate local controls on
1301 the transport process.

1302 Figure 18C shows that three transport events were responsible for the majority of sand
1303 delivery to the foredune over the 9-month observation period. The largest amount of transport
1304 occurred during an event that lasted 90 hours (long duration) with an average wind speed of
1305 12.5 m s^{-1} (moderate to low magnitude). The other two transport events occurred with average
1306 wind speeds of 8.2 and 9.2 m s^{-1} (low magnitude) and lasted 32 and 54 h (long duration),
1307 respectively. Active transport during these events was both time limited (i.e., only observed
1308 during a portion of the wind event) and magnitude limited (i.e., observed transport was less
1309 than predicted). Despite fetch-restricted and moisture-limiting conditions, these three events
1310 delivered 75% of the total amount of sand to the dune during the study period. The remaining
1311 25% was delivered during 24 lesser transport events. Ten of the strongest wind events, which
1312 accounted for 45% of the total predicted sediment input to the dunes, produced no significant
1313 transport at all (Delgado-Fernandez and Davidson-Arnott, 2011). This study shows that
1314 although transport-competent winds may be frequent, only a sub-set of these events may be
1315 effective in transporting sediment toward the foredune given the complex suite of supply-
1316 limiting factors and their seasonal variations.

1317

1318 **Figure 18:** (A) Frequency distribution of potential sediment transport events for the 9-month
 1319 study period. A total of 15 large or very large magnitude wind events during winter months
 1320 were associated with over 50% of the total potential sand transport. (B) Frequency distribution
 1321 of potential sand transport events with onshore flow direction and modified by the cosine
 1322 function, which are believed to be the major contributors to foredune maintenance and
 1323 growth. Large magnitude events still accounted for approximately 50% of potential sediment
 1324 input to the dunes. (C) Observed sand transport towards the foredune measured using a
 1325 combination of techniques (described in Delgado-Fernandez and Davidson-Arnott, 2011). Only
 1326 one of the original large magnitude wind events (in November) actually produced strong
 1327 transport. Two additional medium transport events occurred in the spring. Together, these
 1328 three events accounted for approximately 75% of the total sand delivered to the dunes. Values
 1329 outside the pie charts indicate the percent of potential transport and the number (in brackets)
 1330 of events.
 1331



1332

1333

1334 5.1.3 *Advances in modelling the effect of supply-limited conditions on predicted sand*
1335 *transport to foredunes*

1336 As discussed above, supply limitations play a key role in determining the actual sediment
1337 transport associated with a wind event in coastal environments. This highlights a need to model
1338 supply limitations explicitly when predicting sediment supply to foredunes over periods of
1339 weeks to years. Delgado-Fernandez (2011) used the same dataset to test a supply-limited
1340 modelling approach, which involved filtering the time series to remove all periods when: i) wind
1341 speed was below the threshold for dry sand, ii) when winds were offshore, and iii) during
1342 periods of high surface moisture or coverage by snow and/or ice. Using the theoretical
1343 framework for assessing the impact of the fetch effect (per Bauer and Davidson-Arnott, 2003,
1344 sections 4.2.2 and 4.2.3) the critical fetch length, F_c , was first determined for 'dry' conditions,
1345 where the surface moisture content was <2%, and then for situations of greater moisture
1346 content, between 4 and 10%, to allow for the lengthening of F_c with increasing surface
1347 moisture. When $F_c > F$, the effects of supply limitation can be modeled by any of the
1348 expressions presented in Bauer and Davidson-Arnott (2003), whereas when $F_c < F$, transport
1349 rate is considered to be at its maximum potential.

1350 An example of the model output for a 90-hour storm in November 2007 is shown in Figure
1351 19. Sediment input to the foredune based on wind speed and direction alone was over-
1352 predicted at $Q_n = 9,470 \text{ kg m}^{-1}$ for this event, with maximum transport rate coinciding with the
1353 peak of strong onshore winds (Fig. 19A,E). Large moisture content and short fetch distances
1354 (Fig. 19C,D) imposed a constraint on sediment transport at around 50 hrs into the event and,

1355 when these factors were included in the model (Fig. 19G), the predictions improved
1356 considerably. The initial filtering approach reduced the total predicted input to the foredune
1357 from approximately 86,000 to 36,000 kg m⁻¹. The value was further reduced to about 19,000 kg
1358 m⁻¹ once the supply-limiting effects of fetch and moisture were applied. Values for deposition
1359 measured by erosion-deposition pins and bedframe stations over the same period ranged from
1360 about 4,000 to 15,000 kg m⁻¹. The uncertainty in measured deposition reflects the difficulty in
1361 accounting for the effects of wave erosion and some landward sand transfers (losses) beyond
1362 the foredune, although it is evident that the filtered estimates from the model are much closer
1363 to the measurements than to original, unfiltered predicted values.

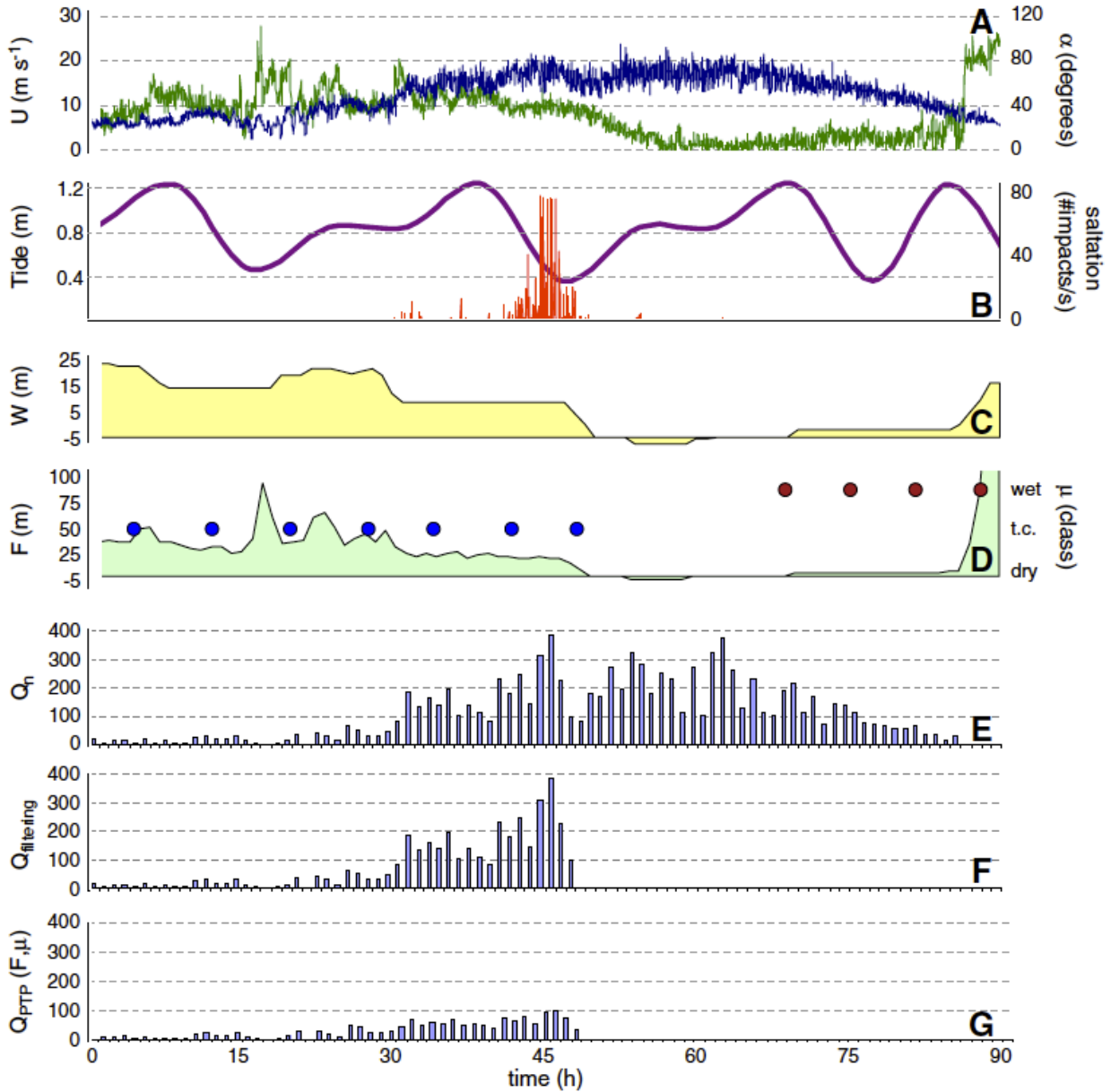
1364 These modelling results at the landform scale, combined with the plot-scale investigations
1365 described above, highlight the need to include supply-limiting factors when predicting sand
1366 transport from the beach to the foredune. The modeling approach reviewed here considers the
1367 effect of increasing moisture content on lengthening the critical fetch (F_c) necessary to achieve
1368 saturated transport, however, it is also possible to model this effect as a limitation on sand
1369 supply from the surface directly (cf., de Vries et al., 2014). Other studies have attempted to
1370 scale up sediment supply to coastal dunes and model their evolution by simply calculating
1371 subaerial barrier volumes and comparing these to foredune volumetric change measurements
1372 (e.g., Miot da Silva and Hesp, 2010), or by using computational approaches that solve simplified
1373 aerodynamics and sand transport relations (e.g., Luna et al., 2011; Duran and Moore, 2014) or
1374 cellular automata approaches (e.g., Baas, 2002; Baas and Neild, 2007; 2010; Zhang et al., 2015;
1375 Keijsers et al., 2016). The utility of these modelling efforts is limited, however, by fundamental

1376 assumptions of saturated flux and the effectiveness of onshore winds over seasons and years.
1377 While incorporation of complexities such as moisture and vegetation may improve some
1378 simulations (e.g., Luna et al., 2011, Zhang et al., 2015; Keijsers et al., 2016), realistic
1379 parameterization of vegetation growth (e.g., seasonal phenology, gradual succession) and
1380 related roughness effects and sand trapping efficiency are generally lacking. In addition, there
1381 are limited field measurements to inform and validate such models, which increases the risk of
1382 using expedient oversimplifications (Barchyn et al., 2014).

1383 Finally, sand input from the beach is just one component of the foredune sediment budget.
1384 Controls on dune evolution at the landscape scale must also consider the broader framework of
1385 beach-dune interaction, which includes wave erosion during storms and berm construction and
1386 the onshore welding of nearshore sand bars to the foreshore, as discussed below.

1387

1388 **Figure 19:** Modelling output for a 90-hr storm at the Greenwich Dunes, PEI site starting on 9
 1389 November 2007. A) 2-min records of wind speed, U , and direction, α ; B) saltation intensity and
 1390 tidal elevation; C) beach width, W ; D) fetch distance, F , determined by beach width and wind
 1391 direction, and classified (optically derived) moisture values, μ ; E) hourly potential transport
 1392 based on wind speed and direction, Q_n ; F) output of the filtering step, $Q_{\text{filtering}}$; G) calculated
 1393 transport over isolated potential transport periods, Q_{PTP} , including fetch distance and moisture.
 1394 Transport in E–F expressed in kg m^{-1} . Modified from Delgado-Fernandez (2011: Fig. 10).



1395

1396 5.2. Beach-dune interaction

1397 5.2.1. *Classic understanding of sand supply and coastal dune evolution*

1398 While cycles of foredune erosion during extreme storms and subsequent rebuilding by
1399 aeolian processes over long inter-storm periods have been recognized for decades,
1400 incorporation of this understanding into a holistic conceptual framework stems from the
1401 proceedings of a symposium on beach-dune interaction edited by Psuty (1988). Studies of
1402 beach-dune interaction typically employed either one or some combination of repeated
1403 topographic surveys, mapping from aerial photography, stratigraphic analysis from trenches or
1404 cores, or interpretation of shallow seismic logs (e.g., Olson, 1958; Bigarella, 1979; Thom and
1405 Hall, 1991; Gares and Nordstrom, 1995; Bristow et al., 2000; Hesp, 2013). In the last two
1406 decades, the development of Ground Penetrating Radar (GPR) and airborne or terrestrial LiDAR
1407 has enhanced mapping of landforms in great detail. In addition, analysis of digital imagery
1408 using GIS has greatly increased our ability to use both historical aerial photography and modern
1409 imagery (e.g., Figs. 11, 23) to map landform change at time scales of days to decades. These
1410 technologies provide a compelling means to fill the information gap between the plot scale and
1411 the landform scale. Nevertheless, a key challenge remains in correlating observed
1412 morphological changes of foredunes with the key forcing variables.

1413 At the plot scale, localized erosion and deposition patterns can be understood and crudely
1414 predicted on the basis of the near-surface wind vector and the contributions of a host of
1415 supply-limiting factors listed as 'independent' variables in Table 1. But at the landform scale, all
1416 of the 'independent' variables at the plot scale become 'dependent' variables and, therefore,

1417 the patterns of erosion and deposition that ultimately lead to broad-scale foredune evolution
1418 are governed by such factors as the nature of shoreline progradation or erosion, the emergence
1419 or removal of vegetation cover, and seasonal to decadal changes in the morphodynamic state
1420 of the nearshore system fronting the foredune. Thus, the detailed nuances of sediment
1421 transport at the scale of seconds and hours (i.e., the intra-event dynamics of interest at the plot
1422 scale) become largely irrelevant as attention must shift toward event characterization (i.e.,
1423 kinds of events), inter-event conditions (i.e., processes active between events), and the time-
1424 sequencing of events. In effect, the focus becomes parameterizing the changing nature of
1425 geomorphically effective events over time as conditioned by the broader context within which
1426 beach-dune interaction takes place.

1427 Events leading to dune erosion and potential overwash are controlled by meteorological
1428 factors that govern wave generation, storm surge, and aeolian transport (e.g., Kriebel and
1429 Dean, 1985; Vellinga, 1986; Morton, 2002; Forbes et al., 2004; Thornton et al., 2007; Pye and
1430 Blott, 2008; Roelvink et al., 2009). An additional factor is alongshore variations in beach width
1431 associated with rip current circulation and megacusps (e.g., Komar, 1971; Thornton et al.,
1432 2007), intertidal bar welding (e.g., Aagaard et al., 2004; Anthony et al., 2006) and longshore
1433 sandwave migration (e.g., Inman, 1987; Davidson-Arnott and Stewart, 1988; Davidson-Arnott
1434 and Law, 1990; Ruessink and Jeuken, 2002; Davidson-Arnott and van Heyningen, 2003; Houser
1435 et al, 2008). These controls operate at time scales of months to years.

1436 *5.2.2. Assessing annual to decadal beach-dune interaction*

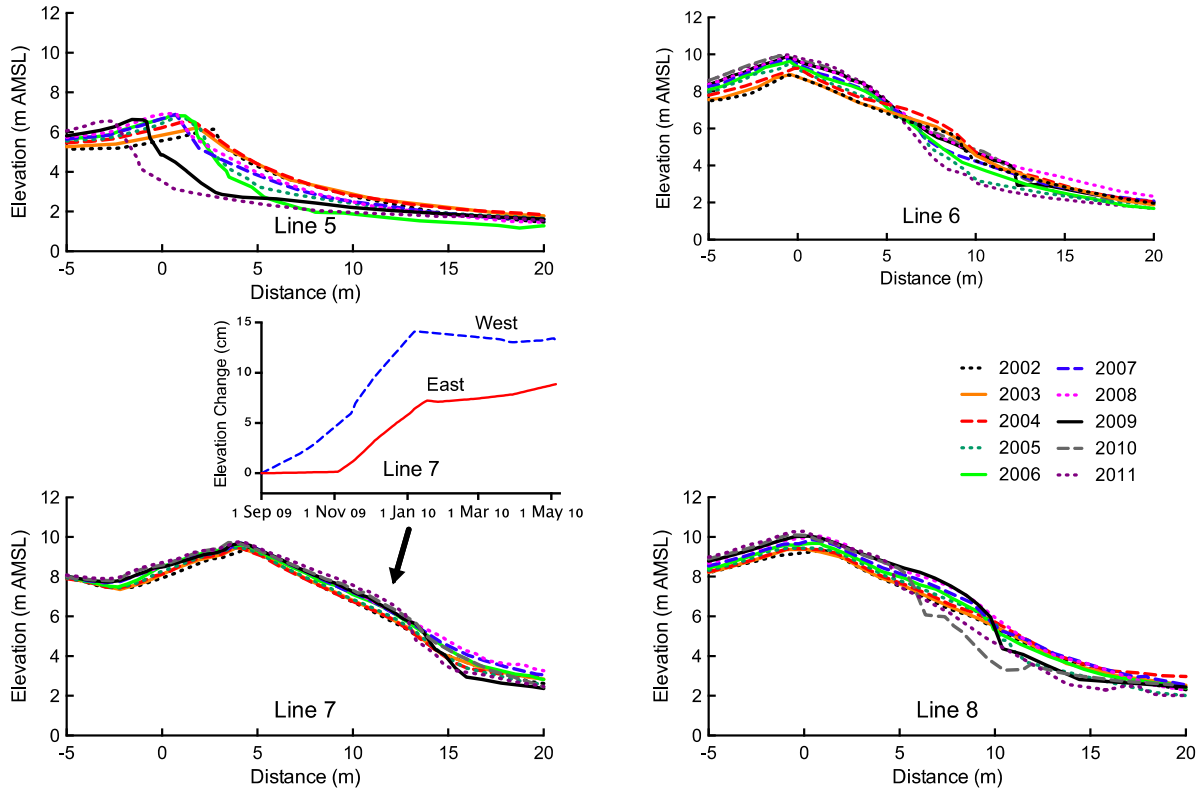
1437 Changes in beach-foredune morphology were quantified at the PEI site using: (i) repeat
1438 topographic surveys of cross-shore profiles, (ii) detailed bedframe measurements of volumetric
1439 changes along each transect (per Davidson-Arnott and Law, 1990), and (iii) hourly remotely
1440 sensed measurement of erosion-deposition pins on the stoss slope of the foredune (see
1441 Delgado-Fernandez et al., 2009; Ollerhead et al., 2013). The site was partitioned into 3 distinct
1442 reaches (see Fig. 1d). Reach 1 extended W about 2 km from the E boundary of PEI National
1443 Park and was oriented $\sim 100^\circ$ - 280° . Reach 2 extended about 3 km to the inlet of St. Peters Bay
1444 and was oriented at 60° - 240° and reach 3 is about 1 km long and extends SE into St. Peters Bay.

1445 Examples of annual topographic profiles are shown in Figure 20 for Lines 5 to 8 in Reach
1446 2 for the period May 2002 to May 2011. These data illustrate how profile response differs in the
1447 alongshore direction (E to W) due to variations in the littoral sediment budget fronting the
1448 beach-dune system. Sediment accretion is evident on the lee slope for all profiles in Reach 2,
1449 indicating landward sand transfers, but the pattern of topographic change on the stoss slope
1450 and back beach is highly variable. On the eastern margins of Reach 2 (e.g., Line 5), the profile
1451 was displaced landward over time due to a negative littoral sediment budget. On the western
1452 margins where there is a positive littoral budget (e.g., Line 8), accretion occurred on the stoss
1453 slope of the foredune while the crest remained relatively stationary. Between Lines 6 and 8,
1454 there is a transition from a negative to a positive littoral budget and, as a consequence, there
1455 was relatively little change in the foredune profile at Line 7.

1456 During the winter 2008-2009 season, there was a major dune scarping event that
1457 eroded the toe of the entire foredune along Reaches 1 and 2. As a result, little sediment moved
1458 onto the foredune at all four lines over the following year, which illustrates how dune scarping
1459 and ramp rebuilding processes pre-condition the broader dune profile response. In short, if the
1460 foredune is scarped, usually during late fall and early winter storms, a dune ramp must re-
1461 establish in order to provide a path for any significant volume of sediment to move up onto the
1462 upper stoss slope. Figure 20 includes an inset graph that shows time-series (2009-2010) trends
1463 from erosion-deposition pin lines installed on the E and W sides of Line 7. The data are mean
1464 values derived from all pins deployed on each line spanning most of the stoss slope. On the E
1465 line, there was a period of relatively little change on the stoss slope (Sept – Nov) followed by
1466 rapid accretion (Nov – Feb) and then no change (Feb – May), whereas on the W line there was
1467 continuous accretion (Sept – Jan) followed by no change afterward. Examination of annual
1468 profiles from 2009 and 2010 shows that this was a period of ramp rebuilding. By mid-November
1469 2009, the ramp had built sufficiently in front of the E line to permit transport onto the stoss
1470 slope and sediment accretion occurred on the stoss slope at both lines of pins thereafter. The
1471 onset of winter terminated the accretion period.

1472

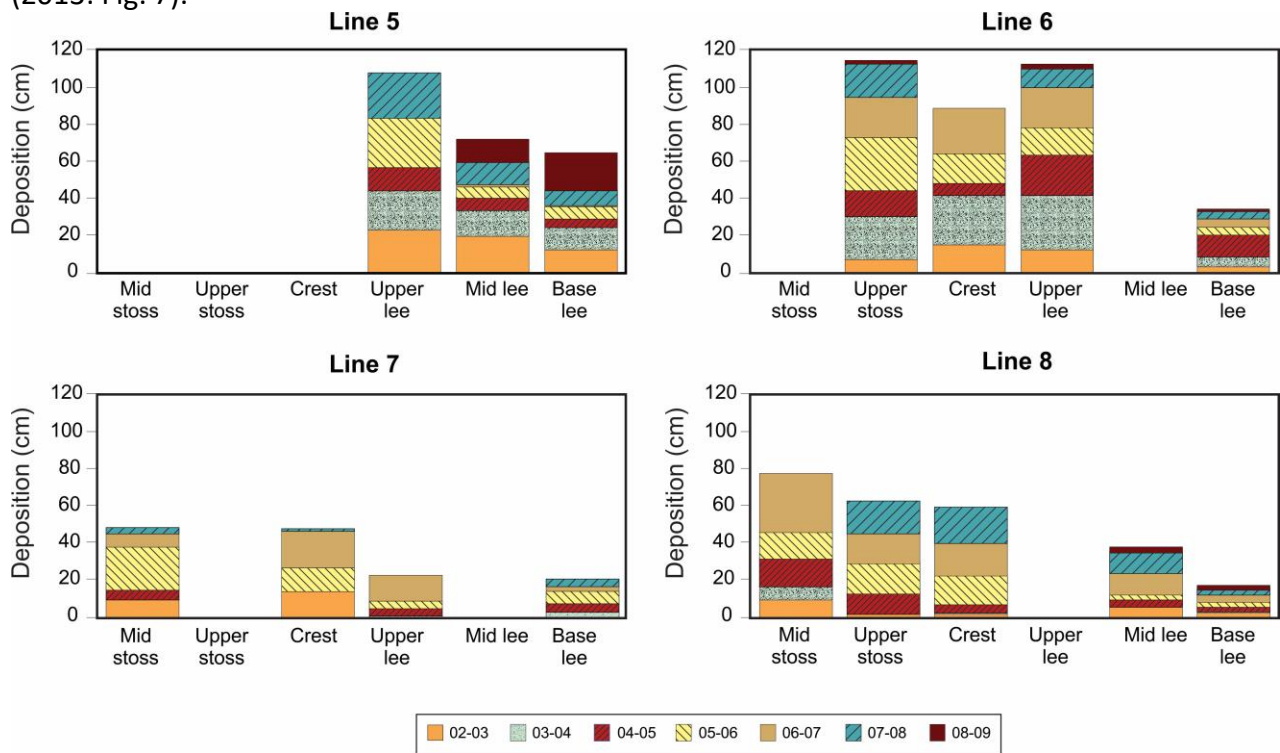
1473 **Figure 20:** Cross-shore topographic profiles for the period 2002-2011 showing differences in
 1474 foredune evolution at Lines 5-8 in Reach 2 at the study site (see Fig. 1d for general locations).



1475
 1476 The patterns illustrated in Figure 20 are also apparent in more detailed bedframe data
 1477 (Fig. 21). At Line 5, no net deposition was recorded on the stoss slope or crest because the
 1478 profile was being displaced landward semi-continuously. Sediment was transported from the
 1479 beach, across the stoss slope, and onto the lee slope, except when there was no ramp present
 1480 (e.g., 2006-2007). Line 5 data also show that when there is a significant scarping event, as in
 1481 2008-2009, sediment can still move onto the lee slope in association with landward
 1482 displacement of the entire profile. At Line 6 there was also no recorded deposition on the mid-
 1483 stoss slope over the seven-year interval. At Lines 7 and 8, where the littoral sediment budget
 1484 transitions from negative to positive, deposition was recorded on the mid-stoss at both lines in

1485 most years, particularly at Line 8 at the W end of Reach 2. Little deposition was recorded on the
 1486 mid and upper stoss slope at Lines 7 and 8 in years like 2003-2004 because sediment was being
 1487 trapped in the incipient foredune though, in subsequent years, sediment was able to move up
 1488 and over the foredune. Seasonal bedframe data and erosion-deposition pin datasets in 2009-
 1489 2010 (not shown) also show that most sediment transport onto the foredune occurs during the
 1490 fall and early winter months. There is a secondary peak in the late winter to early spring when
 1491 the snow and ice cover disappears and the vegetation cover is dormant and of low density
 1492 (Ollerhead et al., 2013).

1493 **Figure 21:** Stacked bar graphs showing the amount and variability of sediment deposition over
 1494 Lines 5-8 for each year period from 2002-2003 to 2008-2009. Modified from Ollerhead et al.
 1495 (2013: Fig. 7).



1496
 1497 The broad picture of beach-dune interaction and evolution that emerges from this
 1498 dataset is one of large inter-annual variability driven by: (i) the magnitude and timing of wind

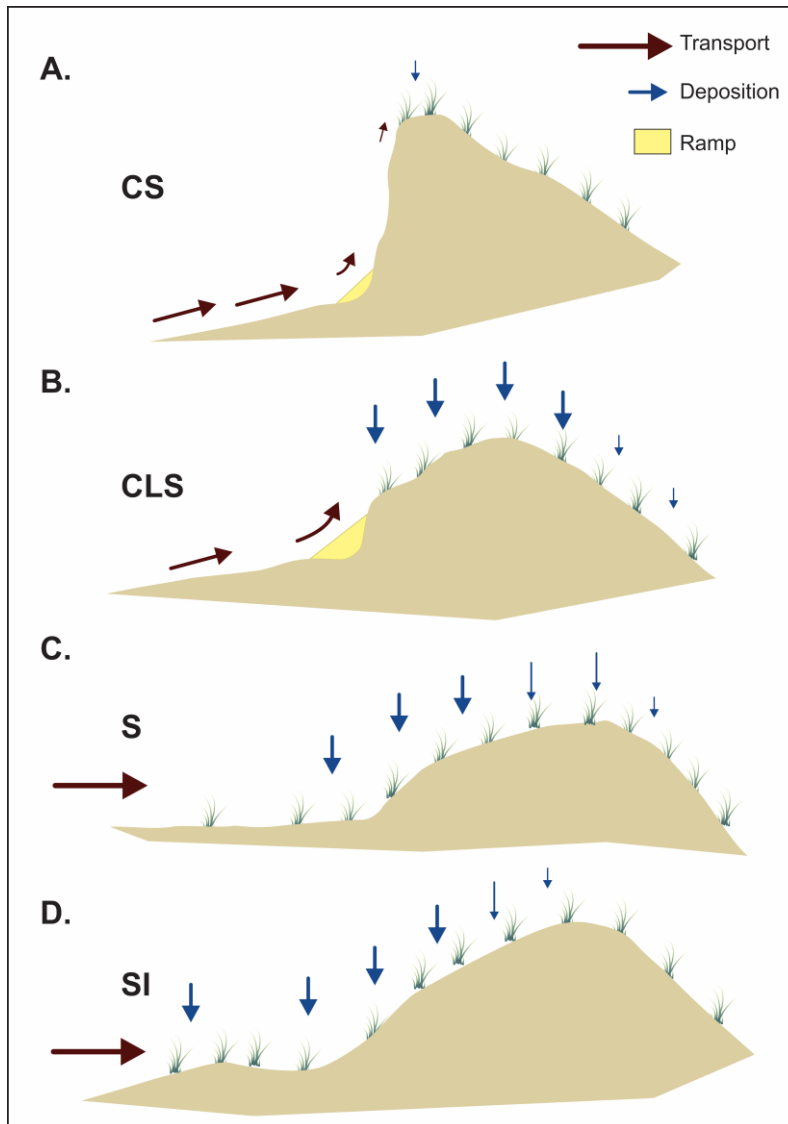
1499 events that yield aeolian transport, (ii) the magnitude and timing of storms that alter the beach
1500 configuration and potentially scarp the dune toe, (iii) the severity of winter temperature and
1501 snow cover conditions, (iv) the spatial variability in beach width at the plot scale due to surface
1502 moisture, wind approach angle, and foreshore accretion/erosion, and (v) landform scale
1503 variation in the littoral sediment budget. Similar patterns have been documented for many
1504 other mid-latitude coasts (e.g., Law and Davidson-Arnott, 1990; Byrne 1997, McKenna Neuman
1505 1990a, 1990b, 1993; Ruz and Allard, 1994; van Dijk and Law, 1995; 2003; Aagaard et al., 2004;
1506 Anthony et al., 2006; Pye and Blott, 2008; Yurk et al., 2014). A specific nuance that became
1507 evident in the PEI research, however, was the role of foredune scarping and the subsequent
1508 development of dune ramps in either precluding or facilitating the transfer of sand to the upper
1509 foredune slope. Similar observations were made by Christiansen (2003) and Christiansen and
1510 Davidson-Arnott (2004). Dune scarp and fill processes and ramp building are understood
1511 conceptually (e.g., Carter et al., 1990), although there are very few field studies of the
1512 processes involved. Plot-scale research on alongshore winds and topographic steering (section
1513 4.1.4) as well as seasonal-interannual topographic profile responses (Ollerhead et al. 2013,
1514 section 5.2.2) provide some insights. If the foredune is scarped, flow deflection may be
1515 significantly different near the scarp than for a non-scarped dune. Winds above the scarp may
1516 be deflected onshore towards the crest while wind flow seaward of the scarp may be deflected
1517 semi-parallel to the beach during oblique and alongshore winds (Hesp et al. 2013). These wind
1518 patterns likely result in dune ramp development because of extended fetch distances that
1519 mobilize sediment on the upper beach, which is deposited near the foredune toe to infill the

1520 eroded areas. Echo dune formation is also common at the base of scarps and is often the first
1521 stage of scarp fill development (Carter et al., 1990; Christiansen and Davidson-Arnott, 2004).
1522 Sand deposition in the lee of echo dunes occurs during onshore winds just above sand
1523 transport threshold and during more oblique winds. Additionally, slumping or avalanching of
1524 the scarp face can occur. All processes lead to infilling of the scarped zone and eventual
1525 rebuilding of the foredune toe ramp. Once the ramp is reconstructed, sediment pathways onto
1526 the stoss slope are re-established.

1527 A conceptual model based on the beach-dune interactions described above is shown in
1528 Figure 22 (see also specific intervals in Fig. 21), which illustrates the following associations: (i)
1529 when the foredune is cliffed and a relatively small ramp is present (CS), very little sediment
1530 reaches the dune crest or lee slope (e.g., Line 5 2006-07); (ii) where the dune is cliffed and a
1531 dune ramp extends over a substantial portion of the lower slope (CLS), moderate to large
1532 amounts of sediment can be delivered to the upper stoss slope, crest and lee slope (e.g., Line 6
1533 2002-03, 2003-04; Line 8 2005-06, 2006-07); (iii) where there is a continuous, vegetated stoss
1534 slope but no substantial incipient foredune (S), moderate amounts of sediment reach the upper
1535 stoss and crest and more limited amounts reach the lee slope (e.g., Line 6 2007-08; Line 7 2002-
1536 03, 2006-07); and (iv) where there is a continuous vegetation cover and a well-developed
1537 incipient foredune (SI), substantial amounts of sediment are trapped in the incipient dune and
1538 lower stoss slope, with small to moderate amounts reaching the crest and little if any reaching
1539 the lee slope (e.g., Line 6 2008-09; Line 7 2007-08, 2008-09; Line 8 2002-03, 2003-04). Further
1540 details of these responses are described in Ollerhead et al. (2013).

1541

1542 **Figure 22:** Conceptual diagram of the four characteristic foredune profile forms found at the
1543 study site. (A) "CS" is a fully cliffed form with stoss slope $> 40^\circ$ that results from high magnitude
1544 wave or storm surge erosion, whereas (B) "CLS" is a cliffed lower stoss slope form resulting
1545 from lower magnitude storms. A ramp may or may not be present at any given time. (C) "S" is a
1546 stoss slope form that has a continuous vegetated slope of $< 40^\circ$ from the dune toe to the crest
1547 and vegetation may extend onto the upper beach, while (D) "SI" is a stoss slope form that has a
1548 continuously vegetated slope and that is fronted by a vegetated incipient foredune that is
1549 capable of trapping significant quantities of aeolian sand transported off the beach. Modified
1550 from Ollerhead et al. (2013: Fig. 6).
1551



1552

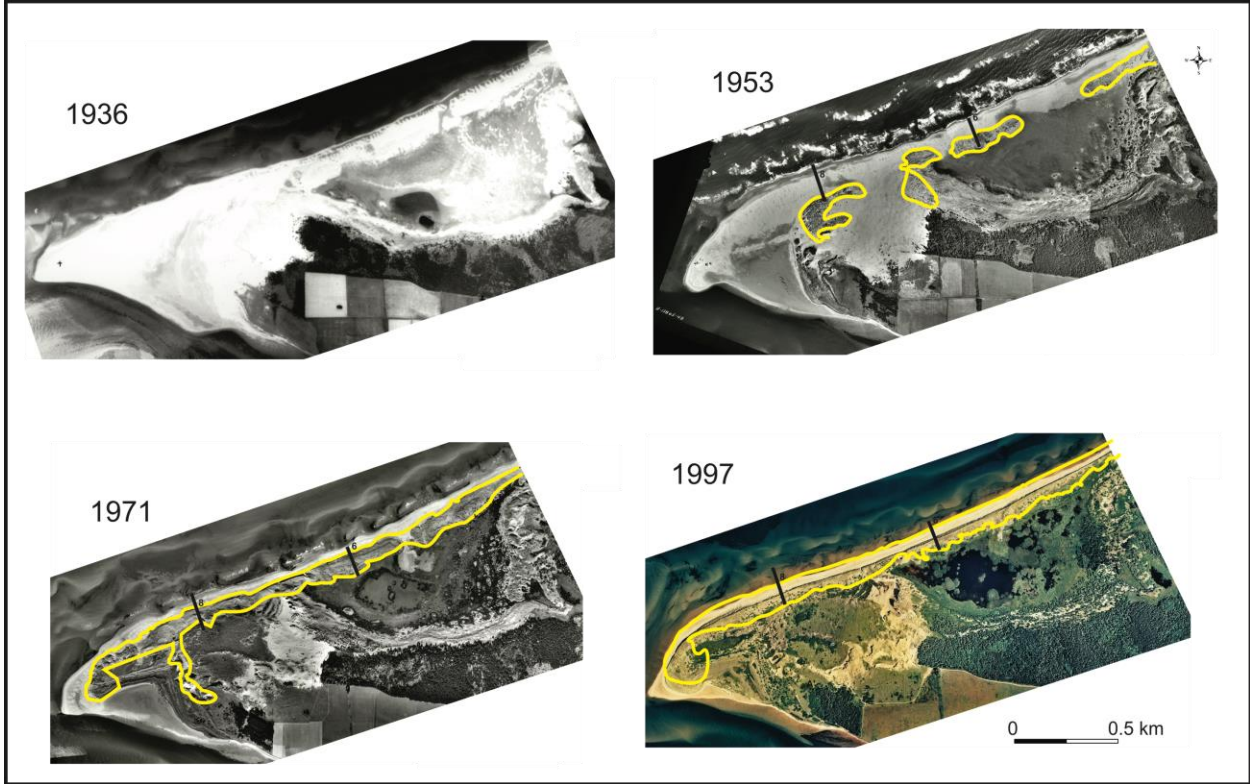
1553 *5.2.3. Decadal scale observations of extreme overwash and foredune recovery*

1554 The field surveying observations at the Greenwich Dunes, PEI site span a period of only one
1555 decade, yet, several major storms occurred during this time and resulted in significant erosion
1556 of the seaward base of the foredunes. The effects were often locally constrained, but in the
1557 winter of 2008-09, the entire shoreline of the study area (and beyond) experienced pronounced
1558 erosion. Barrier breaches and washover fans occurred elsewhere along the north shore of PEI,
1559 but the foredune at Greenwich was not breached. To place this event into context,
1560 examination of historical aerial photographs and local newspaper articles was conducted to see
1561 how often erosive storms had occurred in the past. This research indicated that foredune
1562 breaching had occurred historically, with a particularly intense storm accompanied by a very
1563 high storm surge documented in October 1923 (Mathew et al., 2010). During this time, the
1564 entire dune system along the Greenwich peninsula was eroded and overwashed, creating a
1565 continuous washover terrace that extended up to 600 m inland. Such inundation overwash is
1566 the most severe form of overwash (Sallenger, 2000; Morton, 2002; Donnelly et al., 2006) and
1567 signifies an extreme event in the spectrum of event magnitude. Moreover, evidence from
1568 elsewhere along the north shore of PEI (Simmons, 1982) indicates that this event destroyed the
1569 foredune over most, if not all, of the region. Evidence of this event provided an outstanding
1570 opportunity from which to assess rates of landform recovery (Wolman and Gerson, 1972) in a
1571 beach-dune system.

1572 Mathew et al. (2010) analyzed ortho-rectified mosaics of aerial photographs from 1936,
1573 1953, 1971, and 1997 and produced digital elevation models (DEMs) for each photo year.

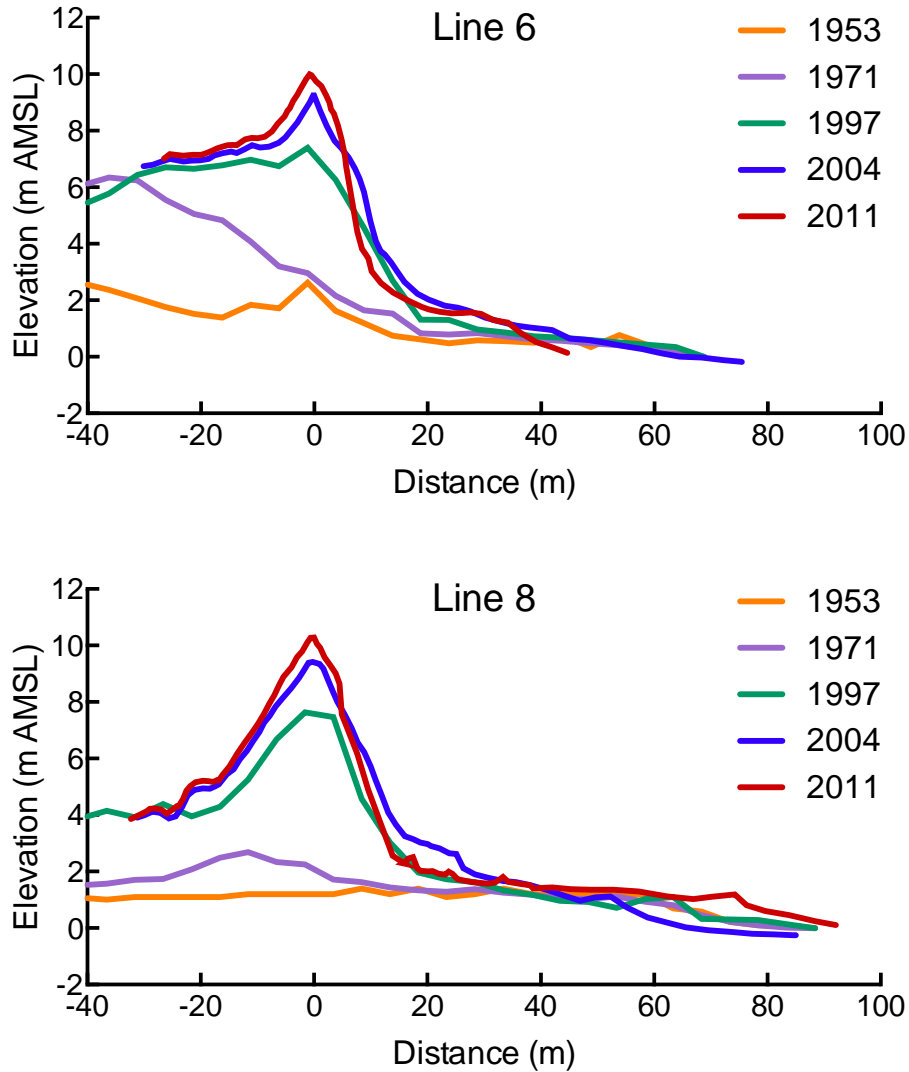
1574 Figure 23 shows the orthophoto mosaics for each year that were analyzed to assess landscape
1575 change and Figure 24 shows extracted topographic profiles at profile locations 6 and 8 (see Figs.
1576 1, 20). In 1936, over a decade after the storm, a wide, unvegetated intertidal zone and beach is
1577 seen with aeolian sand accumulating at the landward edge of the transgressive dunes. Relief
1578 landward of the beach along the shoreline was generally <1 m above mean sea level (aMSL).
1579 Between 1936 and 1953, vegetation established along much of the shoreline and initiated
1580 foredune development in some locations, although there were still several zones of active
1581 overwash. It is likely that the slow rate of vegetation establishment in this 20-year period
1582 reflects almost complete removal of pioneer vegetation by the storm and, thus, the absence of
1583 a nearby source of seeds or reproductive material to re-colonize the area. Less severe
1584 overwash events do not produce such intense 'sterilization' of the substrate (Saunders and
1585 Davidson-Arnott, 1990; Snyder and Boss, 2002). By 1971, a continuous, broad foredune was
1586 present along almost all of the shoreline with a relief of 2-6 m aMSL. In 1997, the foredune
1587 ridge had grown to 6-10 m aMSL and the crest was more continuous and located closer to the
1588 beach. Thus, while washover healing can take place in less than a decade for relatively small
1589 events (Cleary and Hosier, 1979), an event of the magnitude of the 1923 storm required more
1590 than five decades for recovery to a form similar to that found at the site today.
1591

1592 **Figure 23:** Historical aerial photographs showing landscape changes at Greenwich Dunes, PEI
1593 from 1936 to 1997. Locations of cross-shore profiles 6 and 8 (from Figures 1 and 20) are
1594 indicated as well as extent of established foredunes (yellow polygons). Cross-shore topography
1595 along profiles 6 and 8 extracted from the related stereo imagery is shown in Fig. 24. Modified
1596 from Mathew et al. (2010: Fig. 4).
1597



1598

1599 **Figure 24:** Cross-shore topographic profiles extracted from stereo aerial photography by
1600 Mathew et al. (2010) at lines 6 and 8 (see Figs. 1 and 20) from 1953 to 2011 depicting the
1601 extent of vertical accretion and foredune recovery following the major overwash event that
1602 occurred prior to 1936.



1603
1604 At both the plot and landform scale, the potential for foredune erosion and rebuilding at
1605 Greenwich, PEI is highly dependent on the frequency and magnitude of seasonal storm events,
1606 most of which occur in the fall and early winter months (Forbes et al., 2004). While a very large
1607 storm surge accompanied by large waves is necessary to produce the inundation overwash of

1608 the 1923 storm event, the impacts of smaller, less severe storms are also controlled by factors
1609 such as surfzone and beach slope and morphology, foredune height and morphology, littoral
1610 sediment budget, and the time interval between storms (e.g., Houser et al., 2008; Esteves et al.,
1611 2012; Heathfield et al., 2012; Hesp and Smyth, 2016b). The extent and severity of erosion from
1612 an individual storm cannot be predicted by modeling storm surge elevation and wave height
1613 alone. Other factors, such as the presence and effects of dune ramps and incipient dunes, all
1614 influence the extent of erosion and, subsequently, the rate and nature of dune recovery. There
1615 are now a number of approaches to modeling dune erosion and overwash from relatively
1616 simple models based on a few broad beach and water level parameters (e.g., Komar et al.,
1617 1999; Kriebel and Dean, 1993; Larson et al., 2004; Mull and Rugeiro, 2014) to much more
1618 computationally complex 2D cross-shore models such as XBeach (Roelvink et al., 2009; Splinter
1619 and Palmsten, 2012; de Winter et al., 2015) or 3D models such as SWAN offshore and XBeach in
1620 the nearshore (Dissanayake et al., 2014). Rigorous field-testing of these models, however,
1621 requires considerable data on morphology before and after the event, and of ongoing
1622 processes during the storm. None of these models adequately couple nearshore processes to
1623 aeolian processes in the true sense of beach-dune interaction. Very recently, Zhang et al. (2015)
1624 coupled a process-based nearshore model and a cellular automata aeolian model to simulate
1625 historical foredune change on the Baltic Coast. Due to the extent and limitations of model
1626 calibration, however, accurate prediction of future coastline change at scales of years to
1627 decades remains elusive.

1628

1629 **6. Landscape scale**

1630 In PEI, two controls dominate beach-dune morphodynamics and evolution at the landscape
1631 scale. First is the regional RSL trend, which has been rising at a rate of about 0.3 m century⁻¹ for
1632 the past 6,000 years. Second is the rapid erosion of relatively soft bedrock leading to recession
1633 rates of 0.3-1.0 m a⁻¹ and high sand supply to the littoral system (Forbes et al., 2004; Webster,
1634 2012). The focus of the PEI research at the landscape scale was on understanding the effects of
1635 the ongoing RSL transgression and the influence on the littoral and dune sediment budgets and
1636 resulting evolution of the beach-dune system. Two particular questions were addressed: 1)
1637 How do observations of decadal scale dune dynamics align with expected responses per the
1638 Bruun (1962) model of coastline response to sea-level rise?, and; 2) What is the nature of
1639 foredune morphological change (i.e., equilibrium shape and size), if any, associated with
1640 ongoing sea-level transgression?

1641 **6.1 The classic view of the response of coastlines to sea-level rise: the Bruun model**

1642 For decades, much effort has been centred on understanding and predicting the response
1643 of sandy coastal systems to sea-level rise using the “Bruun Rule” (Bruun, 1962; Schwartz, 1967;
1644 SCOR Working Group 89, 1991; Mimura and Nobuoka, 1995; List et al., 1997; Zhang et al., 2004;
1645 Pilkey and Cooper 2004; Rosati et al., 2013), which predicts that a sandy coast will respond to
1646 progressively rising sea levels by shoreline erosion and recession. The volume of eroded
1647 sediment is transported offshore and deposited as a layer with a thickness equal to the rise in
1648 sea level (Fig. 25). Thus, the sink for sediment is offshore, which implies that the sediment is
1649 lost to the nearshore system as further sea-level rise forces the wave-base upwards. In PEI,

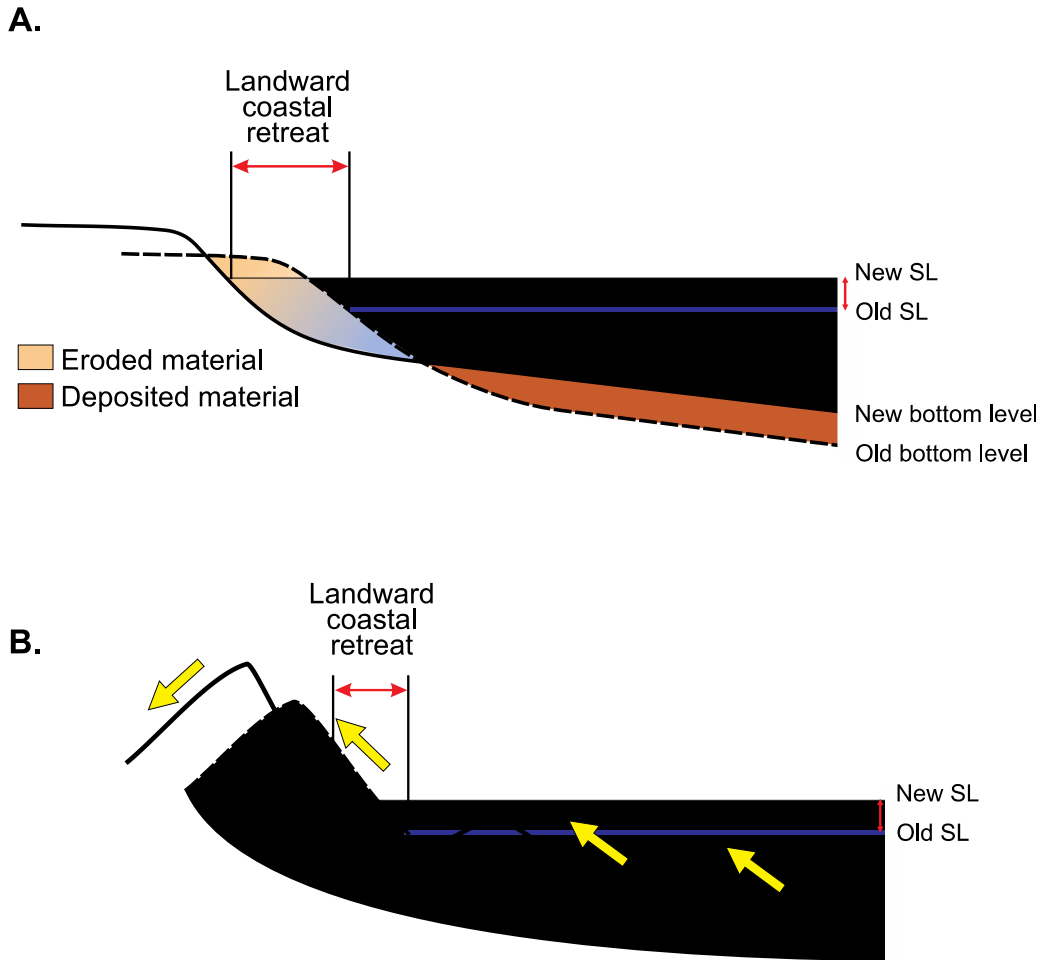
1650 sea-level rise over the past 6,000 years should have resulted in very large volumes of sand
1651 deposited in the nearshore. However, it is evident from surveys by Forbes et al. (2004) that the
1652 shoreface is sediment starved beyond the nearshore bar system. Furthermore, a huge volume
1653 of sediment is stored in inlet tidal deltas and in beach and dune deposits on the mainland or on
1654 barriers. Thus, the Bruun model appears not to apply to the PEI coastline, and similar
1655 conclusions have been reached for a handful of other coasts (e.g., Rosati et al., 2013; Aagaard,
1656 2014).

1657 6.2 A new perspective on the response of beach-dune systems to sea-level rise: the RD-
1658 A model

1659 Based on previous work on the dynamics of nearshore bar systems and research on beach-
1660 dune morphological changes in PEI, Davidson-Arnott (2005) proposed a conceptual model (aka
1661 the RD-A model) of the response of mainland sandy beach and dune systems to sea-level rise
1662 that envisions onshore migration of sediments in the nearshore and consequent landward and
1663 upward translation of the beach-dune profile. In the RD-A model, the primary sediment sinks
1664 are landward of the nearshore, not offshore, and the equilibrium nearshore profile is
1665 maintained as its spatial position migrates (Fig. 25).

1666

1667 **Figure 25:** Schematic illustrations of the Bruun (1962) model of beach profile response to rising
 1668 sea level (A) showing erosion of the upper beach and deposition in the nearshore to a thickness
 1669 equivalent to the rise in sea level, and the RD-A model (B) showing erosion and landward
 1670 migration of the nearshore profile and transgression of the beach and foredune under the same
 1671 amount of sea-level rise. Modified from Davidson-Arnott (2005: Figs. 1 and 2).
 1672



1673 It is now recognized from various lines of evidence that RSL on sandy coasts is generally
 1674 accompanied by erosion of sand from the outer shoreface and onshore transport resulting in
 1675 the accumulation of large sediment bodies on land and in shallow water. For instance, seismic
 1676 profiling and coring off the East and Gulf coasts of the USA and elsewhere in the world have
 1677 revealed that the Holocene transgression resulted in reworking and onshore transport of
 1678 sediments on the shelf as RSL rose, leading to the formation of ravinement surfaces that persist
 1679

1680 to the present (e.g., Belknap and Kraft, 1981; Niederoda et al., 1985; Siringan and Anderson,
1681 1994; Rodriguez et al., 2001; Dillenburg and Hesp, 2009; Goff, 2014; Schwab et al., 2014, Goff et
1682 al., 2015). This is also supported by recent analysis of shoreline change and profile evolution
1683 (e.g., Short, 2010; Schwab et al., 2013; Rosati et al., 2013; Houston and Dean, 2014).

1684 Sediment budget studies based on long-term monitoring and individual field experiments
1685 at Skallingen, Denmark, have shown that sand is transferred from the lower to upper shoreface
1686 in response to ongoing sea-level rise (Aagaard et al., 2004; Aagaard and Sorensen, 2012, 2013).
1687 These empirical studies are supported by numerical modeling of sand transport by wave events
1688 (Aagaard, 2014) at five different sites. A simulation of sand transport for one year using the
1689 model showed net sediment transfers that compared well to transport rates estimated from
1690 nearshore bar migration and aeolian accretion (Aagaard, 2014). This work provides a
1691 mechanism through which the landward transfer of sediments, necessary for translation of the
1692 nearshore profile in equilibrium with sea-level rise, occurs as envisaged by the RD-A model.

1693 There is also increasing recognition that on gently sloping coasts, landward translation of
1694 barriers often involves overwash and inlet processes that move large volumes of sediment
1695 landward (e.g., Dean and Mauremeyer, 1983; Rosati et al., 2013), such as the accretion of
1696 barriers on the east coast of Australia towards the end of the Holocene transgression (e.g., Roy
1697 et al., 1994; Hesp and Short, 1999; Cowell et al., 1995, 2003). On mainland dunes, landward
1698 translation of the foredune occurs by aeolian transport over the dune crest and deposition on
1699 the lee slope, as our annual surveys and other studies show (Ollerhead et al., 2013; Hesp and
1700 Walker 2013: Figs. 10 and 11, see also section 5.2.2). Appreciable amounts of sand may be

1701 transported tens of metres landward of the crest during strong wind events, thus providing a
1702 deposit over which the foredune can subsequently migrate (Arens, 1996; Aagaard et al., 2004;
1703 Christiansen and Davidson-Arnott, 2004; Hesp et al., 2009, 2013; Petersen et al., 2011;
1704 Ollerhead et al., 2013). This is also the mechanism by which landward transgressive dune
1705 systems can be fed (e.g., Anderson and Walker, 2006). According to the RD-A model, if the
1706 sediment budget is relatively neutral (e.g., Line 7), the beach-dune profile will translate
1707 landward in equilibrium with sea-level rise and the transgression distance, R , associated with
1708 the rise in sea level can be measured by migration of the dune toe position. In so doing, one
1709 would need to account for the local nearshore context over shorter time frames, as
1710 demonstrated by the variable responses observed in Fig. 20 (Line 5 to Line 8).

1711 The RD-A model is a simple 2-D model that is best applied to specific cases such as confined
1712 headland-bay beach systems where there are no significant alongshore transfers of sand. On
1713 most exposed coasts, however, it is necessary to consider the complexities introduced by
1714 negative or positive littoral sediment budgets and other factors that may influence the
1715 dynamics of beach-dune interaction locally. The positive littoral sediment budget at Line 8
1716 appears to have counter-balanced the landward translation of the profile due to RSL rise for at
1717 least a decade, while at Line 5, where the sediment budget is negative, ongoing translation of
1718 the shoreline is clearly taking place (Fig. 20). Although these associations are apparent when
1719 examining a decade of topographic profile changes, these trends may be significantly altered
1720 over periods of centuries. Thus, at the landscape scale, even a large overwash event such as

1721 the storm of 1923 can be viewed simply as part of the ongoing 'normal' processes leading to
1722 landward translation of the profile (Mathew et al., 2010) according to the RD-A model.

1723 On shorelines characterized by barriers, tidal inlets, estuaries, and lagoons with large
1724 accommodation space, the controls on shoreline displacement become highly complex. This
1725 applies to much of the north coast of PEI, to the east coast of the USA, and to areas such as the
1726 Wadden Sea in western Europe. In these situations, alongshore transfers and accommodation
1727 space in lagoons are major controls on coastal evolution and it is increasingly recognized that
1728 these 3D sediment transfers have to be modeled explicitly in order to understand the
1729 morphodynamic character of the beach-dune profile and nearshore system (e.g., Stive, 2004;
1730 Stive et al., 2009; Hinckel et al., 2013; Ranasinghe et al., 2013; Moore et al., 2014).
1731 Consideration must also be given to other factors that influence alongshore variations in post-
1732 storm dune recovery (e.g., Houser, 2013) such as controls imposed by shallow bedrock outcrops
1733 on the potential for shoreline transgression.

1734

1735 **7. Summary and Conclusions**

1736 7.1 The persistent challenges of scale in beach-dune geomorphology

1737 A continuing challenge for geomorphology, as with many multidisciplinary Earth sciences, is
1738 that most knowledge about how natural systems function is bounded by scale-specific
1739 constraints inherent to the theories, methodologies, and objects of study that are adopted or
1740 constructed in the scientific process. Occasionally, efforts are made to broaden perspectives by
1741 considering knowledge from closely allied fields or sub-fields, which often have different
1742 methodological and/or theoretical underpinnings. In so doing, a more nuanced understanding
1743 of the dynamics of natural systems is often derived that is informed by alternative perspectives
1744 and different scales of inquiry. This paper attempts to provide such a 'scale aware' perspective
1745 on coastal-aeolian morphodynamics and evolution, based in part on the vast literature on
1746 aeolian processes on coasts and deserts worldwide, but primarily on a decade-long research
1747 program at the Greenwich Dunes, PEI, Canada. This research program incorporated
1748 experimental and monitoring methods spanning the plot (micro), landform (meso), and
1749 landscape (macro) scales. It is argued that this approach has led to a more holistic (i.e., multi-
1750 scalar), focussed, and comprehensive (albeit incomplete) understanding of a discrete beach-
1751 dune system than has been undertaken previously.

1752 An example of the dilemma posed by the scalar boundedness of empirical geomorphic
1753 knowledge in this research is the disconnect in knowledge gained between the detailed process
1754 observations of sand transport activity and related beach-dune conditions (sections 5.1.2, 5.1.3)
1755 and the morphological response observations provided by the seasonal cross-shore beach-dune

1756 profiles (section 5.2.2). The former provides key information on the regime of sand transport,
1757 erosion, and deposition processes presumed to be representative at a seasonal scale, while the
1758 latter yields key insight on the magnitude and direction of seasonal to interannual topographic
1759 and sediment budget changes in the beach-dune system. Despite some spatial and temporal
1760 overlap (e.g., profile 7 exists in the area of coverage of the camera monitoring system) and the
1761 respective richness of these datasets, there remains significant scalar incompatibility or
1762 incompleteness between them. For instance, in the absence of information on how and when
1763 sediments were mobilized between all of the surveys and at all locations, it is only with much
1764 caution and many limitations that one can extrapolate how the temporally-limited and
1765 spatially-discrete observations of the transport regime might translate from seasonal or decadal
1766 trends in beach-dune morphology or sediment budgets. Similarly, it is incredibly difficult to
1767 retrodict prior system states that preconditioned the present observed conditions. So, despite
1768 great efforts here to span spatial and temporal scales of process-response interactions, there
1769 remain some appreciable gaps at scale transitions, in particular.

1770 7.2 Plot scale complexities encourage consideration of landscape scale linkages

1771 The plot scale research at the Greenwich Dunes, PEI, provided significant insights into the
1772 widely recognized inability of conventional sediment transport models to predict sand mass flux
1773 moving across the beach-dune system as a function of wind strength alone (e.g., Sherman and
1774 Li, 2011). Multiple supply-limiting constraints (e.g., surface moisture, grain size and texture,
1775 bed roughness, salt crusts, vegetation) and transport-limiting factors (e.g., vegetation, coarse
1776 lag deposits, wrack) collectively result in sand transport intermittency. Many of these factors,

1777 and their effects on sand transport, are spatially variable as the wind field transitions from the
1778 nearshore to the foreshore, across the back beach, and on to the foredune. However, the plot
1779 scale research also showed that these factors are coupled and co-evolve both in space and
1780 time, with often counter-intuitive outcomes depending on feedback relationships. For
1781 example, the veering of wind direction from cross-shore to oblique approach angles can
1782 strongly influence the delivery of sand to the foredune by way of the fetch effect. Generally,
1783 sand transport increases across the back beach due to increasing fetch distance, however, less
1784 may be delivered to the foredune because total sediment transport across the dune toe line
1785 decreases in proportion to the cosine of the wind angle (e.g., Bauer and Davidson-Arnott, 2003;
1786 Delgado-Fernandez, 2010). Similarly, as the incident wind begins to interact with foredune
1787 topography, and the vegetation thereon, there can be considerable changes in wind speed and
1788 direction as a result of flow deflection, streamline compression or expansion, flow acceleration
1789 or deceleration, vegetation density and distribution, and related secondary flow patterns (e.g.,
1790 flow steering, separation, reversal, jet formation) with significant implications for sand
1791 transport pathways (e.g., Walker et al., 2006; Walker et al., 2009a; 2009b; Bauer et al., 2012;
1792 Hesp et al., 2009; 2015; Hesp and Smyth, 2016). Turbulence within the boundary layer is
1793 influenced significantly by these wind-topography interactions and this research, along with the
1794 findings of other researchers, suggests there is some commonality in the turbulent signatures
1795 found at key locations such as the foredune crest and toe (e.g., Chapman et al., 2012; 2013;
1796 Wiggs et al., 1996b; Wiggs and Weaver, 2012). This work also indicates that there is sufficient
1797 uncertainty surrounding the association of turbulent Reynolds Stress with sand flux to question

1798 whether or not this parameter is a reliable indicator of wind strength for predicting aeolian
1799 sand transport over complex terrain.

1800 There also remain significant gaps in our knowledge with regard to how and when
1801 sediment is moved from the nearshore to the foreshore and, eventually, to the foredune
1802 (Houser, 2009; Houser and Ellis, 2013). Furthermore, it remains unclear as to what types of
1803 events are most significant in growing or maintaining foredunes. For instance, the importance
1804 of offshore winds in maintaining foredunes or contributing to the development of sand ramps
1805 and healing wave-cut dune scarps has become recognised increasingly (e.g., Jackson et al.,
1806 2011; Lynch et al., 2009; 2010; Bauer et al., 2015). Other external factors such as wave run-up,
1807 tidal and storm surge inundation, salt spray, rainfall, snow/ice cover, and progressive
1808 sediment stripping and deflation during transport events also present spatial and temporal
1809 complexities in the aeolian sand transport process. At times, therefore, it is possible to have
1810 some portions of the beach where there is no transport because wind strength is insufficient to
1811 entrain sediments, other portions where wind strength is adequate but surface controls restrict
1812 the rate of sand supply (leading to intermittency), and yet other areas where there is sufficient
1813 wind and sand available to yield substantial transport. All of the complexities resulting from
1814 flow-landform-transport interactions over beaches and dunes at the time scales of single events
1815 and seasons, thus, begot consideration of broader landscape scale controls.

1816 7.3 Bridging the plot to landform scale transition

1817 In response to the complexities at work at the plot scale, standard equilibrium models of
1818 sand transport often fail to produce accurate estimates across beaches and over foredunes.

1819 This serves as a reminder that conceptualizing and modelling sediment transport across beach-
1820 dune systems as controlled by singular factors in isolation is an inadequate approach. The
1821 collective body of research reviewed in this paper also highlights how information about the
1822 broader (landform scale) context is critically important. The conceptual scheme in Table 1
1823 shows that, in order to understand sediment transport rate and patterns of erosion and
1824 deposition across the beach (i.e., the dependent variables), one requires knowledge of the
1825 independent variables (e.g., wind speed, wind approach angle, surface debris, vegetation, salt
1826 crusts, surface moisture, snow or ice cover, beach width and slope) as well as knowledge of a
1827 few key parameters such as foredune size and geometry and vegetation species, distribution,
1828 cover density, height, and morphology. However, at the landform scale, these all become
1829 dependent variables (i.e., things we want to predict or better understand) that are governed by
1830 a range of independent variables (e.g., wave climatology, climatic conditions, geological
1831 setting). In turn, these independent variables dictate the overall supply of sediment available
1832 for beach-dune development. In other words, to improve understanding of sediment transport
1833 and beach-dune morphodynamics at a particular site, landform-scale factors that influence
1834 plot-scale dynamics must be factored in. Essentially, a typology of events is required that
1835 distinguishes them according to their character and effectiveness in yielding geomorphic
1836 change on the beach-dune profile, and that includes information on their magnitude,
1837 frequency, and duration of occurrence.

1838 The research at Greenwich Dunes attempted to provide information that links the plot
1839 scale to the landform scale. For example, the monitoring and modelling work of Delgado-

1840 Fernandez and Davidson-Arnott (2011) and Delgado-Fernandez et al. (2009, 2012, 2013a)
1841 demonstrates that a simple aeolian transport regime assessment, such as the Fryberger and
1842 Dean (1979) model, is inadequate for predicting long-term sand supply to foredunes as it does
1843 not consider the range of supply-limiting conditions in coastal regions that occur. For instance,
1844 intense winter storm events with powerful winds, which would yield significant transport per
1845 the Fryberger and Dean (1979) model, are often insignificant in terms of sediment delivery to
1846 the foredunes simply because the beach is covered by snow and ice. Similarly, strong wind
1847 events must also be considered in relation to the surface moisture state of the beach, which is
1848 controlled by precipitation amounts, relative humidity, solar forcing, tidal stage, and storm
1849 surge. During the nine-month photographic observation period of transport activity at the PEI
1850 study site, only three (of 184) wind events accounted for 75% of the total sand delivered to the
1851 foredune. Sand transport over the foredune was further influenced by the density of
1852 vegetation cover (Ollerhead et al., 2013), which also has a seasonal signature that must be
1853 accounted for in long-term modelling.

1854 7.4 Bridging the landform to landscape scale transition

1855 The transition from landform to landscape scales is similarly critical, as demonstrated by
1856 the cross-shore profiles measured for over a decade at the Greenwich Dunes site (Figure 20).
1857 Some regions (e.g., line 5) suggest a continuous and progressive landward migration of the
1858 dune with little change in overall profile form. In contrast, other sites (e.g., line 8) shows a
1859 relatively stable crest location with seaward progradation of the stoss slope, while others (e.g.,
1860 line 7) remained stable and virtually unchanged. This suggests a transition from a negative

1861 littoral sediment budget to the East (line 5) to a positive budget to the west (line 8). Clearly, a
1862 linear extrapolation of any individual trend from these locations would suggest very different
1863 styles of shoreline evolution over the next century. Thus, the littoral sediment budget affects
1864 the beach width, which in turn influences: i) the fetch effect and, hence, potential sediment
1865 delivery to the foredune as well as, ii) the propensity for wave scarping of the dune toe during
1866 high water storm events. The presence of a scarp or a sand ramp at the base of the dune also
1867 strongly influences the ability of sand to move onto the stoss slope and toward the dune crest.

1868 To understand how this coastline might evolve over the next century requires additional
1869 information at the landscape scale on rates of relative sea-level rise, the broader geological
1870 context of the north shore of PEI, as well as the history of regional coastal change as
1871 documented in archives (e.g., Mathew et al. 2006) and via proxy data in the sedimentological
1872 record. As uniformitarianism would suggest, these are perhaps our best indicators of what may
1873 happen in the future, but ideally this information could be integrated back into the landform
1874 scale and then to the plot scale, so as to provide a deeper understanding of how we might
1875 reliably predict the future rather than simply extrapolate trends. For example, framing the
1876 understanding of coastline evolution within the RD-A model for the response of sandy beach-
1877 dune systems under rising sea levels challenges scientists to predict the events that yield the
1878 landward (and upward) translation of the beach-dune profile from year-to-year. In turn, this
1879 requires the capacity to predict the nature of sediment transport processes across beach-dune
1880 systems at the plot scale, which leads us back to the uncertain nature of the relation between
1881 sediment flux and wind strength.

1882 Much has been written about the unlikely prospects for 'upscaling' micro-scale knowledge
1883 of Earth surface system function obtained via scientific reductionism to macro-scale system
1884 outcomes (e.g., Sherman, 1995; Bauer and Sherman, 1999; Bauer et al., 1999), especially in
1885 light of such challenges as error propagation in models, chaotic behavior in non-linear systems,
1886 and climate non-stationarity. One might ask then, "If we are doing science in the service of
1887 coastal resource managers who are interested primarily in landform and landscape scale
1888 outcomes, why even bother with plot-scale experiments?" The answer, it seems, is to provide a
1889 more holistic understanding of the system under investigation (or under management), in
1890 terms of the range of processes, feedbacks, controls, and linkages between scales of
1891 interaction, to thereby reduce the probability of making incorrect assumptions or predictions
1892 about the future. Knowledge and understanding at each of the scale domains is not
1893 independent of the other, and there has to be consilience or unity of knowledge (Wilson, 1998).
1894 So, from a management perspective, given the increasing pressures and impacts of global
1895 climatic and environmental change, there is a clear need for more applied, integrated, multi-
1896 scalar knowledge. Ignoring the context provided by knowledge at shorter and longer scales
1897 then seems like a perilous course of action.

1898

1899 **8. Acknowledgements**

1900 Foremost, the authors acknowledge the incredible research partnership and support
1901 provided by Parks Canada Agency (PCA) at the Greenwich Dunes in Prince Edward Island (PEI)
1902 National Park. PCA staff A. Doyle (Maintenance Supervisor), D. Lajeunesse and K. Tulk (Park
1903 Ecologists), and R. Steadman and P. McCabe (Wardens) provided invaluable assistance and
1904 encouragement throughout our years of research. A multitude of student researchers and
1905 assistants were also instrumental to this work, including: R. Bams, J. Booth, C. Chapman, I.
1906 Darke, P. Johnson, G. Manson, L. Olsen, K. Pearce, K. Penrose, A. Pons, K. Powell, H. Rhew, R.
1907 Smith, M. Sojan, M. Trites, and Y. Yang. The research was supported financially by grants from
1908 PCA-PEI National Park to R. Davidson-Arnott, J. Ollerhead and I. Walker with additional research
1909 funding from the Natural Sciences and Engineering Research Council of Canada (NSERC)
1910 Discovery Grant and Special Research Opportunities programs to Davidson-Arnott, Ollerhead,
1911 and Walker. I. Walker also recognizes research infrastructure support from the Canada
1912 Foundation for Innovation (CFI) Leader's and New Opportunities programs and support from
1913 UVic and Arizona State University. B. Bauer acknowledges support from UBC-Okanagan and P.
1914 Hesp recognizes contributions from Flinders University, LSU, and the U.S. National Science
1915 Foundation (NSF). J. Ollerhead recognizes logistical support from the Mount Allison Coastal
1916 Wetlands Institute, funded by CFI. I. Delgado-Fernandez acknowledges substantial support
1917 from the University of Guelph and funding from the Ontario Graduate Scholarship program. T.
1918 Smyth recognizes recognizes support from Flinders University and Liverpool Hope University.

1919 Incredibly helpful graphical assistance was provided by M. Puddister and fantastic technical
1920 support with instrumentation by M. Finoro and S. McLean. Finally, we thank T. Horscroft of
1921 Elsevier for the invitation to provide this review as well as two anonymous reviewers and the
1922 Associate Editor who provided constructive comments that vastly improved the manuscript.
1923

1924 **9. References**

- 1925 Aagaard, T., 2014. Sediment supply to beaches: Cross-shore sand transport on the lower
1926 shoreface, *J. Geophys. Res-Earth*. 119. doi:10.1002/2013JF003041.
- 1927 Aagaard, T., Davidson-Arnott, R., Greenwood B., Nielsen, J. 2004. Sediment supply from
1928 shoreface to dunes: linking sediment transport measurements and long term
1929 morphological evolution. *Geomorphology* 60, 205-224.
- 1930 Aagaard, T., Sørensen, P., 2012. Coastal profile response to sea level rise: a process-based
1931 approach. *Earth Surf. Proc. Land*. 37, 354-362.
- 1932 Aagaard, T., Sørensen, P., 2013. Sea level rise and the sediment budget of an eroding barrier on
1933 the Danish North Sea coast. *J. Coastal Res. Special Issue No. 65*.
- 1934 Anderson, R.S., Haff, P.K., 1991. Wind modification and bed response during saltation of sand in
1935 air. *Acta Mech. Supplementum* 1, 21–52.
- 1936 Anderson, J.L., Walker, I.J., 2006. Airflow and sand transport variations within a backshore-
1937 parabolic dune plain complex: NE Graham Island, British Columbia, Canada.
1938 *Geomorphology* 77, 17–34.
- 1939 Anthony, E. J., Vanhee, S., Ruz, M., 2006. Short-term beach-dune sand budgets on the North
1940 Sea coast of France: Sand supply from shoreface to dunes, and the role of wind and
1941 fetch. *Geomorphology* 81, 316-329.
- 1942 Arens, B., 1996. Rates of aeolian sand transport on a beach in a humid temperate climate.
1943 *Geomorphology* 17, 3–18.
- 1944 Arens, S.M., 1996a. Patterns of sand transport on vegetated foredunes. *Geomorphology* 17,
1945 339–350.
- 1946 Arens, S.M., 1996b. Sediment dynamics of a coastal foredune at Schiermonnikoog, The
1947 Netherlands. In: Jones, P.S., Healy, M.G., Williams, A.T. (Eds.), *Studies in European*
1948 *Coastal Management*. Samara Publishing, Cardigan. pp. 137–146.
- 1949 Arens, S.M., Kaam-Peters, V., Van Boxel, J.V., 1995. Air flow over foredunes and implications for
1950 sand transport. *Earth Surf. Proc. Land*. 20(4), 315-332.
- 1951 Arens, S.M., van Kaam, P., van Boxel, J.H., 1995. Airflow over foredunes and implications for
1952 sand transport. *Earth Surf. Proc. Land*. 20, 315-325.
- 1953 Atherton, R.J., Baird, A.J., Wiggs, G.F.S., 2001. Inter-tidal dynamics of surface moisture content
1954 on a meso-tidal beach. *J. Coastal Res.* 17, 482–489.
- 1955 Baas, A.C.W., 2002. Chaos, fractals and self-organization in coastal geomorphology: simulating
1956 dune landscapes in vegetated environments. *Geomorphology*, 48(1–3), 309–328.

- 1957 Baas, A.C.W., 2003. The formation and behavior of aeolian streamers. PhD thesis, University of
1958 Southern California, Los Angeles, CA. 412 pp.
- 1959 Baas, A.C.W., 2004. Evaluation of saltation flux impact responders (Safires) for measuring
1960 instantaneous aeolian sand transport intensity. *Geomorphology* 59, 99–118.
- 1961 Baas, A.C.W., 2006. Wavelet power spectra of aeolian sand transport by boundary layer
1962 turbulence. *Geophys. Res. Lett.* 33, L05403.
- 1963 Baas, A.C.W., Nield, J.M., 2007. Modelling vegetated dune landscapes. *Geophysical Research*
1964 *Letters*, 34(6), L06405.
- 1965 Baas, A.C.W., Nield, J.M., 2010. Ecogeomorphic state variables and phase-space construction
1966 for quantifying the evolution of vegetated aeolian landscapes. *Earth Surf. Proc. Land.*
1967 35(6), 717-731.
- 1968 Baas, A.C.W., Sherman, D.J., 2005a. Formation and behaviour of aeolian streamers. *J. Geophys.*
1969 *Res-Earth.* 110, F13011.
- 1970 Baas, A.C.W., Sherman, D.J., 2005b. Spatiotemporal variability of aeolian sand transport in a
1971 coastal dune environment. *J. Coastal Res.*, 1198–1205.
- 1972 Baddock, M.C., Wiggs, G.F.S., Livingstone, I., 2011. A field study of mean and turbulent flow
1973 characteristics upwind, over and downwind of barchan dunes. *Earth Surf. Proc. Land.*
1974 36(11), 1435-1448.
- 1975 Bagnold, R.A., 1941. The physics of blown sand and desert dunes. Methuen, London. 265 pp.
- 1976 Barchyn, T.E., Hugenholtz, C.H., 2010. Field comparison of four piezoelectric sensors for
1977 detecting aeolian sediment transport. *Geomorphology* 120, 368–371.
- 1978 Barchyn, T.E., Hugenholtz, C.H., Li, B., McKenna Neuman, D., Sanderson, R.S., 2014. From
1979 particle counts to flux: wind tunnel testing and calibration of the ‘Wenglor’ Aeolian
1980 sediment transport sensor. *Aeolian Res.* 15, 311–318.
- 1981 Bauer, B.O., Namikas, S.L., 1998. Design and field test of a continuously weighing, tipping-
1982 bucket assembly for aeolian sand traps. *Earth Surf. Proc. Land.* 23, 1171-1183.
- 1983 Bauer, B.O., Sherman, D.J., 1999. Coastal dune dynamics: problems and prospects. In: Goudie,
1984 A.S., Livingstone, I., Stokes, S. (Eds.), *Aeolian Environments, Sediments and Landforms.*
1985 Wiley, Chichester. pp. 71–104.
- 1986 Bauer, B.O., Davidson-Arnott, R.G.D., 2014. Aeolian particle flux profiles and transport
1987 unsteadiness. *J. Geophys. Res-Earth.* 119, doi:10.1002/2014JF003128
- 1988 Bauer, B.O., Sherman, D.J., Nordstrom, K.F., Gares, P.A., 1990. Aeolian transport measurement
1989 and prediction across a beach and dune at Castroville, California. In: Nordstrom, K.F.,
1990 Psuty, N.P., Carter, R.W.G. (Eds.), *Coastal Dunes: Form and Process.* John Wiley,
1991 Chichester. pp. 39–55.

- 1992 Bauer, B.O., Davidson-Arnott, R.G.D., Nordstrom, K.F., Ollerhead, J., Jackson, N.L., 1996.
 1993 Indeterminacy in aeolian sediment transport across beaches. *J. Coastal Res.* 12, 641–
 1994 653.
- 1995 Bauer, B.O., Yi, J., Namikas, S.L., Sherman, D.J., 1998. Event detection and conditional averaging
 1996 in unsteady aeolian systems. *J. Arid Environ.* 39, 345–375.
- 1997 Bauer, B.O., Veblen, T.T., and Winkler, J.A., 1999. Old methodological sneakers: fashion and
 1998 function in a cross-training era. *Annals of the Association of American Geographers*
 1999 89(4): 679-687.
- 2000 Bauer, B.O., Davidson-Arnott, R.G.D., 2003. A general framework for modelling sediment supply
 2001 to coastal dunes including wind angle, beach geometry and fetch effects.
 2002 *Geomorphology* 49, 89–108.
- 2003 Bauer, B.O., Houser, C.A., Nickling, W.G., 2004. Analysis of velocity profile measurement from
 2004 wind tunnel experiments with saltation. *Geomorphology* 59, 81-98.
- 2005 Bauer, B.O., Davidson-Arnott, R.G.D., Hesp, P.A., Namikas, S.L., Ollerhead, J., Walker, I.J., 2009.
 2006 Aeolian sediment transport on a beach: surface moisture, wind fetch, and mean
 2007 transport. *Geomorphology* 105, 106–116.
- 2008 Bauer, B.O., Davidson-Arnott, R.G.D., Walker, I.J., Hesp, P.A., Ollerhead, J., 2012. On the
 2009 importance of wind direction as a primary control on sediment transport response
 2010 across a beach-dune system. *Earth Surf. Proc. Land.* 37, 1661-1677.
 2011 doi:10.1002/esp.3306.
- 2012 Bauer, B.O., Walker, I.J., Baas, A.C.W., Jackson, D.W.T., McKenna Neumann, C., Wiggs, G.F.S.,
 2013 Hesp, P.A., 2013. Critical reflections on the Coherent Flow Structures paradigm in
 2014 aeolian geomorphology. Chapter 8. In: Venditti, J.G., Best, J.L., Church, M., and Hardy,
 2015 R.J., (Eds.), *Coherent Flow Structures at Earth's Surface*. John Wiley and Sons, Ltd. pp
 2016 111-134.
- 2017 Bauer, B.O., Hesp, P.A., Walker, I.J., Davidson-Arnott, R.G.D., 2015. Sediment transport
 2018 (dis)continuity across a beach–dune profile during an offshore wind event.
 2019 *Geomorphology* 245, 135–148.
- 2020 Belknap, D.F., Kraft, J.C., 1981. Preservation potential of transgressive coastal lithosomes on the
 2021 U.S. Atlantic shelf. *Mar. Geol.* 42, 429–442.
- 2022 Bennett, S.J., Best, J.L., 1995. Mean flow and turbulence structure over fixed, two- dimensional
 2023 dunes: implications for sediment transport and bedform stability. *Sedimentology* 42,
 2024 491–514.
- 2025 Best, J.L., 1993. On the interactions between turbulent flow structure, sediment transport and
 2026 bedform development: some considerations from recent experimental research. In:
 2027 Clifford, N.J., French, J.R., Hardisty, J., (Eds.), *Turbulence: Perspectives on Flow and*
 2028 *Sediment Transport*. Wiley, Chichester. pp. 61–92.

- 2029 Best, J.L., Kostaschuk, R.A., 2002. An experimental study of turbulent flow over a low-angle
2030 dune. *J. Geophys. Res-Earth*. 107, 929–955.
- 2031 Beyers, J.H.M., Jackson, D.W.T., Lynch, K., Cooper, J.A.G., Baas, A.C.W., Delgado-Fernandez, I.,
2032 Pierre-Olivier, D., 2010. Field testing and CFD LES simulation of offshore wind flows over
2033 coastal dune terrain in Northern Ireland. Fifth International Symposium on
2034 Computational Wind Engineering (CWE2010), North Carolina, US. May 23-27.
- 2035 Bigarella, J.J., 1979. Structural features at Lagoa dune field, Brazil. McKee (Ed.), *A Study of*
2036 *Global Sand Seas*. USGS Prof. Paper. 1052, 114-133.
- 2037 Blumberg, D.G., Greeley, R., 1996. A comparison of general circulation model predictions to
2038 sand drift and dune orientations. *J. Climatol.* 9, 3248–3259.
- 2039 Bowen A.J., Lindley D., 1977. A wind-tunnel investigation of the wind speed and turbulence
2040 characteristics close to the ground over various escarpment shapes. *Bound-Lay.*
2041 *Meteorol.* 12, 259–271.
- 2042 Bradley, E.F., 1983. The influence of thermal stability and angle of incidence on the acceleration
2043 of wind up a slope. *J. Wind Eng. Ind. Aerod.* 15, 231–242.
- 2044 Bristow, C.S., Chroston, P.N., Bailey, S.D., 2000. The structure and development of foredunes on
2045 a locally prograding coast: insights from ground-penetrating radar surveys, Norfolk,
2046 UK. *Sedimentology* 47(5), 923-944.
- 2047 Bruun, P., 1962. Sea level rise as a cause of shore erosion. *Journal of Waterways and Harbors*
2048 *Division, ASCE* 88, 117-130.
- 2049 Bryan, K.R., Kench, P.S., Hart., D.E., 2008. Multi-decadal coastal change in New Zealand:
2050 evidence, mechanisms and implications. *New Zeal. Geogr.* 64, 117–128.
- 2051 Bullard, J.E., 1997. A note on the use of the Fryberger method for evaluating potential sand
2052 transport by wind. *J. Sediment. Res.* 67 (3A), 499–501.
- 2053 Butterfield, G.R., 1991. Grain transport rates in steady and unsteady turbulent airflows. In:
2054 Barndorff-Nielsen, O.E., Willets, B.B. (Eds.), *Aeolian Grain Transport 1: Mechanics*.
2055 Springer-Verlag, Wien, *Acta Mech. Supplement* 1, 97–122.
- 2056 Butterfield, G.R., 1999. Near-bed mass flux profiles in aeolian sand transport: High-resolution
2057 measurements in a wind tunnel, *Earth Surf. Proc. Land.* 24, 393–412.
- 2058 Byrne, M.L., 1997. Seasonal sand transport through a trough blowout at Pinery Provincial Park,
2059 Ontario. *Can. J. Earth Sci.* 34, 1460–1466.
- 2060 Carson, M.A., Maclean, P.A., 1986. Development of hybrid Aeolian dunes: the William River
2061 dune field, Northwest Saskatchewan, Canada. *Can. J. Earth Sci.* 23 (12), 1974–1990.

- 2062 Carter, R.W.G., Hesp, P.A., Nordstrom, K., 1990. Geomorphology of erosional dune landscapes.
2063 In: Nordstrom, K., N. Psuty and R.W.G. Carter (Editors), Coastal Dunes: Processes and
2064 Morphology: 217-250. J. Wiley and Sons.
- 2065 Chapman, C.A., Walker, I.J., Hesp, P.A., Bauer, B.O., Davidson-Arnott, R.G.D., 2012. Turbulent
2066 Reynolds Stress and quadrant event activity in wind flow over a coastal foredune,
2067 Geomorphology 151-152, 1-12: doi: 10.1016/j.geomorph.2011.11.015
- 2068 Chapman, C.A., Walker, I.J., Hesp, P.A., Bauer, B.O., Davidson-Arnott, R.G.D., Ollerhead, J., 2013.
2069 Reynolds Stress and sand transport over a vegetated foredune, Earth Surf. Proc. Land.
2070 38, 1735–1747: DOI: 10.1002/esp.3428.
- 2071 Chapman, D.M., 1990. Aeolian sand transport - an optimized model. Earth Surf. Proc. Land. 15,
2072 751–760.
- 2073 Chepil, W.S., Milne, R.A., 1939. Comparative study of soil drifting in the field and in a wind
2074 tunnel. Science and Agriculture 19, 249–257.
- 2075 Christiansen, M.B., 2003. Effects of dune ramps on sediment supply to coastal foredunes:
2076 Skallingen, SW Denmark. Proceedings Coastal Sediments 2003. CD-ROM Published by
2077 World Scientific Publishing Corp. and East Meets West Productions, Texas, USA.
- 2078 Christiansen, M.B., Davidson-Arnott, R.G.D., 2004. The effects of dune ramps on sediment
2079 supply to coastal foredunes, Skallingen Denmark. Geografisk Tidsskrift. Danish Journal of
2080 Geography 104, 29-41.
- 2081 Cleary, W.J., Hosier, P.E., 1979. Geomorphology, washover history, and inlet zonation: Cape
2082 Lookout, N.C. to Bird Island, N.C. In: Leatherman, S.P. (Ed.) Barrier Islands: from the Gulf
2083 of St. Lawrence to the Gulf of Mexico. Academic Press. New York, pp. 237-271.
- 2084 Coldwater Consulting, 2011. Geomorphic Shoreline Classification of Prince Edward Island.
2085 Report prepared for Prince Edward Island Department of Environment, Energy and
2086 Forestry, Charlottetown, PEI and the Atlantic Climate Adaptation Solutions Association,
2087 66 pp.
- 2088 Cowell, P.J., Roy, P.S., Jones, R.A., 1995. Simulation of large-scale coastal change using a
2089 morphological behaviour model. Mar. Geol. 126, 45-61.
- 2090 Cowell, P.J., Stive, M.J.F., Niedoroda, A.W., de Vriend, H.J., Swift, D.J.P., Kaminsky, G.M.,
2091 Capobianco, M., 2003. The coastal-tract (part 1): a conceptual approach to aggregated
2092 modeling of low-order coastal change. J. Coastal Res. 19, 812–827.
- 2093 Darke, I., Davidson-Arnott, R.G.D., Ollerhead, J., 2009 Measurement of beach surface moisture
2094 using surface brightness. J. Coastal Res. 25, 248–256.
- 2095 Darke, I., McKenna Neuman, C., 2008. Field study of beach water content as a guide to wind
2096 erosion potential. J. Coastal Res. 24, 1200– 1208.

- 2097 Davidson-Arnott, R.G.D., 2005. A conceptual model of the effects of sea-level rise on sandy
2098 coasts. *J. Coastal Res.* 21, 1166-1172.
- 2099 Davidson-Arnott, R.G.D., Bauer, B.O., 2009. Aeolian sediment transport on a beach: Thresholds,
2100 intermittency, and high frequency variability. *Geomorphology* 105, 117-126.
- 2101 Davidson-Arnott, R.G.D., Bauer, B.O, Walker, I.J. Hesp, P.A., Ollerhead, J., Chapman, C., 2012.
2102 High-frequency sediment transport responses on a vegetated foredune. *Earth Surf. Proc.*
2103 *Land.* 37, 1227-1241. DOI: 10.1002/esp.3275.
- 2104 Davidson-Arnott, R.G.D., Bauer, B.O., Walker, I.J., Hesp, P.A., Ollerhead, J., Delgado-Fernandez,
2105 I., (2009), Instantaneous and mean aeolian sediment transport rate on beaches: An
2106 intercomparison of measurements from two sensor types, *J. Coastal Res.* SI 56, 297-301.
- 2107 Davidson-Arnott, R.G.D., Dawson, J.D., 2001. Moisture and fetch effects on rates of aeolian
2108 sediment transport, Skallingen, Denmark. *Proceedings Canadian Coastal Conference,*
2109 *Quebec City. CCSEA,* pp. 309–321.
- 2110 Davidson-Arnott, R.G.D., Law, M.N., 1990. Seasonal patterns and controls on sediment supply
2111 to coastal foredunes, Long Point, Lake Erie. In: Nordstrom, K.F., Psuty, N.P. and Carter,
2112 R.W.G. (Eds.), *Coastal Dunes: Form and Process.* John Wiley and Sons, pp. 177-200.
- 2113 Davidson-Arnott, R.G.D., Law, M.N., 1996. Measurement and prediction of long-term sediment
2114 supply to coastal foredunes. *J. Coastal Res.* 12, 654-663.
- 2115 Davidson-Arnott, R.G.D., McQuarrie, K., Aagaard, T., 2005. The effects of wind gusts on aeolian
2116 sediment transport on a beach. *Geomorphology* 68, 115–129.
- 2117 Davidson-Arnott, R.G.D., Stewart, C.J., 1987. The effect of longshore sandwaves on dune
2118 erosion and accretion, Long Point, Ontario. *Proceedings Canadian Coastal Conference,*
2119 *National Research Council of Canada,* pp. 131-144.
- 2120 Davidson-Arnott, R.G.D., van Heyningen, A., 2003. Migration and sedimentology of longshore
2121 sandwaves, Long Point, Lake Erie, Canada. *Sedimentology* 50, 1123-1137.
- 2122 Davidson-Arnott, R.G.D., Yang, Y., Ollerhead, J., Hesp, P.A., Walker, I.J., 2008. The effects of
2123 surface moisture on aeolian sediment transport threshold and mass flux on a beach.
2124 *Earth Surf. Proc. Land.,* 55-74.
- 2125 de Vries, S., van Thiel de Vries, J.S.M., van Rijn, L.C., Arens, S.M., Ranasinghe, R., 2014. Aeolian
2126 sediment transport in supply limited situations. *Aeolian Res.* 12, 75-85.
- 2127 de Winter, R.C., Gongriep, F., Ruessink, B.G., 2015. Observations and modeling of alongshore
2128 variability in dune erosion at Egmond aan Zee, the Netherlands. *Coast. Eng.* 99, 167–
2129 175.
- 2130 Dean, R.G., Maurmeyer, E.M., 1983. Models for beach profile response. In: Komar, P.D. (Ed.),
2131 *Handbook of Coastal Processes and Erosion,* C.R.C. Press, Florida, US, pp. 151-166.

- 2132 Delgado-Fernandez, I., 2010. A review of the application of the fetch effect to modeling sand
2133 supply to coastal foredunes. *Aeolian Res.* 2, 61–67.
- 2134 Delgado-Fernandez, I., 2011. Meso-scale modelling of aeolian sediment input to coastal dunes.
2135 *Geomorphology* 130:230-243 doi:10.1016/j.geomorph.2011.04.001.
- 2136 Delgado-Fernandez, I., Davidson-Arnott, R.G.D., 2011. Meso-scale aeolian sediment input to
2137 coastal dunes: The nature of aeolian transport events. *Geomorphology* 126, 217-232.
- 2138 Delgado-Fernandez, I., Davidson-Arnott, R.G.D., Bauer, B.O., Walker, I.J. Ollerhead, J., 2013a.
2139 Evaluation of the optimal resolution for characterizing the effect of beach surface
2140 moisture derived from remote sensing on aeolian transport and deposition. *J. Coastal*
2141 *Res.* 2 (65), 1277-1282.
- 2142 Delgado-Fernandez, I., Davidson-Arnott, R.G.D., Bauer, B.O., Walker, I.J., Ollerhead, J. Rhew, H.,
2143 2012. Assessing aeolian beach-surface dynamics using a remote sensing approach.
2144 *Earth Surf. Proc. Land.* 37, 1651-1660. doi:10.1002/esp.3303.
- 2145 Delgado-Fernandez, I., Davidson-Arnott, R.G.D. Ollerhead, J., 2009. Application of a remote
2146 sensing technique to the study of coastal dunes. *J. Coastal Res.* 25, 1160-1167.
- 2147 Delgado-Fernandez, I., Jackson, D.W.T., Cooper, J.A.G., Baas, A.C.W., Beyers, J.H., Lynch, K.,
2148 2013b. Field characterization of three-dimensional lee-side airflow patterns under
2149 offshore winds at a beach–dune system. *J. Geophys. Res-Earth.* 118, 706–721.
- 2150 Dillenburg, S.R. Hesp, P.A., 2009. Coastal Barriers—An Introduction. In: *Geology and*
2151 *Geomorphology of Holocene Coastal Barriers of Brazil.* Springer Berlin Heidelberg. pp. 1-
2152 15.
- 2153 Dissanayake, P., Brown, B., Karunaratna, H., 2014. Modelling storm-induced beach/dune
2154 evolution: Sefton coast, Liverpool Bay, UK. *Mar. Geol.* 357, 225–242.
- 2155 Dong, Z., Wang, H., Liu, X., Wang, X. (2004). The blown sand flux over a sandy surface: A wind
2156 tunnel investigation on the fetch effect. *Geomorphology*, 57(1–2), 117–127.
- 2157 Dong, Z., Qian, G., Luo, W., Wang, H., 2006. Analysis of the mass flux profiles of an aeolian
2158 saltating cloud. *J. Geophys. Res-Earth.* 111, D16111.
- 2159 Dong, Z., J. Lu, J., Man, D., Lu, D., Qian, G., Zhang, Z., Luo, W., 2011. Equations for the near-
2160 surface mass flux density profile of wind-blown sediments, *Earth Surf. Proc. Land.* 36,
2161 1292–1299.
- 2162 Donnelly, C., Kraus, N., Larson, M., 2006. State of knowledge of modeling of coastal overwash. *J.*
2163 *Coastal Res.*, 965-991.
- 2164 Drake, T.G., Shreve, R.L., Dietrich, W.E., Whiting, P.J., Leopold, L.B., 1988. Bedload transport of
2165 finegravel observed by motion-picture photography. *J. Fluid Mech.* 192, 193–217. J

- 2166 Durán, O., Herrmann, H., 2006. Modeling of saturated sand flux. *Journal of Statistical Mechanics*
2167 7, P07011.
- 2168 Durán, O., Moore, L.J., 2013. Vegetation controls on the maximum size of coastal dunes.
2169 *Proceedings of the National Academy of Sciences* 110 (43), 17217–17222.
- 2170 Edwards, B.L. Namikas, S.L., 2009. Small-scale variability in surface moisture on a fine-grained
2171 beach: Implications for modeling aeolian transport. *Earth Surf. Proc. Land.* 34, 1333-
2172 1338.
- 2173 Edwards, B.L., Schmutz, P.P., Namikas, S.L., 2012. Comparison of Surface Moisture
2174 Measurements with Depth-Integrated Moisture Measurements on a Fine-Grained
2175 Beach. *J. Coastal Res.* 29, 1284-1291.
- 2176 Ellis, J.T., Morrison, R.F., Priest, B.H., 2009a. Measuring the transport of aeolian sand with a
2177 microphone system. *Geomorphology* 105, 87–94.
- 2178 Ellis, J.T., Li, B., Farrell, E.J., Sherman, D.J., 2009b. Protocols for characterizing aeolian mass-flux
2179 profiles. *Aeolian Res.* 1, 19–26.
- 2180 Ellis, J.T., Sherman, D.J., 2013. Fundamentals of aeolian sediment transport: wind-blown sand.
2181 Ch. 11.6 in: Lancaster, N, Sherman, DJ, Baas, ACW (eds.), Vol. 11: *Aeolian*
2182 *Geomorphology*. pp 85-108. In: Shroder, JF (editor in chief) *Treatise on Geomorphology*.
2183 Elsevier: Oxford.
- 2184 Ellis, J.T., Sherman, D.J., Farrell, E.J., Li, B., 2012. Temporal and spatial variability of aeolian sand
2185 transport: implications for field measurements. *Aeolian Res.* 3, 379–387.
- 2186 Esteves, L.S., Brown, J.M., Williams, J.J., Lymbery, G., 2012. Quantifying thresholds for
2187 significant dune erosion along the Sefton Coast, Northwest, England. *Geomorphology*.
2188 143–144, 52–61.
- 2189 Farrell, E.J., Sherman, D.J., Ellis, J.T., Li, B., 2012. Vertical distribution of grain size for wind
2190 blown sand. *Aeolian Res.* 7, 51-61.
- 2191 FitzGerald, D.M., Fenster, M.S., Argow, B.A., Buynevich, I.V., 2008. Coastal impacts due to sea-
2192 level rise. *Annual Review of Earth and Planetary Sciences* 36, 601-647.
- 2193 Forbes, D.L., Parkes, G.S., Manson, G.K., Ketch, L.A., 2004. Storms and shoreline retreat in the
2194 southern Gulf of St. Lawrence. *Mar. Geol.* 210, 169-204.
- 2195 Frank, A., Kocurek, G., 1996a. Airflow up the stoss slope of sand dunes: limitations of current
2196 understanding. *Geomorphology* 17, 47–54.
- 2197 Frank, A., Kocurek, G., 1996b. Toward a model of airflow on the lee side of aeolian dunes.
2198 *Sedimentology* 43, 451–458.
- 2199 Franke, J., Hirsch, C., Jensen, A.G., Krus, H.W., Schatzmann, M., Westbury, P.S., Miles, S.D.,
2200 Wisse, J.A., Wright, N.G., 2004. Recommendations on the use of CFD in wind

- 2201 engineering. In: van Beeck, J.P.A.J. (Ed.), COST Action C14, Impact of Wind and Storm on
 2202 City Life Built Environment. Proceedings of the International Conference on Urban Wind
 2203 Engineering and Building Aerodynamics, 5–7 May 2004. von Karman Institute, Sint-
 2204 Genesisius-Rode, Belgium.
- 2205 Fryberger, S.G., 1980. Dune forms and wind regime, Mauritania, West Africa: implications for
 2206 past climate. *Palaeocology of Africa* 12, 79–96.
- 2207 Fryberger, S.G. Dean, D., 1979. Dune forms and wind regime. In: McKee, E.D. (Ed.), *A Study of*
 2208 *Global Sand Seas*. U.S. Geological Survey, Professional Paper 1052, 141-151.
- 2209 Gares, P. A., Nordstrom, K. F., 1995. A cyclic model of foredune blowout evolution for a leeward
 2210 coast: Island Beach, New Jersey. *Annals of the Association of American Geographers* 85,
 2211 1-20.
- 2212 Gillette, D.A., Herbert, G., Stockton, P.H., Owen, P.R., 1996. Causes of the fetch effect in wind
 2213 erosion. *Earth Surf. Proc. Land.* 21, 641–659.
- 2214 Goff, J.A., 2014. Seismic and core investigation of Panama City, Florida, reveals sand ridge
 2215 influence on formation of the shoreface ravinement. *Continental Shelf Research* 88, 34–
 2216 46.
- 2217 Goff, J.A., Flood, R. D., Austin, J.A.Jr., Schwab, W.C., Christensen, B., Browne, C.M., Denny, J.F.,
 2218 Baldwin, W.E., 2015. The impact of Hurricane Sandy on the shoreface and inner shelf of
 2219 Fire Island, NewYork: Large bedform migration but limited erosion. *Continental Shelf*
 2220 *Research* 98, 13-25.
- 2221 Heathfield, D.K., Walker, I.J., Atkinson, D.E., 2013. Erosive water level regime and climatic
 2222 variability forcing of beach–dune systems on south-western Vancouver Island, British
 2223 Columbia, Canada. *Earth Surf. Proc. Land.* 38, 751-762.
- 2224 Hesp, P.A., 1988a. Surfzone, beach and foredune interactions on the Australian southeast coast.
 2225 In: Psuty, N.P. (Ed.), *Dune/Beach Interaction*. *J. Coastal Res. Special Issue* 3, 15–25.
- 2226 Hesp, P.A., 1988b. Morphology, dynamics and internal stratification of some established
 2227 foredunes in southeast Australia. In: Hesp, P.A., Fryberger, S. (Eds.), *Eolian Sediments*.
 2228 *Journal of Sedimentary Geology.* 55, 17–41.
- 2229 Hesp, P.A., 1989. A review of biological and geomorphological processes involved in the
 2230 initiation and development of incipient foredunes. In: Gimingham, C.H., Ritchie, W.,
 2231 Willetts, B.B., and Willis, A.J. (Eds.) *Coastal Sand Dunes*. *Proc. Roy. Soc. Edinburgh*
 2232 *Section B (Biol. Sci.)* 96, pp. 181-202.
- 2233 Hesp, P.A., 2002. Foredunes and blowouts: initiation, geomorphology and dynamics.
 2234 *Geomorphology* 48, 245-268.
- 2235 Hesp, P.A., 2013. Conceptual models of the evolution of transgressive dune field
 2236 systems. *Geomorphology* 199, 138-149.

- 2237 Hesp, P.A., Pringle, A., 2001. Wind flow and topographic steering within a trough blowout. J.
2238 Coastal Res. Special Issue 34, 597–601.
- 2239 Hesp, P.A., Short, A.D., 1999. Barrier morphodynamics. In: Short, A.D. (Ed.), Handbook of Beach
2240 and Shoreface Morphodynamics. John Wiley and Sons, Chichester, UK, pp. 307-333.
- 2241 Hesp, P.A., Smyth, T.A.G., Nielsen, P., Walker, I.J., Bauer, B.O., Davidson-Arnott, R.G.D., 2015.
2242 Flow deflection over a foredune. *Geomorphology* 230, 64-74.
- 2243 Hesp, P.A., Walker, I.J., 2012. Three-dimensional airflow within a bowl blowout: Greenwich
2244 Dunes, Prince Edward Island, Canada. *Aeolian Res.* 3, 389-399.
- 2245 Hesp, P.A., Walker, I.J., 2013. Fundamentals of Aeolian Sediment Transport: Coastal Dunes. Ch.
2246 11.17 in: Lancaster, N, Sherman, DJ, Baas, ACW (eds.), Vol. 11: *Aeolian Geomorphology*.
2247 pp 328-355. In: Shroder, JF (ed.) *Treatise on Geomorphology*. Elsevier: Oxford.
- 2248 Hesp, P.A., Walker I.J., Chapman, C.A., Davidson-Arnott, R.G.D., Bauer, B.O., 2013. Aeolian
2249 dynamics over a coastal foredune, Prince Edward Island, Canada. *Earth Surf. Proc. Land*.
2250 38, 1566-1575. DOI: 10.1002/esp.3444.
- 2251 Hesp, P.A., Walker, I.J., Davidson-Arnott, R.G.D., Ollerhead, J., 2005. Flow dynamics over a
2252 vegetated foredune at Prince Edward Island, Canada. *Geomorphology* 65, 71–84.
- 2253 Hesp, P.A., Walker, I.J., Namikas, S.L., Davidson-Arnott, R.G.D., Bauer, B.O., Ollerhead, J., 2009.
2254 Storm wind flow over a foredune, Prince Edward Island, Canada *J. Coastal Res. SI* 56,
2255 312–316.
- 2256 Hesp, P.A., Smyth, T.A.G., 2016a. Jet flow over foredunes. *Earth Surface Processes and*
2257 *Landforms*, 1735, 1727–1735.
- 2258 Hesp, P.A., Smyth, T.A.G., 2016b. Surfzone-beach-dune interactions: Review and the role of the
2259 intertidal beach. *J. Coastal Research S.I.* 75: 8-12.
- 2260 Hinkel, J., Nicholls, R.J., Tol, R.J., Wang, Z.B., Hamilton, J.M., Boot, G., Vafeidis, A.T., McFadden,
2261 L., Ganopolski, A., Klein, R.J.T., 2013. A global analysis of erosion of sandy beaches and
2262 sea-level rise: An application of DIVA. *Global and Planetary Change* 111, 150–158.
- 2263 Houser, C., 2009. Synchronization of transport and supply in beach-dune interaction. *Prog.*
2264 *Phys. Geog.* 33(6), 733-746
- 2265 Houser, C., 2013. Alongshore variation in the morphology of coastal dunes: Implications for
2266 storm response. *Geomorphology* 199, 48–61.
- 2267 Houser, C., Ellis, J., 2013. Beach and Dune Interaction. Ch. 10.10 in: Sherman, D.J. (ed.), Vol.
2268 10: *Aeolian Geomorphology*. pp 267-288. In: Shroder, JF (editor in chief) *Treatise on*
2269 *Geomorphology*. Elsevier: Oxford.
- 2270 Houser, C., Hapke, C., Hamilton, S., 2008. Controls on coastal dune morphology, shoreline
2271 erosion and barrier island response to extreme storms. *Geomorphology* 100, 223-240.

- 2272 Houston, J.R., Dean, R.G., 2014. Shoreline change on the east coast of Florida. *J. Coastal Res.* 30,
2273 647-660.
- 2274 Howard, A.D., Morton, J.B., Gad-El-Hak, M., Pierce, D.B., 1978. Sand transport model of barchan
2275 dune equilibrium. *Sedimentology* 25, 307–338.
- 2276 Hsu, S.A., 1977. Boundary-layer meteorological research in the coastal zone. In: Walker, H.J.
2277 (Ed.), *Geoscience and Man, Research Techniques in Coastal Environments*, Dept.
2278 *Geography and Anthropology*, Louisiana State University, US, pp. 99–111.
- 2279 Hsu, S.A., 1987. Structure of air flow over sand dunes and its effect on aeolian sand transport in
2280 coastal regions. In: Kraus, C. (Ed), *Coastal Sediments '87*, American Society of Civil
2281 Engineers, New York, US, pp. 188–201.
- 2282 Hunt, J.C.R., Leibovich, S., Richards, K.J., 1988. Turbulent shear flows over low hills. *Q. J. Roy.
2283 Meteor. Soc.* 114, 1435–1470.
- 2284 Hunter, R., Richmond, B.M., Alpha, T.R., 1983. Storm-controlled oblique dunes of the Oregon
2285 coast. *Geol. Soc. Am. Bull.* 94, 1450–1465.
- 2286 Inman, D.L., 1987. Accretion and erosion waves on beaches. *Shore and Beach* 55, 61-66.
- 2287 Jackson, D.W.T., 1996. A new, instantaneous aeolian sand trap design for field use.
2288 *Sedimentology* 43, 791–796.
- 2289 Jackson, D.W.T., Beyers, J.H.M., Lynch, K., Cooper, J.A.G., Baas, A.C.W., Delgado-Fernandez, I.,
2290 2011. Investigation of three-dimensional wind flow behaviour over coastal dune
2291 morphology under offshore winds using computational fluid dynamics (CFD) and
2292 ultrasonic anemometry. *Earth Surf. Proc. Land*. DOI: 10.1002/esp.2139.
- 2293 Jackson, P.S., Hunt, J.C.R., 1975. Turbulent wind flow over a low hill. *Q. J. Roy. Meteor. Soc.* 101,
2294 929–955.
- 2295 Jackson, N.L., Nordstrom, K.L., 1998. Aeolian transport of sediment on a beach during and after
2296 rainfall, Wildwood, NJ, USA. *Geomorphology* 22, 151–157.
- 2297 Jackson, R.G., 1976. Sedimentological and fluid-dynamic implications of the turbulent bursting
2298 phenomenon in geophysical flows. *J. Fluid Mech.* 77, 531–560.
- 2299 James, T.S., Henton, J.A., Leonard, L.J., Darlington, A., Forbes, D.L., Craymer, M., 2014. Relative
2300 Sea-level Projections in Canada and the Adjacent Mainland United States; Geological
2301 Survey of Canada. Open File 7737, 67 p.
- 2302 Jensen, N.O., Zeman, O., 1985. Perturbations to mean wind and turbulence in flow over
2303 topographic forms. In: Barndorff-Nielsen, O.E., Moller, J.T., Rasmussen, K.R., Willets, B.B.
2304 (Eds.), *Proceedings of International Workshop on the Physics of Blown Sand*.
2305 Department of Theoretical Statistics, Institute of Mathematics, University of Aarhus,
2306 Denmark, pp. 351–368.

- 2307 Kawamura, R., 1951. Study of Sand Movement by Wind. Univ of Tokyo, Rept. Inst. Tech. 5.
 2308 Translated (1965) as University of California Hydraulics Engineering Laboratory Report
 2309 HEL 2-8, Berkeley, California.
- 2310 Kok, J., Renno, N., 2009. A comprehensive numerical model of steady state saltation. J.
 2311 Geophys. Res- Atmos. 114, D17204.
- 2312 Komar, P.D., 1971. Nearshore cell circulation and the formation of giant cusps. Geol. Soc. Am.
 2313 Bull. 82, 2643-50.
- 2314 Komar, P.D., McDougal, W.G., Marra, J.J., Ruggiero, P., 1999. The rational analysis of setback
 2315 distances: Applications to the Oregon Coast. Shore and Beach 67(1), 41–49.
- 2316 Kostaschuk, R.A., Shugar, D.H., Best, J.L., Parsons, D.R., Lane, S.N., Hardy, R.J., Orfeo, O., 2009.
 2317 Suspended sediment transport and deposition over a dune: Rio Parana, Argentina. Earth
 2318 Surf. Proc. Land. 34, 1605–1611.
- 2319 Kriebel, D.L., Dean, R.G., 1985. Numerical simulation of time-dependent beach and dune
 2320 erosion. Coast. Eng. 9: 221–245.
- 2321 Kriebel, D.L., Dean, R.G., 1993. Convolution method for time dependent beach-profile response.
 2322 Journal of Waterway, Port, and Coastal Engineering 119(2), 204–226.
- 2323 Kroon, A., Hoekstra, P., 1990. Eolian sediment transport on a natural beach. J. Coastal Res. 6,
 2324 367–380.
- 2325 Lancaster, N., 1985. Variations in wind velocity and sand transport rates on the windward flanks
 2326 of desert sand dunes. Sedimentology 32, 581–593.
- 2327 Lancaster, N., Nickling, W.G., McKenna Neuman, C., Wyatt, V.E., 1996. Sediment flux and
 2328 airflow on the stoss slope of a barchan dune. Geomorphology 17, 55–62.
- 2329 Larson, M., Erikson L. Hanson, H., 2004. An analytical model to predict dune erosion due to
 2330 wave impact. Coast. Eng.. 51, 675–696.
- 2331 Law, M.N., Davidson-Arnott, R.G.D., 1990. Seasonal controls on aeolian processes on the beach
 2332 and foredune. Proceedings Symposium on Coastal Sand Dunes, Sept. 1990, Guelph,
 2333 Ontario. National Research Council of Canada, pp. 49-68.
- 2334 Leenders, J.K., van Boxel, J.H., Sterk, G., 2005. Wind forces and related saltation transport.
 2335 Geomorphology 71, 357–372.
- 2336 Lettau, K., Lettau, H., 1977. Experimental and micrometeorological field studies of dune
 2337 migration. In: Lettau, K., Lettau, H. (Eds.), Exploring the World's Driest Climate. IES
 2338 Report 101, University of Wisconsin Press, Madison, US, pp. 110-147.
- 2339 List, J.H., Sallenger, A.H., Hansen, M.E., Jaffe, B.E., 1997. Accelerated relative sea-level rise and
 2340 rapid coastal erosion: testing a causal relationship for the Louisiana barrier islands. Mar.
 2341 Geol. 140, 347-363.

- 2342 Luna, M.C.M.M., Parteli, E.J.R., Durán, O., Herrmann, H.J., 2011. Model for the genesis of
2343 coastal dune fields with vegetation. *Geomorphology* 129, 215–224.
- 2344 Lynch, K., Delgado-Fernandez, I., Jackson, D.W.T., Cooper, J.A.G., Baas, A.C.W., Beyers, J.H.M.,
2345 2013. Alongshore variation of aeolian sediment transport on a beach, under offshore
2346 winds. *Aeolian Res.* 8, 11-18.
- 2347 Lynch, K., Jackson, D.W.T., Cooper, A.G., 2006. A remote-sensing technique for the
2348 identification of aeolian fetch distance. *Sedimentology* 53, 1381–1390.
- 2349 Lynch, K., Jackson, D.W.T., Cooper, J.A.G., 2008. Aeolian fetch distance and secondary airflow
2350 effects: the influence of micro-scale variables on meso-scale foredune development.
2351 *Earth Surf. Proc. Land.* 1005, 991–1005.
- 2352 Lynch, K., Jackson, D.W.T., Cooper, J.A.G., 2009. Foredune accretion under offshore winds.
2353 *Geomorphology* 105(1–2), 139–146.
- 2354 Lynch, K., Jackson, D.W.T., Cooper, J.A.G., 2010. Coastal foredune topography as a control on
2355 secondary airflow regimes under offshore winds. *Earth Surf. Proc. Land.* 35(3), 344–353.
- 2356 Manson, G.K., Davidson-Arnott, R.G.D., Forbes, D.L., 2015 modelled nearshore sediment
2357 transport in open-water conditions, central north shore of Prince Edward Island,
2358 Canada. *Can. J. Earth Sci.* 53, 101-118: 10.1139/cjes-2015-009.
- 2359 Manson, G.K., Forbes, D.L., Parkes, G., 2002a. Wind climatology. In: Forbes D.L., Shaw, R.W.
2360 (Eds.), *Coastal Impacts of Climate Change and Sea-level Rise on Prince Edward Island.*
2361 Open File 4261, Geological Survey of Canada, Ottawa, Canada. p. 34
- 2362 Martin, R.L., Barchyn, T.E., Hugenholtz, C.H., Jerolmack, D.J., 2014. Timescale dependence of
2363 aeolian sand flux observations under atmospheric turbulence. *J. Geophys. Res- Atmos.*
2364 118, 1-15. doi:10.1002/jgrd.50687, 2013.
- 2365 Mathew, S., Davidson-Arnott, R.G.D., Ollerhead, J., 2010. Evolution of a beach/dune system
2366 following overwash during a catastrophic storm: Greenwich Dunes, Prince Edward
2367 Island, 1936-2005. *Can. J. Earth Sci.* 47, 273-290.
- 2368 McKenna Neuman, C., 1990a. Observations of winter aeolian transport and niveo-aeolian
2369 deposition at Crater Lake, Pagnirtung Pass, N.W.T., Canada. *Permafrost Periglac.* 1,
2370 235–247.
- 2371 McKenna Neuman, C., 1990b. Role of sublimation in particle supply for aeolian transport in cold
2372 environments. *Geogr. Ann. A.* 72A, 329–335.
- 2373 McKenna Neuman, C., 1993. A review of aeolian transport processes in cold environments.
2374 *Prog. Phys. Geog.* 17, 137–155.
- 2375 McKenna Neuman, C., Lancaster, N., Nickling, W.G., 1997. Relations between dune morphology,
2376 air flow, and sediment flux on reversing dunes, Silver Peak, Nevada. *Sedimentology* 44,
2377 1103–1113.

- 2378 McKenna Neuman, C., Lancaster, N., Nickling, W.G., 2000. Effect of unsteady winds on sediment
2379 transport intermittency along the stoss slope of a reversing dune. *Sedimentology* 47,
2380 211–226.
- 2381 McKenna Neuman, C., Langston, G., 2006. Measurement of water content as a control of
2382 particle entrainment by wind. *Earth Surf. Proc. Land.* 31(3), 303–317.
- 2383 McKenna Neuman, C., Muljaars Scott, M., 1998. A wind tunnel study of the influence of pore
2384 water on aeolian sediment transport. *J. Arid Environ.* 39, 403–419.
- 2385 McLean, R., Shen, J.S., 2006. From foreshore to foredune: foredune development over the last
2386 30 years at Moruya Beach, NSW, Australia. *J. Coastal Res.* 22, 28–36.
- 2387 McLean, S.R., Smith, J.D., 1986. A model for flow over two-dimensional bed forms. *J. Hydraulic
2388 Engineering* 112: 300-317.
- 2389 Mikklesen, H.E., 1989. Wind flow and sediment transport over a low coastal dune. *Geoskrifter*
2390 32. Institute of Geology, University of Aarhus, Denmark, 60 pp.
- 2391 Mimura, N., Nobuoka, H., 1995. Verification of Bruun Rule for the estimate of shoreline retreat
2392 caused by sea-level rise. In: Dally, W.R., Zeidler, R.B. (Eds.), *Coastal Dynamics 95*,
2393 American Society of Civil Engineers, New York, US, pp. 607–616.
- 2394 Miot da Silva, G., Hesp, P., 2010. Coastline orientation, aeolian sediment transport and
2395 foredune and dunefield dynamics of Moçambique beach, southern Brazil.
2396 *Geomorphology* 120, 258-278.
- 2397 Moore, L.J., Patsch, K., List, J.H., Williams, S.J., 2014. The potential for sea-level-rise-induced
2398 barrier island loss: Insights from the Chandeleur Islands, Louisiana, USA *Mar. Geol.* 355,
2399 244–259.
- 2400 Morton, R.A., 2002. Factors controlling storm impacts on coastal barriers and beaches - a
2401 preliminary basis for real-time forecasting. *J. Coastal Res.* 18, 486–501.
- 2402 Mull, J., Ruggiero, P., 2014. Estimating Storm-Induced Dune Erosion and Overtopping along U.S.
2403 West Coast Beaches. *J. Coastal Res.* 30(6), 1173-1187
- 2404 Mulligan, K.R., 1988. Velocity profiles measured on the windward slope of a transverse dune.
2405 *Earth Surf. Proc. Land.* 13, 573–582.
- 2406 Namikas, S.L., 2003. Field measurement and numerical modeling of aeolian mass flux
2407 distributions on a sandy beach. *Sedimentology* 50, 303–326.
- 2408 Namikas, S.L., Bauer, B.O., Sherman, D.J., 2003. Influence of averaging interval on shear velocity
2409 estimates for aeolian transport modeling. *Geomorphology.* 53, 235–246.
- 2410 Namikas, S.L., Sherman, D.J., 1995. A review of the effects of surface moisture content on
2411 aeolian sand transport. In: Tchakerian, V.P. (Ed.), *Desert Aeolian Processes*. Chapman &
2412 Hall, London, pp. 269–293.

- 2413 Nelson, J.M., Smith, J.D., 1989. Mechanics of flow over ripples and dunes. *J. Geophys. Res-*
2414 *Earth.* 94, 8146–8162.
- 2415 Nickling, W.G., 1988. The initiation of particle movement by wind. *Sedimentology* 35, 499–511.
- 2416 Nickling, W.G., Davidson-Arnott, R.G.D., 1990. Aeolian sediment transport on beaches and
2417 coastal sand dunes. *Proceedings of the Symposium on Coastal Sand Dunes.* National
2418 Research Council of Canada. pp. 1–35.
- 2419 Niedoroda, A.W., Swift, D.J., Figueiredo, A.G., Freeland, G.L., 1985. Barrier island evolution,
2420 middle Atlantic shelf, USA Part II: Evidence from the shelf floor. *Mar. Geol.* 63(1), 363-
2421 396.
- 2422 Nordstrom, K., Jackson, N.L., 1992. Effect of source width and tidal elevation changes on
2423 Aeolian transport on an estuarine beach. *Sedimentology* 769–778.
- 2424 Nordstrom, K.F., Jackson, N.L., 1993. The role of wind direction in eolian transport on a narrow
2425 sand beach. *Earth Surf. Proc. Land.* 18, 675-685.
- 2426 Ollerhead, J., Davidson-Arnott, R.G.D., Walker, I.J., Mathew, S., 2013. Annual to decadal
2427 morphodynamics of the foredune system at Greenwich Dunes, Prince Edward Island,
2428 Canada. *Earth Surf. Proc. Land.* 38, 284–298.
- 2429 Olson, J. S., 1958. Lake Michigan dune development 3. Lake level, beach and dune oscillations.
2430 *J. Geol.* 66, 473-483.
- 2431 Paola, C., Voller, V.R., 2005. A generalized Exner equation for sediment mass balance. *J.*
2432 *Geophys. Res-Earth.* 110, F04014. <http://dx.doi.org/10.1029/2004JF000274>.
- 2433 Parsons, D.R., Walker, I.J., Wiggs, G.F.S., 2004. Numerical modelling of flow structures over
2434 idealised transverse Aeolian dunes of varying geometry. *Geomorphology* 59, 149–164.
- 2435 Pearce, K.I., Walker, I.J., 2005. Frequency and magnitude biases in the ‘Fryberger’ model, with
2436 implications for characterizing geomorphically effective winds. *Geomorphology* 68, 39-
2437 55.
- 2438 Petersen, P.S., Hilton, M.J., Wakes, S.J., 2011. Evidence of æolian sediment transport across an
2439 *Ammophila arenaria*-dominated foredune, Mason Bay, Stewart Island. *NZ Geographer*
2440 67, 174–189.
- 2441 Pilkey, O.H., Cooper, J.A.G., 2004. Society and sea level rise. *Science* 303(5665), p.1781.
- 2442 Psuty, N.P., 1988, Sediment budget and dune/beach interaction. *J. Coastal Res. Special Issue*, 3,
2443 1-4.
- 2444 Pye, K., Blott, S.J., 2008. Decadal-scale variation in dune erosion and accretion rates: an
2445 investigation of the significance of changing storm tide frequency and magnitude on the
2446 Sefton coast, UK. *Geomorphology* 102, 652–666.

- 2447 Ranasinghe, R., Callaghan, D., Stive, M.J.F., 2012. Estimating coastal recession due to sea level
2448 rise: beyond the Bruun rule. *Climatic Change* DOI 10.1007/s10584-011-0107-8.
- 2449 Rasmussen, K.R., 1989. Some aspects of flow over coastal dunes. In: Gimingham, C.H., Ritchie,
2450 W., Willetts, B.B., Willis, A.J. (Eds.), *Coastal Sand Dunes*. Proceedings of the Royal Society
2451 of Edinburgh 96B, pp. 129–147.
- 2452 Rasmussen, K.R., Mikkelsen, H.E., 1998. On the efficiency of vertical array aeolian field traps,
2453 *Sedimentology* 45, 789–800.
- 2454 Reed, D.J., Davidson-Arnott, R.G.D., Perillo, G.M.E., 2009. Estuaries, Coastal Marshes, Tidal Flats
2455 and Coastal Dunes. Chapter 5. In: Slaymaker, O. (Ed.), *Landscape Changes in the 21st*
2456 *Century*. Cambridge University Press, Cambridge, UK, pp. 130-167.
- 2457 Robert, A., Roy, A.G., DeSerres, B., 1996. Turbulence at a roughness transition in a depthlimited
2458 flow over a gravel bed. *Geomorphology* 16, 175– 187.
- 2459 Rodriguez, A.B., Fassell, M.L., Anderson, J.B., 2001. Variations in shore face progradation and
2460 ravinement along the Texas coast, Gulf of Mexico. *Sedimentology* 48, 837–853.
- 2461 Roelvink, D., Reniers, A., van Dongeren, A., van Thiel de Vries, J., McCall, R., Lescinski, J., 2009.
2462 Modelling storm impacts on beaches, dunes and barrier islands. *Coast. Eng.* 56, 1133–
2463 1152.
- 2464 Rosati, J.D., Dean, R.G., Walton, T.L., 2013. The modified Bruun Rule extended for landward
2465 transport. *Mar. Geol.* 340, 71-81.
- 2466 Rotnicka, J., 2013. Aeolian vertical mass flux profiles above dry and moist sandy beach surfaces,
2467 *Geomorphology* 187, 27-37, doi:10.1016/j.geomorph.2012.12.032.
- 2468 Roy, A.G., Biron, P., DeSerres, B., 1996. On the necessity of applying a rotation to instantaneous
2469 velocity measurements in river flows. *Earth Surf. Proc. Land.* 21, 817–827.
- 2470 Roy, A.G., Buffin-Belanger, T., Lamarre, H., Kirkbride, A.D., 2004. Size, shape and dynamics of
2471 large-scale turbulent flow structures in a gravel-bed river. *J. Fluid Mech.* 500, 1-27.
- 2472 Roy, P.S., Cowell, P.J., Ferland, M.A., Thom, B.G. 1994. Wave-dominated coasts. In: Carter,
2473 R.W.G. and Woodroffe, C.D. (Eds.), *Coastal Evolution*. Cambridge University Press, UK,
2474 517 pp.
- 2475 Ruessink, B.G., Jeuken, M.C.J.L., 2002. Dunefoot dynamics along the Dutch coast. *Earth Surf.*
2476 *Proc. Land.* 27, 1043-1056.
- 2477 Ruz, M.-H., Allard, H., 1994. Foredune development along a subarctic emerging coastline,
2478 eastern Hudson Bay, Canada. *Mar. Geol.* 117, 57-74.
- 2479 Sallenger, A.H., 2000. Storm impact scale for barrier islands. *J. Coastal Res.* 16, 890-895.
- 2480 Sarre, R.D., 1988. Evaluation of aeolian sand transport equations using intertidal zone
2481 measurements, Saunton Sands, England. *Sedimentology* 35 (4), 671-679.

- 2482 Sarre, R., 1989. The morphological significance of vegetation and relief on coastal foredune
2483 processes. *Z. Geomorphol. N.F.* 73, 17–31.
- 2484 Sauermann, G., Kroy, K., Herrmann, H.J., 2001. Continuum saltation model for sand dunes.
2485 *PHys. Rev. E.* 64(3 Pt 1), 031305.
- 2486 Saunders, K.E., Davidson-Arnott, R.G.D., 1990. Coastal dune response to natural disturbances.
2487 In: Davidson-Arnott, R.G.D. (Ed.), *Proceedings of the Symposium on Coastal Sand Dunes.*
2488 National Research Council of Canada, pp. 321-346.
- 2489 Schönfeldt, H.J., von Löwis, S., 2003. Turbulence-driven saltation in the atmospheric boundary
2490 layer. *Meteorol. Z.* 12: 257–268.
- 2491 Schumm, S.A., Lichty, R.W., 1965. Time, space, and causality in geomorphology. *Am. J. Sci.* 263,
2492 110–119.
- 2493 Schwab, W.C., Baldwin, W.E., Denny, J.F., Hapke, C.J., Gayes, J.T., List, J.H., Warner, J. C., 2014.
2494 Modification of the Quaternary stratigraphic framework of the inner- continental shelf
2495 by Holocene marine transgression: an example offshore of Fire Island, N.Y. *Mar. Geol.*
2496 355, 346–360.
- 2497 Schwab, W.C., Baldwin, W.E., Hapke, C.J., Lentz, E.E., Gayes, P.T., Denny, J.F., List, .H., Warner,
2498 J.C., 2013. Geologic evidence for onshore sediment transport from the inner continental
2499 shelf: Fire Island, New York. *J. Coastal Res.* 29, 526–544.
- 2500 Schwartz, M.L., 1967. The Bruun theory of sea-level rise as a cause of shore erosion. *J. Geol.* 75,
2501 76-92.
- 2502 SCOR Working Group 89, 1991. The response of beaches to sea level changes: a review of
2503 predictive models. *J. Coastal Res.* 7, 895–921.
- 2504 Shao, Y., Raupach, M.R., 1992. The overshoot and equilibrium of saltation. *J. Geophys. Res-*
2505 *Atmos.* 97, 20559-20564.
- 2506 Sherman, D.J., 1995. Problems of scale in the modeling and interpretation of coastal
2507 dunes. *Mar. Geol.* 124(1), 339-349.
- 2508 Sherman, D.J., Hotta, S., 1990. Aeolian sediment transport: theory and measurement. In:
2509 Nordstrom, K.F., Psuty, N.P., Carter, R.W.G. (Eds.), *Coastal Dunes: Form and Process.*
2510 John Wiley and Sons Ltd, West Sussex, UK, pp. 17–37.
- 2511 Sherman, D.J., Bauer, B.O., 1993. Dynamics of beach-dune systems. *Prog. Phys. Geog.* 17, 413-
2512 447.
- 2513 Sherman, D.J., Li, B., 2011. Predicting aeolian sand transport rates: A reevaluation of models.
2514 *Aeolian Research* 3(4): 371-378 DOI:10.1016/j.aeolia.2011.06.002.
- 2515 Sherman, D.J., Bauer, B.O., Carter, R.W.G., Jackson, D.W.T., McCloskey, J., Davidson-Arnott,
2516 R.G.D., Gares, P.A., Jackson, N.L., Nordstrom, K.F., 1994. The AEOLUS Project: Measuring

- 2517 coastal wind and sediment systems, Coastal Dynamics '94. Waterway, Port, Coastal and
2518 Ocean Division, ASCE, pp. 476–487.
- 2519 Sherman, D.J., Jackson, D.W.T., Namikas, S.L., Wang, J., 1998. Wind-blown sand on beaches: an
2520 evaluation of models. *Geomorphology* 22: 113-133.
- 2521 Sherman, D.J., Li, B., Farrell, E.J., Ellis, J.T., Cox, W.D., Maia, L.P., Sousa, P.H.G.O., 2011.
2522 Measuring aeolian saltation: A comparison of sensors, *J. Coastal Res.* 59, 280–290.
- 2523 Sherman, D.J., Swann, C., Barron, J.D., 2014. A high-efficiency, low-cost aeolian sand trap.
2524 *Aeolian Res.* 13, 31–34.
- 2525 Short, A.D., 2010. Role of geological inheritance in Australian beach morphodynamics. *Coast.*
2526 *Eng.* 57(2), 92-97.
- 2527 Short, A.D., Hesp, P.A., 1982. Wave, beach and dune interactions in southeast Australia. *Mar.*
2528 *Geol.* 48, 259–284.
- 2529 Shugar, D.H., Kostaschuk, R.A., Best, J.L., Parsons, D.R., Lane, S.N., Orfeo, O., Hardy, R.J., 2010.
2530 On the relationship between flow and suspended sediment transport over the crest of a
2531 sand dune, Rio Parana, Argentina. *Sedimentology* 57, 252–272.
- 2532 Simmons, M.D., 1982. Have catastrophic storms shaped [PEI]'s North Shore? Some
2533 observations which suggest an important role for unusually large storms.
2534 In: *Proceedings Workshop on Atlantic Coastal Erosion and Sedimentation*, Halifax.
2535 National Research Council, Associate Committee on Shoreline Erosion and
2536 Sedimentation, Ottawa, Canada, pp. 23-36.
- 2537 Siringan, F.P., Anderson, J.B., 1994. Modern shoreface and inner-shelf storm deposits off the
2538 East Texas Coast, Gulf of Mexico. *J. Sediment. Res.* 64, 99–110.
- 2539 Smyth, T.A.G., 2016. A review of Computational Fluid Dynamics (CFD) airflow modelling over
2540 aeolian landforms. *Aeolian Research*, 22, 153-164.
- 2541 Smyth, T.A.G., Hesp, P.A., 2015. Aeolian dynamics of beach scraped ridge and dyke
2542 structures. *Coast. Eng.* 99, 38-45.
- 2543 Smyth, T.A.G., Jackson, D.W.T., Cooper, J.A.G. 2011. CFD modeling of three- dimensional airflow
2544 over dune blowouts. *J. Coastal Res.* SI64, 314–318.
- 2545 Smyth, T.A.G., Jackson, D.W.T., Cooper, J.A.G. 2012. High resolution measured and modelled
2546 three-dimensional airflow over a coastal bowl blowout. *Geomorphology* 177–178, 62-
2547 73.
- 2548 Snyder, R., Boss, C., 2002. Recovery and stability in barrier island plant communities. *J. Coastal*
2549 *Res.* 18 (3), 530–536.
- 2550 Spaan, W.P., van den Abeele, G.D., 1991. Wind borne particle measurements with acoustic
2551 sensors. *Soil Technol.* 4, 51–63.

- 2552 Spies, P.J., McEwan, I.K., Butterfield, G.R., 2000. One-dimensional transitional behavior in
2553 saltation, *Earth Surf. Proc. Land.*, 505–518.
- 2554 Splinter, K.D., Palmsten, M.L., 2012. Modeling dune response to an east coast low. *Mar. Geol.*
2555 329–331, 46–57.
- 2556 Sterk, G., Jacobs, A.F.G., van Boxel, J.H., 1998. The effect of turbulent flow structures on
2557 saltation sand transport in the atmospheric boundary layer. *Earth Surf. Proc. Land.* 28,
2558 877–887.
- 2559 Stive, M.J.F., 2004. How important is global warming for coastal erosion? *Climatic Change.* 64,
2560 27-39.
- 2561 Stive, M.J.F., Ranasinghe, R., Cowell, P., 2009. Sea level rise and coastal erosion. In: Kim, Y. (Ed.),
2562 *Handbook of Coastal and Ocean Engineering.* World Scientific. pp 1023–1038.
- 2563 Stockton, P.H., Gillette, D.A., 1990. Field measurement of the sheltering effect of vegetation on
2564 erodible land surfaces. *Land Degrad. Rehabil.* 2, 77–85.
- 2565 Stout, J.E., Zobeck, T.M., 1997. Intermittent saltation. *Sedimentology* 44, 959–970.
- 2566 Svasek, J.N., Terwindt, J.H.J., 1974. Measurements of sand transport by wind on a natural
2567 beach. *Sedimentology* 21, 311–322.
- 2568 Sweet, M.L., Kocurek, G., 1990. An empirical model of aeolian dune lee-face airflow.
2569 *Sedimentology* 37. 1023–1038.
- 2570 Thom, B.G., Hall, W., 1991. Behaviour of beach profiles during accretion and erosion dominated
2571 periods. *Earth Surf. Proc. Land.*, 113–127.
- 2572 Thorn, C.E., Welford, M.R., 1994. The equilibrium concept in geomorphology. *Ann. Assoc. Am.*
2573 *Geogr.* 84(4), 666-696.
- 2574 Thornton, E.B., MacMahan, J., Sallenger, A.H., 2007. Rip currents, megacusps, and eroding
2575 dunes. *Mar. Geol.* 240, 151–167.
- 2576 Tsoar, H., Rasmussen, K.R., Sorensen, M., Willetts, B.B., 1985. Laboratory studies of flow over
2577 dunes. In: Barndorff-Nielsen, O.E., Moller, J.T., Rasmussen, K.K., Willetts, B.B. (Eds.),
2578 *Proceedings of the International Workshop on the Physics of Blown Sand,* University of
2579 Aarhus, Denmark, pp. 327–350.
- 2580 Valyrakis, M., Diplas, P., Dancy, C.L., Greer, K., 2010. Role of instantaneous force magnitude
2581 and duration on particle entrainment. *J. Geophys. Res-Earth.* 115, 1–18.
- 2582 van de Poll, H.W., 1983. *Geology of Prince Edward Island.* Energy and Minerals Branch, PEI
2583 Department of Energy and Forestry, Charlottetown, PEI. Paper 83-1, 66pp.
- 2584 van Dijk, D., Law, J., 1995. Sublimation and aeolian sand movement from a frozen surface:
2585 experimental results from Presqu'ile Beach, Ontario. *Geomorphology* 11, 177-187.

- 2586 Van Dijk, D., Law, J., 2003. The rate of grain release by pore-ice sublimation in cold-aeolian
2587 environments. *Geogr. Ann. A.* 85(1), 99-113.
- 2588 Vellinga, P., 1986. Beach and dune erosion during storm surges. PhD. Thesis, Delft University of
2589 Technology, Delft, The Netherlands, (Publication 372, Delft Hydraulics).
- 2590 Venditti, J.G., Bauer, B.O., 2005. Turbulent flow over a dune: Green River, Colorado. *Earth Surf.*
2591 *Proc. Land.* 30(3), 289-304.
- 2592 Wahid, A.H., 2008. GIS-based modeling of wind-transported sand on the Qaa Plain Beach,
2593 southwestern Sinai, Egypt. *J. Coastal Res.* 24(4), 936–943.
- 2594 Wal, A., McManus, J., 1993. Wind regime and sand transport on a coastal beach–dune complex,
2595 Tentsmuir, eastern Scotland. In: Pye, K. (Ed.), *The Dynamics and Environmental Context*
2596 *of Aeolian Sedimentary Systems.* The Geological Society, London, UK, pp. 159–171.
- 2597 Walker, I.J., 2005. Physical and logistical considerations of using ultrasonic anemometry in
2598 aeolian sediment transport research. *Geomorphology* 68(1-2), 57-76.
- 2599 Walker, I.J., Barrie, J.V., 2006. Geomorphology and sea-level rise on one of Canada’s most
2600 ‘sensitive’ coasts: Northeast Graham Island, British Columbia. *J. Coastal Res.* SI 39, 220-
2601 226.
- 2602 Walker, I.J., Davidson-Arnott, R.G.D., Hesp, P.A., Bauer, B.O., Ollerhead, J., 2009a. Mean flow
2603 and turbulence responses in airflow over foredunes: new insights from recent research.
2604 *J. Coastal Res.* SI 56, 366–370.
- 2605 Walker, I.J., Hesp, P.A., 2013. Fundamentals of Aeolian Sediment Transport: Airflow Over
2606 Dunes. Ch. 11.7 in: Lancaster, N, Sherman, DJ, Baas, ACW (eds.), Vol. 11: *Aeolian*
2607 *Geomorphology.* pp 109-133. In: Shroder, JF (editor in chief) *Treatise on*
2608 *Geomorphology.* Elsevier: Oxford.
- 2609 Walker, I.J., Hesp, P.A., Davidson-Arnott, R.G.D., Bauer, B.O., Ollerhead, J., 2009b. Response of
2610 three-dimensional flow to variations in the angle of incident flow and profile form of
2611 dunes: Greenwich Dunes, Prince Edward Island, Canada. *Geomorphology* 105, 127-138.
- 2612 Walker, I.J., Hesp, P.A., Davidson-Arnott, R.G.D., Ollerhead, J., 2006. Topographic steering of
2613 alongshore airflow over a vegetated foredune: Greenwich Dunes, Prince Edward Island,
2614 Canada. *J. Coastal Res.* 22, 1278-1291.
- 2615 Walker, I.J., Nickling, W.G., 2002. Dynamics of secondary airflow and sediment transport over
2616 and in the lee of a transverse dunes. *Prog. Phys. Geog.* 26, 47–75.
- 2617 Walker, I.J., Nickling, W.G., 2003. Simulation and measurement of surface shear stress over
2618 isolated and closely spaced transverse dunes in a wind tunnel. *Earth Surf. Proc. Land.* 28,
2619 1111–1124.

- 2620 Walker, I.J., Shugar, D.H., 2013. Secondary flow deflection in the lee of transverse dunes with
2621 implications for dune morphodynamics and migration. *Earth Surf. Proc. Land.* 1642–
2622 1654.
- 2623 Walmsley, J.L., Howard, A.D., 1985. Application of a boundary-layer model to flow over an
2624 eolian dune. *J. Geophys. Res-Atmos.* 90(10), 631–640.
- 2625 Walmsley, J.I., Salmon, J.R., Taylor, P.A., 1982. On the application of a model of boundary-layer
2626 flow over low hills to real terrain. *Boundary Layer Meteorology* 23, 17–46.
- 2627 Wang, X., Dong, Z., Zhang, J., Chen, G., 2002. Geomorphology of sand dunes in the Northeast
2628 Taklimakan Desert. *Geomorphology* 42, 183– 195.
- 2629 Weaver, C.M., Wiggs, G.F.S., 2011. Field measurements of mean and turbulent airflow over a
2630 barchan sand dune. *Geomorphology* 128, 32–41.
- 2631 Webster, T., 2012. Coastline change in Prince Edward Island, 1968-2010 and 2000-2010. Report
2632 prepared for Prince Edward Island Department of Environment, Energy and Forestry,
2633 Charlottetown, PEI and the Atlantic Climate Adaptation Solutions Association, 36 pp.
- 2634 Weng, W.S., Hunt, J.C.R., Carruthers, D.J., Warren, A., Wiggs, G.F.S., Livingstone, A., Castro, I.,
2635 1991. Air flow and sand transport over sand dunes. *Acta Mech. Supplementum* 2, 1–22.
- 2636 Wiggs, G.F.S., Baird, A.J., Atherton, R.J., 2004a. The dynamic effect of moisture on the
2637 entrainment and transport of sand by wind. *Geomorphology* 59, 13–30.
- 2638 Wiggs, G.F.S., Baird, A.J., Atherton, R.J., 2004b. Thresholds of aeolian sand transport:
2639 establishing suitable values. *Sedimentology* 51, 95–108.
- 2640 Wiggs, G.F.S., Livingstone, I., Thomas, D.S.G., Bullard, J.A., 1996a. Airflow and roughness
2641 characteristics over partially vegetated linear dunes in the Southwest Kalahari desert.
2642 *Earth Surf. Proc. Land.* 21, 19–34.
- 2643 Wiggs, G.F.S., Livingstone, I., Warren, A., 1996b. The role of streamline curvature in sand dune
2644 dynamics: evidence from field and wind tunnel measurements. *Geomorphology* 17, 29–
2645 46.
- 2646 Wiggs, G.F.S., Weaver, C.M., 2012. Turbulent flow structures and aeolian sediment transport
2647 over a barchan sand dune. *Geophys. Res. Lett.* 39: L05404.
- 2648 Williams, G.P., 1964. Some aspects of the eolian saltation load. *Sedimentology* 9, 89-104.
- 2649 Wilson, E.O. (1998) *Consilience: The Unity of Knowledge*. Alfred A. Knopf Inc., New York, New
2650 York. 332 pp.
- 2651 Wolman, M.G., Gerson, R., 1978. Relative scales of time and effectiveness of climate in
2652 watershed geomorphology. *Earth Surf. Proc. Land.* 3(2), 189-208.
- 2653 Wolman, M.G., Miller, W.P., 1960. Magnitude and frequency of forces in geomorphic
2654 processes. *J. Geol.* 68, 54-74.

- 2655 Yang, Y., Davidson-Arnott, R.G.D., 2005. Rapid measurement of surface moisture content on a
2656 beach. *J. Coastal Res.* 21, 447–452.
- 2657 Yurk, B., Hansen, E.C., DeVries-Zimmerman, S., Kilibarda, Z., van Dijk, D., Bodenbender, B.,
2658 Krehel, A., Pennings T., 2014. The role of extratropical cyclones in shaping dunes along
2659 southern and southeastern Lake Michigan. In: Fisher, T.G., Hansen, E.C. (Eds.), *Coastline
2660 and Dune Evolution along the Great Lakes*. Geological Society of America Special Paper
2661 508, pp. 167–194, doi:10.1130/2014.2508(10).
- 2662 Zhang, K., Douglas, B.C., Leatherman, S.P., 2004. Global warming and coastal erosion. *Climactic
2663 Change* 64, 41–58.
- 2664 Zhang, W., Schneider, R., Kolbb, J., Teichmann, T., Dudzinska-Nowak, J., Harff, J.C., Till J.J.,
2665 Hanebuth, T.J.J., 2015. Land–sea interaction and morphogenesis of coastal foredunes –
2666 A modeling case study from the southern Baltic Sea coast. *Coast. Eng.* 99, 148-166.